

Toroidal Maps: Schnyder Woods, Orthogonal Surfaces and Straight-Line Representations

Daniel Gonçalves · Benjamin Lévêque

Received: 6 July 2012 / Revised: 1 July 2013 / Accepted: 25 September 2013 /
Published online: 31 October 2013
© Springer Science+Business Media New York 2013

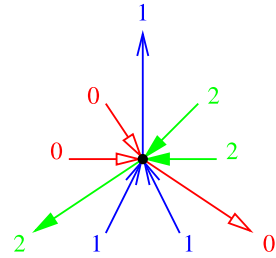
Abstract A Schnyder wood is an orientation and coloring of the edges of a planar map satisfying a simple local property. We propose a generalization of Schnyder woods to graphs embedded on the torus with application to graph drawing. We prove several properties on this new object. Among all we prove that a graph embedded on the torus admits such a Schnyder wood if and only if it is an essentially 3-connected toroidal map. We show that these Schnyder woods can be used to embed the universal cover of an essentially 3-connected toroidal map on an infinite and periodic orthogonal surface. Finally we use this embedding to obtain a straight-line flat torus representation of any toroidal map in a polynomial size grid.

Keywords Schnyder woods · Toroidal graphs · Embedding

1 Introduction

A closed curve on a surface is *contractible* if it can be continuously transformed into a single point. Given a graph embedded on the torus, a *contractible loop* is an edge forming a contractible cycle. Two *homotopic multiple edges* are two edges with the same extremities such that their union forms a contractible cycle. In this paper, we will almost always consider graphs embedded on the torus with no contractible loop and no homotopic multiple edges. We call these graphs *toroidal graphs* for short and keep the distinction with *graph embedded on the torus* that may have contractible loops or homotopic multiple edges. A *map* on a surface is a graph embedded on this surface where every face is homeomorphic to an open disk. A *map embedded on the torus* is a graph embedded on the torus that is a map (it may contains contractible loops or homotopic multiple edges). A *toroidal map* is a toroidal graph that is a map

D. Gonçalves · B. Lévêque (✉)
LIRMM, CNRS, Université Montpellier 2, 161 rue Ada, 34095 Montpellier Cedex 5, France
e-mail: benjamin.leveque@lirmm.fr

Fig. 1 Schnyder property

(it has no contractible loop and no homotopic multiple edges). A *toroidal triangulation* is a toroidal map where every face has size three. A general graph (i.e., not embedded on a surface) is *simple* if it contains no loop and no multiple edges. Since some loops and multiple edges are allowed in toroidal graphs, the class of toroidal graphs is larger than the class of simple toroidal graphs.

The torus is represented by a parallelogram in the plane whose opposite sides are pairwise identified. This representation is called the *flat torus*. The *universal cover* G^∞ of a graph G embedded on the torus is the infinite planar graph obtained by replicating a flat torus representation of G to tile the plane (the tiling is obtained by translating the flat torus along two vectors corresponding to the sides of the parallelogram). Note that a graph G embedded on the torus has no contractible loop and no homotopic multiple edges if and only if G^∞ is simple.

Given a general graph G , let n be the number of vertices and m the number of edges. Given a graph embedded on a surface, let f be the number of faces. Euler's formula says that any map on a surface of genus g satisfies $n - m + f = 2 - 2g$, where the plane is the surface of genus 0, and the torus the surface of genus 1.

Schnyder woods were originally defined for planar triangulations by Schnyder [26].

Definition 1 (Schnyder wood, Schnyder property) Given a planar triangulation G , a *Schnyder wood* is an orientation and coloring of the edges of G with the colors 0, 1, 2 where each inner vertex v satisfies the *Schnyder property* (see Fig. 1 where each color is represented by a different type of arrow):

- Vertex v has outdegree one in each color.
- The edges $e_0(v)$, $e_1(v)$, $e_2(v)$ leaving v in colors 0, 1, 2, respectively, occur in counterclockwise order.
- Each edge entering v in color i enters v in the counterclockwise sector from $e_{i+1}(v)$ to $e_{i-1}(v)$ (where $i + 1$ and $i - 1$ are understood modulo 3).

For higher genus triangulated surfaces, a generalization of Schnyder woods has been proposed by Castelli Aleardi et al. [3], with applications to encoding. Unfortunately, in this definition, the simplicity and the symmetry of the original Schnyder wood are lost. Here we propose an alternative generalization of Schnyder woods for toroidal graphs, with application to graph drawings.

By Euler's formula, a planar triangulation satisfies $m = 3n - 6$. Thus, there are not enough edges in the graph for all vertices to be of outdegree three. This explains

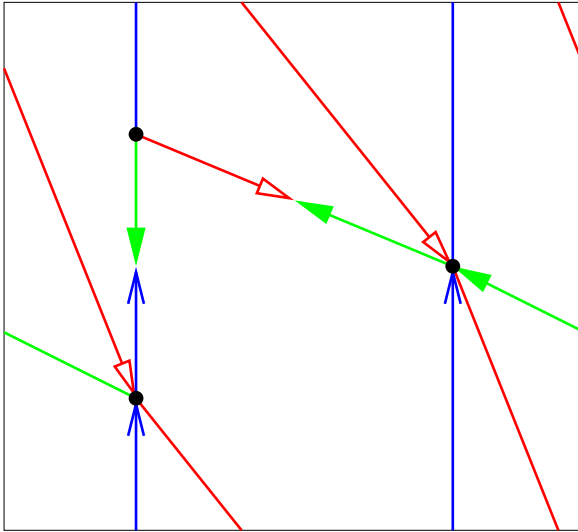


Fig. 2 Example of a Schnyder wood of a toroidal graph

why just some vertices (inner ones) are required to satisfy the Schnyder property. For a toroidal triangulation, Euler’s formula gives exactly $m = 3n$, so there is hope for a nice object satisfying the Schnyder property for every vertex. This paper shows that such an object exists. Here we do not restrict ourselves to triangulations and we directly define Schnyder woods in a more general framework.

Felsner [7, 8] (see also [20]) has generalized Schnyder woods to 3-connected planar maps by allowing edges to be oriented in one direction or in two opposite directions. We also allow edges to be oriented in two directions in our definition.

Definition 2 (Toroidal Schnyder wood) Given a toroidal graph G , a (toroidal) Schnyder wood of G is an orientation and coloring of the edges of G with the colors 0, 1, 2, where every edge e is oriented in one direction or in two opposite directions (each direction having a distinct color), satisfying the following (see example of Fig. 2):

- (T1) Every vertex v satisfies the Schnyder property (see Definition 1)
- (T2) Every monochromatic cycle of color i intersects at least one monochromatic cycle of color $i - 1$ and at least one monochromatic cycle of color $i + 1$.

Note that in this definition each vertex has exactly one outgoing arc in each color. Thus, there are monochromatic cycles and the term “wood” has to be handled with care here. The graph induced by one color is not necessarily connected, but each connected component has exactly one directed cycle. We will prove that all the monochromatic cycles of one color have the same homotopy.

In the case of toroidal triangulations, $m = 3n$ implies that there are too many edges to have bi-oriented edges. Thus, we can use this general definition of Schnyder wood for toroidal graphs and keep in mind that when restricted to toroidal triangulations all edges are oriented in one direction only.

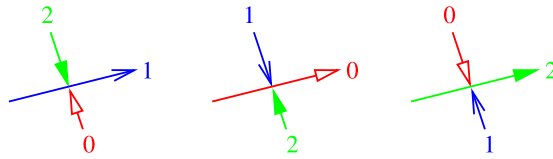


Fig. 3 Rules for the dual Schnyder wood

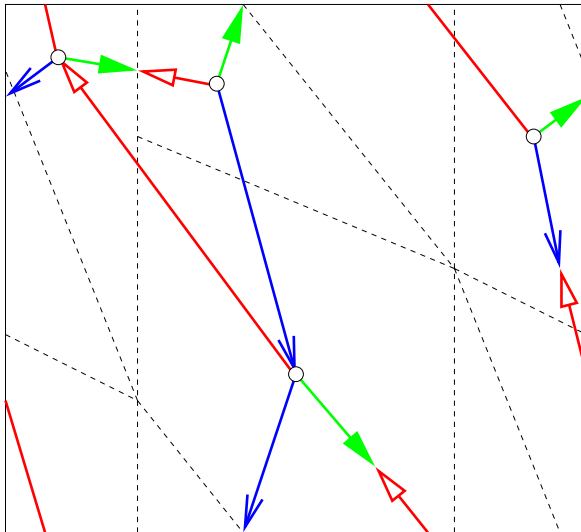


Fig. 4 Dual Schnyder wood of the Schnyder wood of Fig. 2

Extending the notion of essentially 2-connectedness [23], we say that a toroidal graph G is *essentially k -connected* if its universal cover is k -connected. Note that an essentially 1-connected toroidal graph is a toroidal map. We prove that essentially 3-connected toroidal maps are characterized by the existence of Schnyder woods.

Theorem 1 *A toroidal graph admits a Schnyder wood if and only if it is an essentially 3-connected toroidal map.*

The *dual* of a Schnyder wood is the orientation and coloring of the edges of G^* obtained by the rules represented on Fig. 3.

Our definition supports duality and we have the following results.

Theorem 2 *There is a bijection between Schnyder woods of a toroidal map and Schnyder woods of its dual.*

The dual Schnyder wood of the Schnyder wood of Fig. 2 is represented on Fig. 4.

In our definition of Schnyder woods, two properties are required: a local one (T1) and a global one (T2). This second property is important for using Schnyder woods

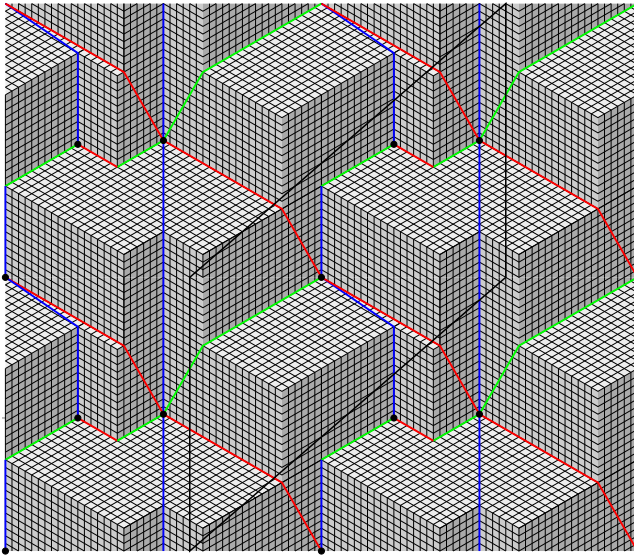


Fig. 5 Geodesic embedding of the toroidal map of Fig. 2

to embed toroidal graphs on orthogonal surfaces, as has been done in the plane by Miller [20] (see also [8]).

Theorem 3 *The universal cover of an essentially 3-connected toroidal map admits a geodesic embedding on an infinite and periodic orthogonal surface.*

A geodesic embedding of the toroidal map of Fig. 2 is represented on Fig. 5. The black parallelogram represents a copy of the graph of Fig. 2; this is the basic tile that is used to fill the plane.

A *straight-line flat torus representation* of a toroidal map G is the restriction to a flat torus of a periodic straight-line representation of G^∞ . The problem of finding a straight-line flat torus representation of a toroidal map was previously solved on exponential size grids [21]. There are several works that represent a toroidal map inside a parallelogram in a polynomial size grid [5, 6], but in these representations the opposite sides of the parallelogram do not perfectly match. In the embeddings obtained by Theorem 3, vertices are not coplanar, but we prove that for toroidal triangulations one can project the vertices on a plane to obtain a periodic straight-line representation of G^∞ . This gives the first straight-line flat torus representation of any toroidal map in a polynomial size grid.

Theorem 4 *A toroidal graph admits a straight-line flat torus representation in a polynomial size grid.*

In Sect. 2, we explain how our definition of Schnyder woods in the torus generalizes the planar case. In Sect. 3, we show that our Schnyder woods are of two fundamentally different types. In Sect. 4, we study the behavior of Schnyder woods

in the universal cover; we define the notion of regions and show that the existence of Schnyder woods for a toroidal graph implies that the graph is an essentially 3-connected toroidal map. In Sect. 5, we define the angle labeling and the dual of a Schnyder wood. In Sect. 6, we show how the definition of Schnyder woods can be relaxed for one of the two types of Schnyder wood. This relaxation is used in the next sections for proving the existence of a Schnyder wood. In Sect. 7, we use a result of Fijavz [13] on the existence of non-homotopic cycles in simple toroidal triangulations to obtain a short proof of existence of Schnyder woods for simple triangulations. In Sect. 8, we prove a technical lemma showing how a Schnyder wood of a graph G can be derived from a Schnyder wood of the graph G' , where G' is obtained from G by contracting an edge. This lemma is then used in Sect. 9 to prove the existence of Schnyder woods for any essentially 3-connected toroidal maps. In Sect. 10, we use Schnyder woods to embed the universal cover of essentially 3-connected toroidal maps on periodic and infinite orthogonal surfaces by generalizing the region vector method defined in the plane. In Sect. 11, we show that the dual map can also be embedded on this orthogonal surface. In Sect. 12, we show that, in the case of toroidal triangulations, this orthogonal surface can be projected on a plane to obtain a straight-line flat torus representation.

2 Generalization of the Planar Case

Felsner [7, 8] has generalized planar Schnyder woods by allowing edges to be oriented in one direction or in two opposite directions. The formal definition is the following:

Definition 3 (Planar Schnyder wood) Given a planar map G , let x_0, x_1, x_2 be three distinct vertices occurring in counterclockwise order on the outer face of G . The *suspension* G^σ is obtained by attaching a half-edge that reaches into the outer face to each of these special vertices. A (*planar*) *Schnyder wood* rooted at x_0, x_1, x_2 is an orientation and coloring of the edges of G^σ with the colors 0, 1, 2, where every edge e is oriented in one direction or in two opposite directions (each direction having a distinct color), satisfying the following (see the example of Fig. 6):

- (P1) Every vertex v satisfies the Schnyder property and the half-edge at x_i is directed outwards and colored i
- (P2) There is no monochromatic cycle.

In the definition given by Felsner [8], property (P2) is in fact replaced by “There is no interior face the boundary of which is a monochromatic cycle”, but the two are equivalent by results of [7, 8].

With our definition of Schnyder woods for toroidal graphs, the goal is to generalize the definition of Felsner. In the torus, property (P1) can be simplified as every vertex plays the same role: there are no special outer vertices with a half-edge reaching into the outer face. This explains property (T1) in our definition. Then if one asks that every vertex satisfies the Schnyder property, there are necessarily monochromatic

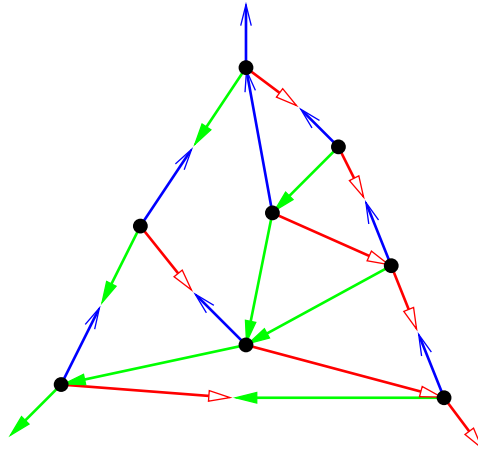


Fig. 6 Example of a Schnyder wood of a planar map

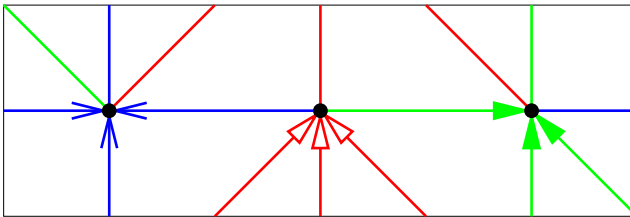


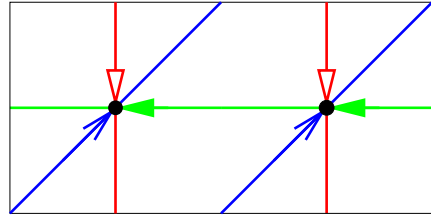
Fig. 7 An orientation and coloring of the edges of a toroidal triangulation satisfying (T1) but not (T2), as there is no pair of intersecting monochromatic cycles

cycles and (P2) is not satisfied. This explains why (P2) has been replaced by (T2) in our generalization to the torus.

It would have been possible to replace (P2) by “there is no contractible monochromatic cycles”, but this is not enough to suit our needs. Our goal is to use Schnyder woods to embed universal covers of toroidal graphs on orthogonal surfaces, as has been done in the plane by Miller [20] (see also [8]). The difference is that our surface is infinite and periodic. In such a representation the three colors 0, 1, 2 correspond to the three directions of the space. Thus, the monochromatic cycles with different colors have to intersect each other in a particular way. This explains why property (T2) is required. Figure 7 gives an example of an orientation and coloring of the edges of a toroidal triangulation satisfying (T1) but not (T2), as there is no pair of intersecting monochromatic cycles.

Let G be a toroidal graph given with a Schnyder wood. Let G_i be the directed graph induced by the edges of color i . This definition includes edges that are half-colored i , and in this case, the edges get only the direction corresponding to color i . Each graph G_i has exactly n edges, so it does not induce a rooted tree (contrarily to planar Schnyder woods). Note also that G_i is not necessarily connected (for example, in the graph of Fig. 8, every Schnyder wood has one color whose corresponding

Fig. 8 A toroidal graph where every Schnyder wood has one color whose corresponding subgraph is not connected



subgraph is not connected). But each component of G_i has exactly one outgoing arc for each of its vertices. Thus, each connected component of G_i has exactly one directed cycle that is a *monochromatic cycle* of color i , or i -cycle for short. Note that monochromatic cycles can contain edges oriented in two directions with different colors, but the *orientation* of an i -cycle is the orientation given by the (half-)edges of color i . The graph G_i^{-1} is the graph obtained from G_i by reversing all its edges. The graph $G_i \cup G_{i-1}^{-1} \cup G_{i+1}^{-1}$ is obtained from the graph G by orienting edges in one or two directions depending on whether this orientation is present in G_i , G_{i-1}^{-1} , or G_{i+1}^{-1} . The following lemma shows that our property (T2) in fact implies that there are no contractible monochromatic cycles.

Lemma 1 *The graph $G_i \cup G_{i-1}^{-1} \cup G_{i+1}^{-1}$ contains no contractible directed cycle.*

Proof Suppose there is a contractible directed cycle in $G_i \cup G_{i-1}^{-1} \cup G_{i+1}^{-1}$. Let C be such a cycle containing the minimum number of faces in the closed disk D bounded by C . Suppose by symmetry that C turns clockwise around D . Then, by (T1), there is no edge of color $i - 1$ leaving the closed disk D . So there is an $(i - 1)$ -cycle in D , and this cycle is C by minimality of C . Then, by (T1), there is no edge of color i leaving D . So, again by minimality of C , the cycle C is an i -cycle. Thus, all the edges of C are oriented clockwise in color i and counterclockwise in color $i - 1$. Then, by (T1), all the edges of color $i + 1$ incident to C have to leave D . Thus, there is no $(i + 1)$ -cycle intersecting C , a contradiction to property (T2). \square

Let G be a planar map and let x_0, x_1, x_2 be three distinct vertices occurring in counterclockwise order on the outer face of G . One can transform G^σ into the following toroidal map G^+ (see Fig. 9): Add a vertex v in the outer face of G . Add three non-parallel and non-contractible loops on v . Connect the three half-edges leaving x_i to v such that there are no two such edges entering v consecutively. Then we have the following.

Theorem 5 *The Schnyder woods of a planar map G rooted at x_0, x_1, x_2 are in bijection with the Schnyder woods of the toroidal map G^+ (where the orientation of one of the loops is fixed).*

Proof (\implies) We are given a Schnyder wood of the planar graph G , rooted at x_0, x_1, x_2 . Orient and color the graph G^+ as in the example of Fig. 9, i.e., the edges of the original graph G have the same color and orientation as in G^σ , the edge from

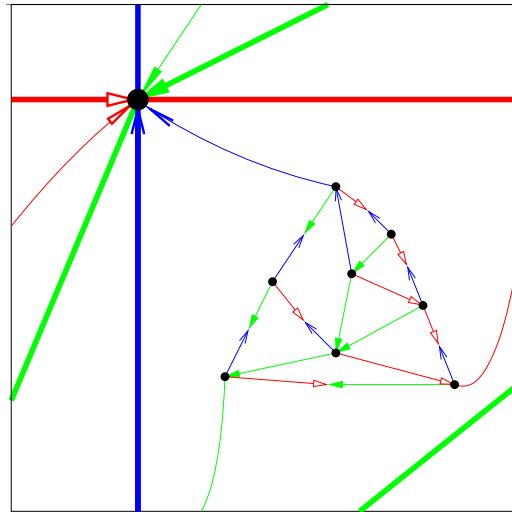


Fig. 9 The toroidal Schnyder wood corresponding to the planar Schnyder wood of Fig. 6

x_i to v is colored i and leaving x_i , and the three loops around v are colored and oriented appropriately so that v satisfies the Schnyder property. Then it is clear that all the vertices of G^+ satisfy (T1). By (P2), we know that G^σ has no monochromatic cycles. All the edges between G and v are leaving G , so there is no monochromatic cycle of G^+ involving vertices of G . Thus, the only monochromatic cycles of G^+ are the three loops around v and they satisfy (T2).

(\Leftarrow) Given a Schnyder wood of G^+ , the restriction of the orientation and coloring to G and the three edges leaving v gives a Schnyder wood of G^σ . The three loops around v are three monochromatic cycles corresponding to three edges leaving v ; thus, they have different colors by (T1). Thus, the three edges between G and v are entering v with three different colors. The three loops around v have to leave v in counterclockwise order 0, 1, 2 and we can assume the colors such that the edge leaving x_i is colored i . Clearly, all the vertices of G^σ satisfy (P1). By Lemma 1, there are no contractible monochromatic cycles in G^+ , so G^σ satisfies (P2). \square

A planar map G is *internally 3-connected* if there exist three vertices on the outer face such that the graph obtained from G by adding a vertex adjacent to the three vertices is 3-connected. Miller [20] (see also [7]) proved that a planar map admits a Schnyder wood if and only if it is internally 3-connected. The following results show that the notion of essentially 3-connected is the natural generalization of internally 3-connected to the torus.

Theorem 6 *A planar map G is internally 3-connected if and only if there exist three vertices on the outer face of G such that G^+ is an essentially 3-connected toroidal map.*

Proof (\implies) Let G be an internally 3-connected planar map. By definition, there exist three vertices x_0, x_1, x_2 on the outer face such that the graph G' obtained from G by adding a vertex adjacent to these three vertices is 3-connected. Let G'' be the graph obtained from G by adding three vertices y_0, y_1, y_2 that form a triangle and by adding the three edges $x_i y_i$. It is not difficult to check that G'' is 3-connected. Since G^∞ can be obtained from the (infinite) triangular grid, which is 3-connected, by gluing copies of G'' along triangles, G^∞ is clearly 3-connected. Thus, G^+ is an essentially 3-connected toroidal map.

(\impliedby) Suppose there exist three vertices on the outer face of G such that G^+ is an essentially 3-connected toroidal map, i.e., G^∞ is 3-connected. A copy of G is contained in a triangle $y_0 y_1 y_2$ of G^∞ . Let G'' be the subgraph of G^∞ induced by this copy plus the triangle, and let x_i be the unique neighbor of y_i in the copy of G . Since G'' is connected to the rest of G^∞ by a triangle, G'' is also 3-connected. Let us now prove that this implies that G is internally 3-connected for x_0, x_1 , and x_2 . This is equivalent to saying that the graph G' , obtained by adding a vertex z connected to x_0, x_1 , and x_2 , is 3-connected. If G' had a separator $\{a, b\}$ or $\{a, z\}$, with $a, b \in V(G') \setminus \{z\}$, then $\{a, b\}$ or $\{a, y_i\}$, for some $i \in [0, 2]$, would be a separator of G'' . This would contradict the 3-connectedness of G'' . So G is internally 3-connected. \square

3 Two Different Types of Schnyder Woods

Two non-contractible closed curves are *homotopic* if one can be continuously transformed into the other. Homotopy is an equivalence relation, and as we are on the torus we have the following.

Lemma 2 *Let C_1, C_2 be two non-contractible closed curves on the torus. If C_1, C_2 are not homotopic, then their intersection is non-empty.*

Two non-contractible oriented closed curves on the torus are *fully homotopic* if one can be continuously transformed into the other by preserving the orientation. We say that two monochromatic directed cycles C_i, C_j of different colors are *reversal* if one is obtained from the other by reversing all the edges ($C_i = C_j^{-1}$). We say that two monochromatic cycles are *crossing* if they intersect but are not reversal. We define the *right side* of an i -cycle C_i , as the right side while “walking” along the directed cycle by following the orientation given by the edges colored i .

Let G be a toroidal graph given with a Schnyder wood.

Lemma 3 *All i -cycles are non-contractible, non-intersecting, and fully homotopic.*

Proof By Lemma 1, all i -cycles are non-contractible. If there exist two such distinct i -cycles that are intersecting, then there is a vertex that has two outgoing edges of color i , a contradiction to (T1). So the i -cycles are non-intersecting. Then, by Lemma 2, they are homotopic.

Suppose that there exist two i -cycles C_i, C'_i that are not fully homotopic. By the first part of the proof, cycles C_i, C'_i are non-contractible, non-intersecting, and homotopic. Let R be the region between C_i and C'_i situated on the right of C_i . Suppose

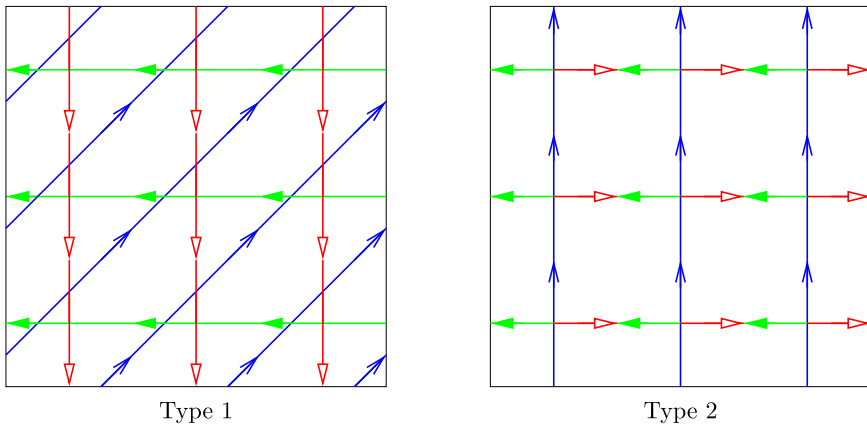


Fig. 10 The two types of Schnyder woods on toroidal graphs

by symmetry that C_i^{-1} is not an $(i + 1)$ -cycle. By (T2), there exists a cycle C_{i+1} intersecting C_i and thus C_{i+1} is crossing C_i . By property (T1), C_{i+1} is entering C_i from its right side and so it is leaving the region R when it crosses C_i . To enter the region R , the cycle C_{i+1} has to enter C_i or C_i' from their left side, a contradiction to property (T1). □

Lemma 4 *If two monochromatic cycles are crossing, then they are of different colors and they are not homotopic.*

Proof By Lemma 3, two crossing monochromatic cycles are not of the same color. Suppose that there exist two monochromatic cycles C_{i-1} and C_{i+1} , of color $i - 1$ and $i + 1$, that are crossing and homotopic. By Lemma 1, the cycles C_{i-1} and C_{i+1} are not contractible. Since $C_{i-1} \neq C_{i+1}^{-1}$ and $C_{i-1} \cap C_{i+1} \neq \emptyset$, the cycle C_{i+1} is leaving C_{i-1} . It is leaving C_{i-1} on its right side by (T1). Since C_{i-1} and C_{i+1} are homotopic, the cycle C_{i+1} is entering C_{i-1} at least once from its right side. This is in contradiction with (T1). □

Let C_i be the set of i -cycles of G . Let $(C_i)^{-1}$ denote the set of cycles obtained by reversing all the cycles of C_i . By Lemma 3, the cycles of C_i are non-contractible, non-intersecting, and fully homotopic. So we can order them as follows: $C_i = \{C_i^0, \dots, C_i^{k_i-1}\}$, $k_i \geq 1$, such that, for $0 \leq j \leq k_i - 1$, there is no i -cycle in the region $R(C_i^j, C_i^{j+1})$ between C_i^j and C_i^{j+1} containing the right side of C_i^j (superscript understood modulo k_i).

We show that Schnyder woods are of two different types (see Fig. 10):

Theorem 7 *Let G be a toroidal graph given with a Schnyder wood. Then all i -cycles are non-contractible, non-intersecting, and fully homotopic, and either:*

- For every pair of two monochromatic cycles C_i, C_j of different colors i, j , the two cycles C_i and C_j are not homotopic and thus intersect (we say the Schnyder wood is of Type 1);

or

- There exists a color i such that $C_{i-1} = (C_{i+1})^{-1}$ and for any pair of monochromatic cycles C_i, C_j of colors i, j , with $j \neq i$, the two cycles C_i and C_j are not homotopic and thus intersect (we say the Schnyder wood is of Type 2, or Type 2.i if we want to specify the color i).

Moreover, if G is a toroidal triangulation, then there are no edges oriented in two directions and the Schnyder wood is of Type 1.

Proof By Lemma 3, all i -cycles are non-contractible, non-intersecting, and fully homotopic. Suppose that there exist a $(i - 1)$ -cycle C_{i-1} and a $(i + 1)$ -cycle C_{i+1} that are homotopic. We prove that the Schnyder wood is of Type 2.i. We first prove that $C_{i-1} = (C_{i+1})^{-1}$. Let C'_{i-1} be any $(i - 1)$ -cycle. By (T2), C'_{i-1} intersects an $(i + 1)$ -cycle C'_{i+1} . By Lemma 3, C'_{i-1} (resp. C'_{i+1}) is homotopic to C_{i-1} (resp. C_{i+1}). So C'_{i-1} and C'_{i+1} are homotopic. By Lemma 4, C'_{i-1} and C'_{i+1} are reversal. Thus, $C_{i-1} \subseteq (C_{i+1})^{-1}$ and so by symmetry $C_{i-1} = (C_{i+1})^{-1}$. Now we prove that for any pair of monochromatic cycles C'_i, C'_j of colors i, j , with $j \neq i$, the two cycles C'_i and C'_j are not homotopic. By (T2), C'_j intersects an i -cycle C_i . Since $C_{i-1} = (C_{i+1})^{-1}$, cycle C'_j is bi-oriented in color $i - 1$ and $i + 1$, and thus we cannot have $C'_j = C_i^{-1}$. So C'_j and C_i are crossing and by Lemma 4, they are not homotopic. By Lemma 3, C'_i and C_i are homotopic. Thus, C'_j and C'_i are not homotopic. Thus, the Schnyder wood is of Type 2.i.

If there are no two monochromatic cycles of different colors that are homotopic, then the Schnyder wood is of Type 1.

For toroidal triangulation, $m = 3n$ by Euler's formula, so there are no edges oriented in two directions, and thus only Type 1 is possible. \square

Note that in a Schnyder wood of Type 1, we may have edges that are in two monochromatic cycles of different colors (see Fig. 2).

We do not know if the set of Schnyder woods of a given toroidal graph has a kind of lattice structure as in the planar case [9]. De Fraysseix et al. [15] proved that Schnyder woods of a planar triangulation are in one-to-one correspondence with the orientation of the edges of the graph where each inner vertex has outdegree three. It is possible to retrieve the coloring of the edges of a Schnyder wood from the orientation. The situation is different for toroidal triangulations. There exist orientations of toroidal triangulations where each vertex has outdegree three but there is no corresponding Schnyder wood. For example, if one considers a toroidal triangulation with just one vertex, the orientations of edges that satisfy (T1) are the orientations where there are not three consecutive edges leaving the vertex (see Fig. 11).

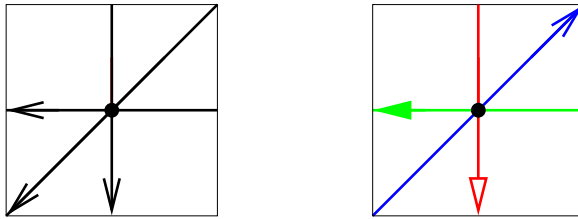


Fig. 11 Two different orientations of a toroidal triangulation. Only the second one corresponds to a Schnyder wood

4 Schnyder Woods in the Universal Cover

Let G be a toroidal graph given with a Schnyder wood. Consider the orientation and coloring of the edges of G^∞ that correspond to the Schnyder wood of G .

Lemma 5 *The orientation and coloring of the edges of G^∞ satisfy the following:*

- (U1) *Every vertex of G^∞ satisfies the Schnyder property*
- (U2) *There is no monochromatic cycle in G^∞ .*

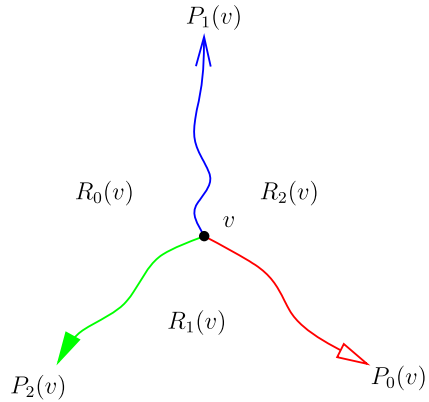
Proof Clearly, (U1) is satisfied. Now we prove (U2). Suppose by contradiction that there is a monochromatic cycle U of color i in G^∞ . Let C be the closed curve of G corresponding to edges of U . If C self-intersects, then there is a vertex of G with two edges leaving v in color i , a contradiction to (T1). So C is a monochromatic cycle of G . Since C corresponds to a cycle of G^∞ , it is a contractible cycle of G , a contradiction to Lemma 1. □

One can remark that properties (U1) and (U2) are the same as in the definition of Schnyder woods for 3-connected planar graphs (properties (P1) and (P2)). Note that if the orientation and coloring of the edges of G^∞ , corresponding to an orientation and coloring of the edges of G , satisfy properties (U1) and (U2), we do not necessarily have a Schnyder wood of G . For example, the graph G^∞ obtained by replicating the graph G of Fig. 7 satisfies (U1) and (U2), whereas the orientation and coloring of G do not make a Schnyder wood as (T2) is not satisfied.

Recall that the notation $\mathcal{C}_i = \{C_i^0, \dots, C_i^{k_i-1}\}$ denotes the set of i -cycles of G such that there is no i -cycle in the region $R(C_i^j, C_i^{j+1})$. As monochromatic cycles are not contractible by Lemma 1, a directed monochromatic cycle C_i^j corresponds to a family of infinite directed monochromatic paths of G^∞ (infinite in both directions of the path). This family is denoted \mathcal{L}_i^j . Each element of \mathcal{L}_i^j is called a *monochromatic line* of color i , or i -line for short. By Lemma 3, all i -lines are non-intersecting and oriented in the same direction. Given any two i -lines L, L' , the unbounded region between L and L' is noted $R(L, L')$. We say that two i -lines L, L' are *consecutive* if no i -lines are contained in $R(L, L')$.

Let v be a vertex of G^∞ . For each color i , vertex v is the starting vertex of a unique infinite directed monochromatic path of color i , denoted $P_i(v)$. Indeed this is a path

Fig. 12 Regions corresponding to a vertex



since there is no monochromatic cycle in G^∞ by property (U2), and it is infinite (in one direction of the path only) because every reached vertex of G^∞ has exactly one edge leaving in color i by property (U1). As $P_i(v)$ is infinite, it necessarily contains two vertices u, u' of G^∞ that are copies of the same vertex of G . The subpath of $P_i(v)$ between u and u' corresponds to an i -cycle of G and thus is part of an i -line of G^∞ . Let $L_i(v)$ be the i -line intersecting $P_i(v)$.

Lemma 6 *The graph $G_i^\infty \cup (G_{i-1}^\infty)^{-1} \cup (G_{i+1}^\infty)^{-1}$ contains no directed cycle.*

Proof Suppose there is a contractible directed cycle C in $G_i^\infty \cup (G_{i-1}^\infty)^{-1} \cup (G_{i+1}^\infty)^{-1}$. Let D be the closed disk bounded by C . Suppose by symmetry that C turns around D clockwise. Then, by (U1), there is no edge of color $i - 1$ leaving the closed disk D . So there is an $(i - 1)$ -cycle in D , a contradiction to (U2). \square

Lemma 7 *For every vertex v and color i , the two paths $P_{i-1}(v)$ and $P_{i+1}(v)$ only intersect on v .*

Proof If $P_{i-1}(v)$ and $P_{i+1}(v)$ intersect on two vertices, then $G_{i-1}^\infty \cup (G_{i+1}^\infty)^{-1}$ contains a cycle, contradicting Lemma 6. \square

By Lemma 7, for every vertex v , the three paths $P_0(v), P_1(v), P_2(v)$ divide G^∞ into three unbounded regions $R_0(v), R_1(v)$, and $R_2(v)$, where $R_i(v)$ denotes the region delimited by the two paths $P_{i-1}(v)$ and $P_{i+1}(v)$. Let $R_i^\circ(v) = R_i(v) \setminus (P_{i-1}(v) \cup P_{i+1}(v))$ (see Fig. 12).

Lemma 8 *For all distinct vertices u, v , we have:*

- (i) *If $u \in R_i(v)$, then $R_i(u) \subseteq R_i(v)$.*
- (ii) *If $u \in R_i^\circ(v)$, then $R_i(u) \subsetneq R_i(v)$.*
- (iii) *There exists i and j with $R_i(u) \subsetneq R_i(v)$ and $R_j(v) \subsetneq R_j(u)$.*

Proof (i) Suppose by symmetry that the Schnyder wood is not of Type 2.($i + 1$). Then in G , i -cycles are not homotopic to $(i - 1)$ -cycles. Thus in G^∞ , every i -line crosses

every $(i - 1)$ -line. Moreover an i -line crosses an $(i - 1)$ -line exactly once and from its right side to its left side by (U1). Vertex v is between two consecutive monochromatic $(i - 1)$ -lines L_{i-1}, L'_{i-1} , with L'_{i-1} situated on the right of L_{i-1} . Let R be the region situated on the right of L_{i-1} , so $v \in R$.

Claim 1 *For any vertex w of R , the path $P_i(w)$ leaves the region R .*

Proof of Claim 1 The i -line $L_i(w)$ has to cross L_{i-1} exactly once and from right to left; thus, $P_i(w)$ leaves the region R . This proves Claim 1. □

The path $P_{i+1}(v)$ cannot leave the region R as this would contradict (U1). Thus, by Claim 1 for $w = v$, we have $R_i(v) \subseteq R$ and so $u \in R$. Moreover, the paths $P_{i-1}(u)$ and $P_{i+1}(u)$ cannot leave region $R_i(v)$ as this would contradict (U1). Thus by Claim 1 for $w = u$, the path $P_i(u)$ leaves the region $R_i(v)$ and so $R_i(u) \subseteq R_i(v)$.

(ii) By (i), $R_i(u) \subseteq R_i(v)$, so the paths $P_{i-1}(u)$ and $P_{i+1}(u)$ are contained in $R_i(v)$. Then none of them can contain v as this would contradict (U1). So all the faces of $R_i(v)$ incident to v are not in $R_i(u)$ (and there is at least one such face).

(iii) By symmetry, we prove that there exists i with $R_i(u) \subsetneq R_i(v)$. If $u \in R_i^c(v)$ for some color i , then $R_i(u) \subsetneq R_i(v)$ by (ii). Suppose now that $u \in P_i(v)$ for some i . By Lemma 7, at least one of the two paths $P_{i-1}(u)$ and $P_{i+1}(u)$ does not contain v . Suppose by symmetry that $P_{i-1}(u)$ does not contain v . As $u \in P_i(v) \subseteq R_{i+1}(v)$, we have $R_{i+1}(u) \subseteq R_{i+1}(v)$ by (i), and as none of $P_{i-1}(u)$ and $P_i(u)$ contains v , we have $R_{i+1}(u) \subsetneq R_{i+1}(v)$. □

Lemma 9 *If a toroidal graph G admits a Schnyder wood, then G is essentially 3-connected.*

Proof Let u, v, x, y be any four distinct vertices of G^∞ . Let us prove that there exists a path between u and v in $G^\infty \setminus \{x, y\}$. Suppose by symmetry, that the Schnyder wood is of Type 1 or Type 2.1. Then the monochromatic lines of color 0 and 2 form a kind of grid; i.e., the 0-lines intersect all the 2-lines. Let L_0, L'_0 be 0-lines and L_2, L'_2 be 2-lines, such that u, v, x, y are all in the interior of the bounded region $R(L_0, L'_0) \cap R(L_2, L'_2)$.

By Lemma 7, the three paths $P_i(v)$, for $0 \leq i \leq 2$, are disjoint except on v . Thus, there exists i , such that $P_i(v) \cap \{x, y\} = \emptyset$. Similarly there exists j , such that $P_j(u) \cap \{x, y\} = \emptyset$. The two paths $P_i(v)$ and $P_j(u)$ are infinite, so they intersect the boundary of $R(L_0, L'_0) \cap R(L_2, L'_2)$. Thus, $P_i(v) \cup P_j(u) \cup L_0 \cup L'_0 \cup L_2 \cup L'_2$ contains a path from u to v in $G^\infty \setminus \{x, y\}$. □

By Lemma 9, if G admits a Schnyder wood, then it is essentially 3-connected, so it is a map and each face is a disk.

Note that if (T2) is not required in the definition of Schnyder woods, then Lemma 9 is false. Figure 13 gives an example of an orientation and a coloring of the edges of a toroidal graph satisfying (T1), such that there are no contractible monochromatic cycles, but where (T2) is not satisfied as there is a 0-cycle not intersecting any 2-cycle. This graph is not essentially 3-connected; indeed, G^∞ is not connected.

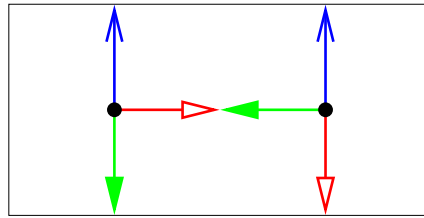


Fig. 13 An orientation and a coloring of the edges of a toroidal graph satisfying (T1) but not essentially 3-connected

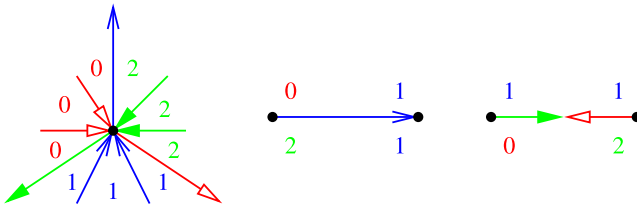


Fig. 14 Angle labeling around vertices and edges

5 Duality of Schnyder Woods

We are given a planar map G , and x_0, x_1, x_2 , three distinct vertices occurring in counterclockwise order on the outer face of G . A *Schnyder angle labeling* [7] of G with respect to x_0, x_1, x_2 is a labeling of the angles of G^σ satisfying the following:

- (L1) The label of the angles at each vertex form, in counterclockwise order, non-empty intervals of 0's, 1's, and 2's. The two angles at the half-edge at x_i have labels $i + 1$ and $i - 1$
- (L2) The label of the angles at each inner face form, in counterclockwise order, non-empty intervals of 0's, 1's, and 2's. At the outer face the same is true in clockwise order.

Felsner [8] proved that, for planar maps, Schnyder woods are in bijection with Schnyder angle labellings. In the toroidal case, we do not see a simple definition of Schnyder angle labeling that would be equivalent to our definition of Schnyder woods. This is due to the fact that, unlike (P2) which is local and can be checked just by considering faces, (T2) is global. Nevertheless, we have one implication.

The *angle labeling corresponding to* a Schnyder wood of a toroidal map G is a labeling of the angles of G such that the angles at a vertex v in the counterclockwise sector between $e_{i+1}(v)$ and $e_{i-1}(v)$ are labeled i (see Fig. 14).

Lemma 10 *The angle labeling corresponding to a Schnyder wood of a toroidal map satisfies the following: the angles at each vertex and at each face form, in counterclockwise order, non-empty intervals of 0's, 1's, and 2's.*

Proof Clearly, the property is true at each vertex by (T1). To prove that the property is true at each face, we count the number of color changes around vertices, faces, and edges. This number of changes is denoted d . For a vertex v there are exactly three changes, so $d(v) = 3$ (see Fig. 14). For an edge e , that can be either oriented in one or two directions, there are also exactly three changes, so $d(e) = 3$ (see Fig. 14). Now consider a face F . Suppose we cycle counterclockwise around F ; then an angle colored i is always followed by an angle colored i or $i + 1$. Consequently, $d(F)$ must be a multiple of 3. Suppose that $d(F) = 0$; then all its angles are colored with one color i . In that case the cycle around face F would be completely oriented in counterclockwise order in color $i + 1$ (and in clockwise order in color $i - 1$). This cycle being contractible, this would contradict Lemma 1. So $d(F) \geq 3$.

The sum of the changes around edges must be equal to the sum of the changes around faces and vertices. Thus $3m = \sum_e d(e) = \sum_v d(v) + \sum_F d(F) = 3n + \sum_F d(F)$. Euler’s formula gives $m = n + f$, so $\sum_F d(F) = 3f$ and this is possible only if $d(F) = 3$ for every face F . \square

There is no converse to Lemma 10. Figure 7 gives an example of a coloring and orientation of the edges of a toroidal triangulation not satisfying (T2) but where the angles at each vertex and at each face form, in counterclockwise order, non-empty intervals of 0’s, 1’s, and 2’s.

Let G be a toroidal graph given with a Schnyder wood. By Lemma 9, G is an essentially 3-connected toroidal map, and thus the dual G^* of G has no contractible loop and no homotopic multiple edges. Let \tilde{G} be a simultaneous drawing of G and G^* such that only dual edges intersect.

The dual of the Schnyder wood is the orientation and coloring of the edges of G^* obtained by the following method (see Figs. 3 and 4): Let e be an edge of G and e^* the dual edge of e . If e is oriented in one direction only and colored i , then e^* is oriented in two directions, entering e from the right side in color $i - 1$ and from the left side in color $i + 1$ (the right side of e is the right side while following the orientation of e). Symmetrically, if e is oriented in two directions in colors $i + 1$ and $i - 1$, then e^* is oriented in one direction only and colored i such that e is entering e^* from its right side in color $i - 1$.

Lemma 11 *Let G be a toroidal map. The dual of a Schnyder wood of a toroidal map G is a Schnyder wood of the dual G^* . Moreover we have:*

- (i) *On the simultaneous drawing \tilde{G} of G and G^* , the i -cycles of the dual Schnyder wood are homotopic to the i -cycles of the primal Schnyder wood and oriented in opposite directions.*
- (ii) *The dual of a Schnyder wood is of Type 2.i if and only if the primal Schnyder wood is of Type 2.i.*

Proof In every face of \tilde{G} , there is exactly one angle of G and one angle of G^* . Thus a Schnyder angle labeling of G corresponds to an angle labeling of G^* . The dual of the Schnyder wood is defined such that an edge e is leaving F in color i if and only if the angle at F on the left of e is labeled $i - 1$ and the angle at F on the right of e is labeled $i + 1$, and such that an edge e is entering F in color i if and only if at

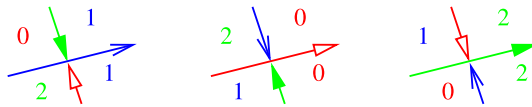


Fig. 15 Rules for the dual Schnyder wood and angle labeling

least one of the angles at F incident to e is labeled i (see Fig. 15). By Lemma 10, the angles at a face form, in counterclockwise order, non-empty intervals of 0’s, 1’s, and 2’s. Thus, the edges around a vertex of G^* satisfy property (T1).

Consider \tilde{G} with the orientation and coloring of primal and dual edges.

Let C be a i -cycle of G^* . Suppose, by contradiction, that C is contractible. Let D be the disk delimited by C . Suppose by symmetry that C is going anticlockwise around D . Then all the edges of G that are dual to edges of C are entering D in color $i - 1$. Thus, D contains an $(i - 1)$ -cycle of G , a contradiction to Lemma 1. Thus, every monochromatic cycle of G^* is non-contractible.

The dual of the Schnyder wood is defined in such a way that an edge of G and an edge of G^* of the same color never intersect in \tilde{G} . Thus the i -cycles of G^* are homotopic to i -cycles of G . Consider a i -cycle C_i (resp. C_i^*) of G (resp. G^*). The two cycles C_i and C_i^* are homotopic. By symmetry, we assume that the primal Schnyder wood is not of Type 2.($i - 1$). Let C_{i+1} be an $(i + 1)$ -cycle of G . The two cycles C_i and C_{i+1} are not homotopic and C_i is entering C_{i+1} on its left side. Thus, the two cycles C_i^* and C_{i+1} are not homotopic, and by the dual rules C_i^* is entering C_{i+1} on its right side. So C_i and C_i^* are homotopic and going in opposite directions.

Suppose the Schnyder wood of G is of Type 1. Then two monochromatic cycles of G of different colors are not homotopic. Thus, the same is true for monochromatic cycles of the dual. So (T2) is satisfied and the dual of the Schnyder wood is a Schnyder wood of Type 1.

Suppose now that the Schnyder wood of G is of Type 2. Assume by symmetry that it is of Type 2.i. Then all monochromatic cycles of color i and j , with $j \in \{i - 1, i + 1\}$, intersect. Now suppose, by contradiction, that there is a j -cycle C^* , with $j \in \{i - 1, i + 1\}$, that is not equal to a monochromatic cycle of color in $\{i - 1, i + 1\} \setminus \{j\}$. By symmetry we can assume that C^* is of color $i - 1$. Let C be the $(i - 1)$ -cycle of the primal that is the first on the right side of C^* in \tilde{G} . By definition of Type 2.i, C^{-1} is an $(i + 1)$ -cycle of G . Let R be the region delimited by C^* and C situated on the right side of C^* . Cycle C^* is not an $(i + 1)$ -cycle, so there is at least one edge of color $i + 1$ leaving a vertex of C^* . By (T1) in the dual, this edge is entering the interior of the region R . An edge of G^* of color $i + 1$ cannot intersect C and cannot enter C^* from its right side. So in the interior of the region R there is at least one $(i + 1)$ -cycle C_{i+1}^* of G^* . Cycle C_{i+1}^* is homotopic to C^* and going in the opposite direction (i.e., C_{i+1}^* and C^* are not fully homotopic). If C_{i+1}^* is not an $(i - 1)$ -cycle, then we can define $R' \subsetneq R$ the region delimited by C_{i+1}^* and C situated on the left side of C_{i+1}^* and as before we can prove that there is an $(i - 1)$ -cycle of G^* in the interior of R' . So in any case, there is an $(i - 1)$ -cycle C_{i-1}^* of G^* in the interior of R and C_{i-1}^* is fully homotopic to C^* . Let $R'' \subsetneq R$ be the region delimited by C^* and C_{i-1}^* situated on the right side of C^* . Clearly, R'' does not contain C . Thus, by the

definition of C , the region R'' does not contain any $(i - 1)$ -cycle of G . But R'' is non-empty and contains at least one vertex v of G . The path $P_{i-1}(v)$ cannot leave R'' , a contradiction. So (T2) is satisfied and the dual Schnyder wood is of Type 2.i. \square

By Lemma 11, we have Theorem 2.

6 Relaxing the Definition

In the plane, the proof of existence of Schnyder woods can be done without too much difficulty, as the properties to be satisfied are only local. In the toroidal case, things are much more complicated, as property (T2) is global. The following lemma shows that property (T2) can be relaxed a bit in the case of Schnyder woods of Type 1.

Lemma 12 *Let G be a toroidal graph given with an orientation and coloring of the edges of G with the colors 0, 1, 2, where every edge e is oriented in one direction or in two opposite directions. The orientation and coloring is a Schnyder wood of Type 1 if and only if it satisfies the following:*

- (T1') *Every vertex v satisfies the Schnyder property.*
- (T2') *For each pair i, j of different colors, there exists an i -cycle intersecting a j -cycle.*
- (T3') *There are no monochromatic cycles C_i, C_j of different colors i, j such that $C_i = C_j^{-1}$.*

Proof (\implies) If we have a Schnyder wood of Type 1, then property (T1') is satisfied, as it is equal to property (T1). Property (T1) implies that there always exist monochromatic cycles of each color, and thus property (T2') is a relaxation of (T2). Property (T3') is implied by definition of Type 1 (see Theorem 7).

(\impliedby) Conversely, suppose we have an orientation and coloring satisfying (T1'), (T2'), (T3'). We prove several properties.

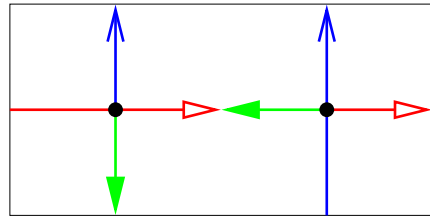
Claim 2 *All i -cycles are non-contractible, non-intersecting, and homotopic.*

Proof of Claim 2 Suppose there is a contractible monochromatic cycle. Let C be such a cycle containing the minimum number of faces in the closed disk D bounded by C . Suppose by symmetry that C turns around D clockwise. Let i be the color of C . Then, by (T1'), there is no edge of color $i - 1$ leaving the closed disk D . So there is an $(i - 1)$ -cycle in D and this cycle is C by minimality of C , a contradiction to (T3').

If there exist two distinct i -cycles that are intersecting, then there is a vertex that has two outgoing edges of color i , a contradiction to (T1'). So the i -cycles are non-intersecting. Then, by Lemma 2, they are homotopic. This proves Claim 2. \square

Claim 3 *If two monochromatic cycles are intersecting, then they are not homotopic.*

Fig. 16 An orientation and coloring of the edges of toroidal graph satisfying (T1') and (T2') but that is not a Schnyder wood



Proof of Claim 3 Suppose by contradiction that there exist C, C' , two distinct directed monochromatic cycles that are homotopic and intersecting. By Claim 2, they are not contractible and of different color. Suppose C is an $(i - 1)$ -cycle and C' an $(i + 1)$ -cycle. By (T1'), C' is leaving C on its right side. Since C, C' are homotopic, the cycle C' is entering C at least once from its right side, a contradiction with (T1'). This proves Claim 3. \square

We are now able to prove that (T2) is satisfied. Let C_i be any i -cycle of color i . We have to prove that C_i intersects at least one $(i - 1)$ -cycle and at least one $(i + 1)$ -cycle. Let j be either $i - 1$ or $i + 1$. By (T2'), there exists an i -cycle C'_i intersecting a j -cycle C'_j of color j . The two cycles C'_i, C'_j are not reversal by (T3'); thus, they are crossing. By claim (3), C'_i and C'_j are not homotopic. By Claim 2, C_i and C'_i are homotopic. Thus, by Lemma 2, C_i and C'_j are not homotopic and intersecting.

Thus, (T1) and (T2) are satisfied, and the orientation and coloring are a Schnyder wood. By (T3') and Theorem 7 it is a Schnyder wood of Type 1. \square

Note that for toroidal triangulations, there are no edges oriented in two directions in an orientation and coloring of the edges satisfying (T1'), by Euler's formula. So (T3') is automatically satisfied. Thus, in the case of toroidal triangulations it is sufficient to have properties (T1') and (T2') to have a Schnyder wood. This is not true in general, as shown by the example of Fig. 16 that satisfies (T1') and (T2') but that is not a Schnyder wood. There is a monochromatic cycle of color 1 that is not intersecting any monochromatic cycle of color 2, so (T2) is not satisfied.

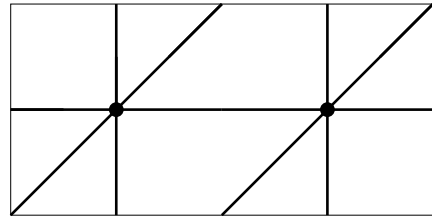
7 Existence for Simple Triangulations

In this section we present a short proof of existence of Schnyder woods for simple triangulations. Sections 8 and 9 contain the full proof of existence for essentially 3-connected toroidal maps.

Fijavz [13] proved a useful result concerning the existence of particular non-homotopic cycles in toroidal triangulations with no loop and no multiple edges. (Recall that in this paper we are less restrictive, as we allow non-contractible loops and non-homotopic multiple edges.)

Theorem 8 ([13]) *A simple toroidal triangulation contains three non-contractible and non-homotopic cycles that all intersect on one vertex and that are pairwise disjoint otherwise.*

Fig. 17 A toroidal triangulation that does not contain three non-contractible and non-homotopic cycles that all intersect on one vertex and that are pairwise disjoint otherwise



Theorem 8 is not true for all toroidal triangulations, as shown by the example on Fig. 17.

Theorem 8 can be used to prove the existence of particular Schnyder woods for simple toroidal triangulations. We first need the following lemma.

Lemma 13 *If G is a connected near-triangulation (i.e., all inner faces are triangles) whose outer boundary is a cycle, and with three vertices x_0, x_1, x_2 on its outer face such that the three outer paths between the x_i are chordless, then G' is internally 3-connected for vertices x_i .*

Proof Let G' be the graph obtained from G by adding a vertex z adjacent to the three vertices x_i . We have to prove that G' is 3-connected. Let S be a separator of G' of minimum size and suppose by contradiction that $1 \leq |S| \leq 2$. Let $G'' = G' \setminus S$.

For $v \in S$, the vertices of $N_{G'}(v) \setminus S$ should appear in several connected components of G'' , otherwise $S \setminus \{v\}$ is also a separator of G' . Since G is a near-triangulation, the neighbors of an inner vertex v of G form a cycle, and thus there are at least two vertex-disjoint paths between any two vertices of $N(v)$ in $G' \setminus \{v\}$. So S contains no inner vertex of G . Similarly, the three neighbors of z in G' belong to a cycle of $G' \setminus \{z\}$ (the outer boundary of G), so S does not contain z . Thus, S contains only vertices that are on the outer boundary of G .

Let $v \in S$. Vertex v is on the outer face of G , so its neighbors in G form a path P where the two extremities of P are the two neighbors of v on the outer face of G . So S contains an inner vertex u of P . Vertex u is also on the outer face of G , so uv is a chord of the outer cycle of G . As the three outer paths between the x_i are chordless, we have that u, v lie on two different outer paths between pairs of x_i . But then all the vertices of $P \setminus \{u\}$ are in the same components of G'' because of z , a contradiction. \square

Theorem 9 *A simple toroidal triangulation admits a Schnyder wood with three monochromatic cycles of different colors all intersecting on one vertex and that are pairwise disjoint otherwise.*

Proof Let G be a simple toroidal triangulation. By Theorem 8, let C_0, C_1, C_2 be three non-contractible and non-homotopic cycles of G that all intersect on one vertex x and that are pairwise disjoint otherwise. By eventually shortening the cycles C_i , we can assume that the three cycles C_i are chordless. By symmetry, we can assume that the six edges e_i, e'_i of the cycles C_i incident to x appear around x in the counterclockwise order $e_0, e'_2, e_1, e'_0, e_2, e'_1$ (see Fig. 18). The cycles C_i divide G into two regions, denoted R_1, R_2 such that R_1 is the region situated in the counterclockwise sector

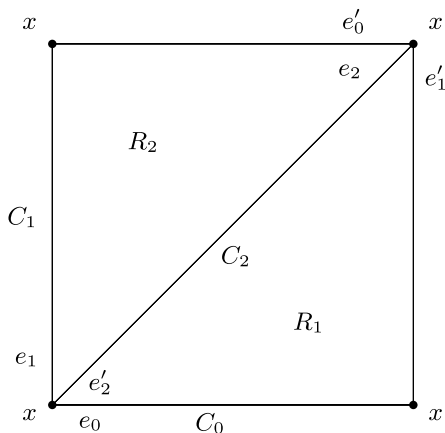
between e_0 and e'_2 of x and R_2 is the region situated in the counterclockwise sector between e'_2 and e_1 of x . Let G_i be the subgraph of G contained in the region R_i (including the three cycles C_i).

Let G'_1 (resp. G'_2) be the graph obtained from G_1 (resp. G_2) by replacing x by three vertices x_0, x_1, x_2 , such that x_i is incident to the edges in the counterclockwise sector between e_{i+1} and e'_i (resp. e'_i and e_{i-1}) (see Fig. 19). The two graphs G'_1 and G'_2 are near-triangulation and the C_i are chordless, so by Lemma 13, they are internally 3-connected planar maps for vertices x_i . The vertices x_0, x_1, x_2 appear in counterclockwise order on the outer face of G'_1 and G'_2 . By a result of Miller [20] (see also [7, 8]), the two graphs G'_i admit planar Schnyder woods rooted at x_0, x_1, x_2 . Orient and color the edges of G that intersect the interior of R_i by giving them the same orientation and coloring as in a planar Schnyder wood of G'_i . Orient and color the cycle C_i in color i such that it is entering x by edge e'_i and leaving x by edge e_i . We claim that the orientation and the coloring that are obtained form a toroidal Schnyder wood of G (see Fig. 19).

Clearly, any interior vertex of the region R_i satisfies (T1). Let us show that (T1) is also satisfied for any vertex v of a cycle C_i distinct from x . In a Schnyder wood of G'_1 , the cycle C_i is oriented in two directions, from x_{i-1} to x_i in color i and from x_i to x_{i-1} in color $i - 1$. Thus the edge leaving v in color $i + 1$ is an inner edge of G'_1 and vertex v has no edges entering in color $i + 1$. Symmetrically, in G'_2 the edge leaving v in color $i - 1$ is an inner edge of G'_2 and vertex v has no edges entering in color $i - 1$. Then one can paste G'_1 and G'_2 along C_i , orient C_i in color i , and see that v satisfies (T1). The definition of the G'_i and the orientation of the cycles are done so that x satisfies (T1). The cycles C_i being pairwise intersecting, (T2') is satisfied, so by Lemma 12, the orientation and coloring form a Schnyder wood. \square

Note that in the Schnyder wood obtained by Theorem 9, we do not know if there are several monochromatic cycles of one color or not. So given any three monochromatic cycles of different color, they might not all intersect on one vertex. But for any two monochromatic cycles of different color, we know that they intersect exactly once. We wonder whether Theorem 9 can be modified as follows: Does a simple

Fig. 18 Notation of the proof of Theorem 9



toroidal triangulation admit a Schnyder wood such that there is just one monochromatic cycle per color? Moreover, can one require that the monochromatic cycles of different colors pairwise intersect exactly once? Or, as in Theorem 9, that they all intersect on one vertex and that they are pairwise disjoint otherwise?

8 The Contraction Lemma

We prove the existence of Schnyder woods for essentially 3-connected toroidal maps by contracting edges until we obtain a graph with just a few vertices. Then the graph can be decontracted step by step to obtain a Schnyder wood of the original graph.

Given a toroidal map G , the *contraction* of a non-loop edge e of G is the operation consisting of continuously contracting e until its two ends are merged. We denote the obtained graph as G/e . On Fig. 20 the contraction of an edge e is represented. We consider three different cases corresponding to whether the faces adjacent to the edge e are triangles or not. Note that only one edge of each set of homotopic multiple edges that is possibly created is preserved.

The goal of this section is to prove the following lemma, which plays a key role in the proof of Sect. 9.

Lemma 14 *If G is a toroidal map given with a non-loop edge e whose extremities are of degree at least three and such that G/e admits a Schnyder wood of Type 1, then G admits a Schnyder wood of Type 1.*

The proof of Lemma 14 is long and technical. In the planar case, an analogous lemma can be proved without too much difficulty (see Sect. 2.6 of [12]), as there are special outer vertices where the contraction can be done to reduce the case analysis and as properties (P1) and (P2) are local and not too difficult to preserve during the decontraction process.

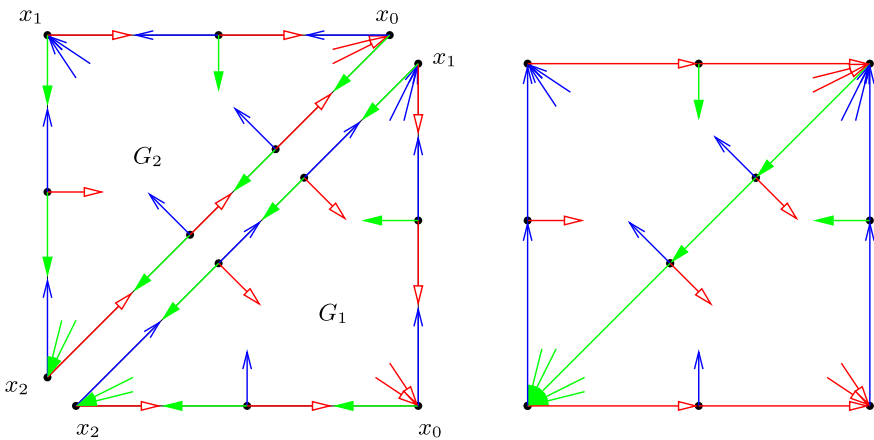


Fig. 19 Gluing two planar Schnyder woods into a toroidal one to prove Theorem 9

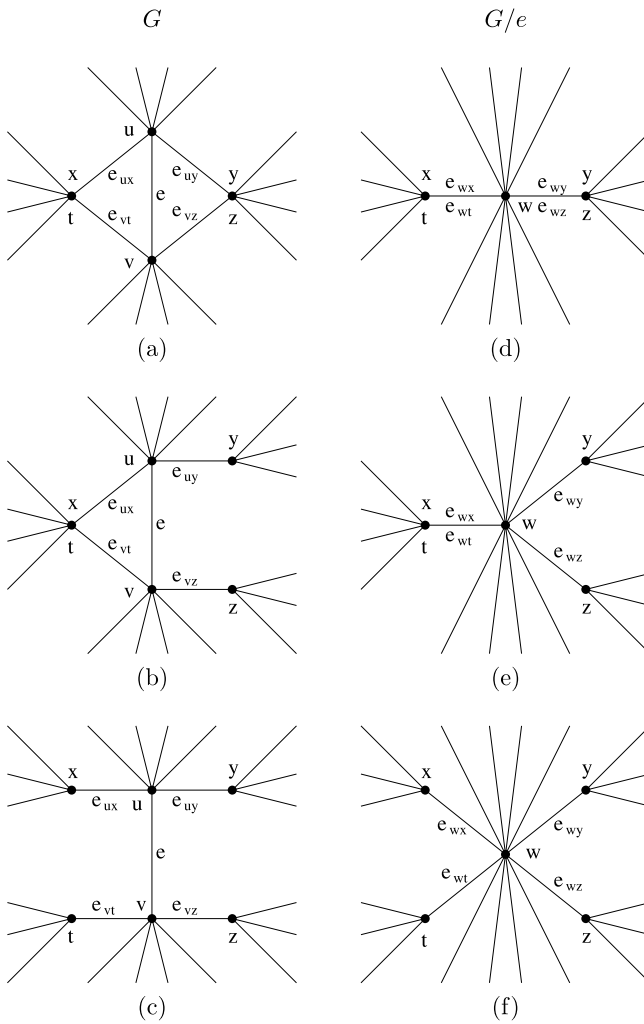


Fig. 20 The contraction operation

In the toroidal case there is a huge case analysis for the following reasons. One has to consider the three different kinds of contractions depicted on Fig. 20. For each of these cases, one must consider the different ways that the edges can be oriented and colored (around the contraction point) in G/e . For each of these cases, one must show that the Schnyder wood G/e can be extended to a Schnyder wood of G . This would be quite easy if one just has to satisfy (T1), which is a local property, but satisfying (T2) is much more complicated. Instead of proving (T2), that is considering intersections between every pair of monochromatic cycles, we prove (T2') and (T3'), which is equivalent for our purposes by Lemma 12. Property (T2') is simpler than (T2), as it considers just one intersection for each pair of colors instead of all the intersections. Even with this simplification, proving (T2') is the main difficulty of the proof. For

each considered case, one has to analyze the different ways in which the monochromatic cycles go through the contracted vertex or not and show that there always exist a coloring and orientation of G where (T2') is satisfied. Some cases are non-trivial and involve the use of lemmas like Lemmas 15 and 16.

Lemma 15 *Let G be a toroidal map given with a Schnyder wood and let y, w be two vertices of G such that $e_i(y)$ is entering w . Suppose that there is a directed path Q_{i-1} of color $i - 1$ from y to w , and a directed path Q_{i+1} of color $i + 1$ from y to w . Consider the two directed cycles $C_{i-1} = Q_{i-1} \cup \{e_i(y)\}^{-1}$ and $C_{i+1} = Q_{i+1} \cup \{e_i(y)\}^{-1}$. Then C_{i-1} and C_{i+1} are not homotopic.*

Proof By Lemma 1, the cycles C_{i-1} and C_{i+1} are not contractible. Suppose that C_{i-1} and C_{i+1} are homotopic. The path Q_{i+1} is leaving C_{i-1} at y on the right side of C_{i-1} . Since C_{i-1} and C_{i+1} are homotopic, the path Q_{i+1} is entering C_{i-1} at least once from its right side. This is in contradiction with (T1). \square

The sector $[e_1, e_2]$ of a vertex w , for e_1 and e_2 two edges incident to w , is the counterclockwise sector of w between e_1 and e_2 , including the edges e_1 and e_2 . The sectors $]e_1, e_2]$, $[e_1, e_2[$, and $]e_1, e_2[$ are defined analogously by excluding the corresponding edges from the sectors.

Lemma 16 *Let G be a toroidal map given with a Schnyder wood and let w, x, y be three vertices such that $e_{i-1}(x)$ and $e_{i+1}(y)$ are entering w . Suppose that there is a directed path Q_{i-1} of color $i - 1$ from y to w , entering w in the sector $[e_i(w), e_{i-1}(x)]$, and a directed path Q_{i+1} of color $i + 1$ from x to w , entering w in the sector $[e_{i+1}(y), e_i(w)]$. Consider the two directed cycles $C_{i-1} = Q_{i-1} \cup \{e_{i+1}(y)\}^{-1}$ and $C_{i+1} = Q_{i+1} \cup \{e_{i-1}(x)\}^{-1}$. Then either C_{i-1} and C_{i+1} are not homotopic or $C_{i-1} = C_{i+1}^{-1}$.*

Proof By Lemma 1, the cycles C_{i-1} and C_{i+1} are not contractible. Suppose that C_{i-1} and C_{i+1} are homotopic and that $C_{i-1} \neq C_{i+1}^{-1}$. Since $C_{i-1} \neq C_{i+1}^{-1}$, the cycle C_{i+1} is leaving C_{i-1} . By (T1) and the assumption on the sectors, C_{i+1} is leaving C_{i-1} on its right side. Since C_{i-1} and C_{i+1} are homotopic, the path Q_{i+1} is entering C_{i-1} at least once from its right side. This is in contradiction with (T1). \square

We are now able to prove Lemma 14.

Proof of Lemma 14 Let u, v be the two extremities of e . Vertices u and v are of degree at least three. Let x, y (resp. z, t) be the neighbors of u (resp. v) such that x, v, y (resp. z, u, t) appear consecutively and in counterclockwise order around u (resp. v) (see Fig. 20(c)). Note that u and v are distinct by the definition of edge contraction, but that x, y, z, t are not necessarily distinct, nor necessarily distinct from u and v . Depending on whether the faces incident to e are triangles or not, we are, by symmetry, in one of the three cases of Fig. 20(a, b, c). Let $G' = G/e$ and consider a Schnyder wood of Type 1 of G' . Let w be the vertex of G' resulting from the contraction of e .

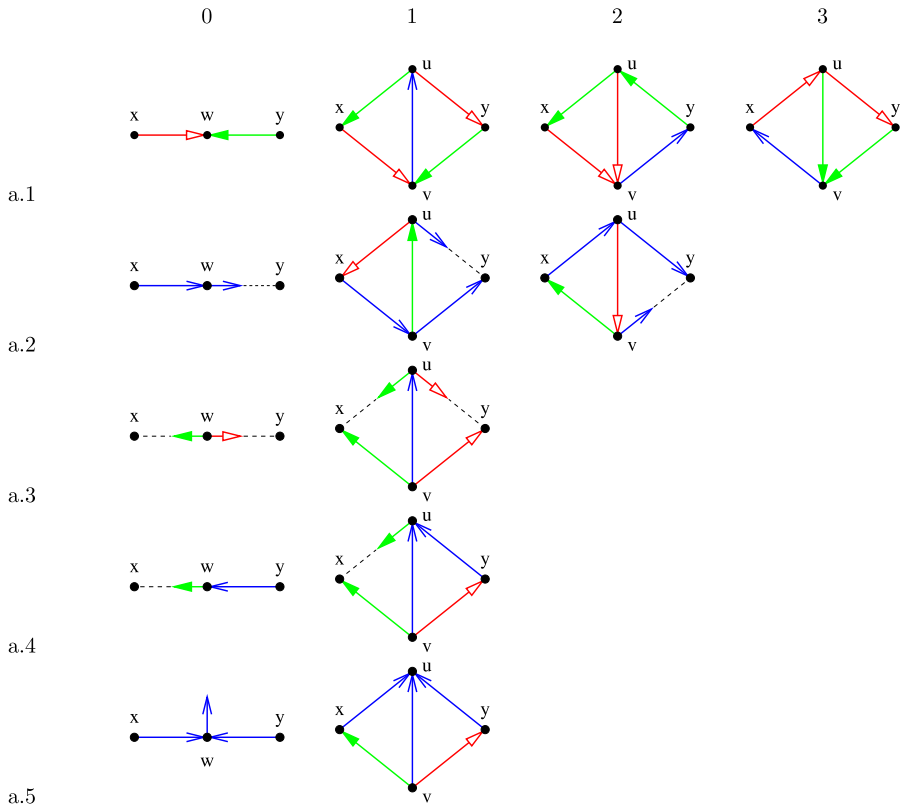


Fig. 21 Decontraction rules for case (a)

For each case (a), (b), (c), there are different cases corresponding to the different possibilities of orientation and coloring of the edges $e_{wx}, e_{wy}, e_{wz}, e_{wt}$ in G' . For example, for case (a), there should be 6 cases depending on if e_{wx} and e_{wy} are both entering w , both leaving w , or one entering w and one leaving w (3 cases), multiplied by the coloring, both of the same or not (2 cases). The case where w has two edges leaving in the same color is impossible by (T1). So, by symmetry, only 5 cases remain represented by figures $a.k.0$, for $k = 1, \dots, 5$, on Fig. 21 (in the notation $\alpha.k.l$, $\alpha.k$ indicates the line on the figures and l the column). For cases (b) and (c), there are more cases to consider, but the analysis is similar. These cases are represented in the first columns of Figs. 22 and 23. On these figures, a dotted half-edge represents the possibility for an edge to be unidirected or bidirected. In the last case of each figure, we have indicated where the edge is leaving in color 1, as there are two possibilities (up or down).

In each case $\alpha.k$, $\alpha \in \{a, b, c\}$, we show how one can color and orient the edges of G to obtain a Schnyder wood of G from the Schnyder wood of G' . Only the edges $e, e_{ux}, e_{uy}, e_{vt}, e_{vz}$ of G have to be specified; all the other edges of G keep the orientation and coloring of their corresponding edge in G' . In each case $\alpha.k$, there might be several possibilities for coloring and orienting these edges to satisfy (T1). Only

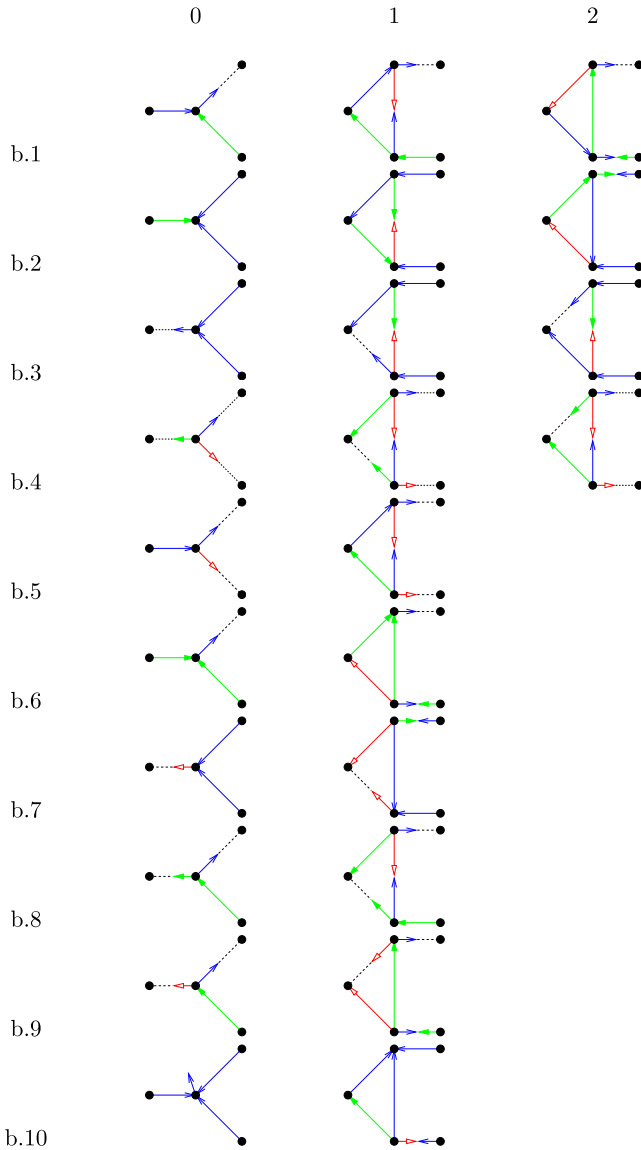


Fig. 22 Decontraction rules for case (b)

some of these possibilities, the ones that are useful for our purpose, are represented on figures $\alpha.k.\ell$, $\ell \geq 1$, of Figs. 21 through 23. A dotted half-edge represents the fact that the edge is unidirected or bidirected like the corresponding half-edge of G' .

In each case $\alpha.k$, $\alpha \in \{a, b, c\}$, we show that one of the colorings $\alpha.k.\ell$, $\ell \geq 1$, gives a Schnyder wood of Type 1 of G . By Lemma 12, we just have to prove that, in each case $\alpha.k$, there is one coloring satisfying (T1'), (T2'), and (T3'). Properties

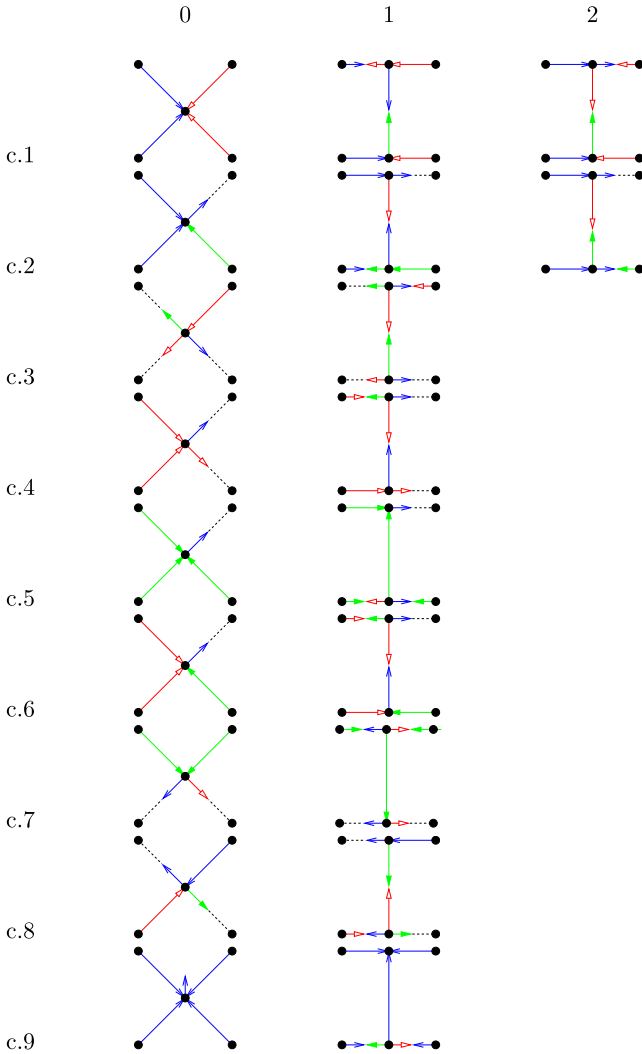


Fig. 23 Decontraction rules for case (c)

(T1') and (T3') are satisfied for any colorings $\alpha.k.\ell$, $\ell \geq 1$, but this is not the case for property (T2'). This explains why several possible colorings of G must be considered.

(T1') One can easily check that in all the cases $\alpha.k.\ell$, property (T1') is satisfied for every vertex of G . To do so one can consider the angle labeling around vertices $w, x, y, (z), (t)$ of G' in the case $\alpha.k.0$. Then one can see that this angle labeling exports well around vertices $u, v, x, y, (z), (t)$ of G and thus the Schnyder property is satisfied for these vertices. On Fig. 24, an example is given on how the angle labeling is modified during the decontraction process. It corresponds to case $c.2.1$ where the dotted half-edge is unidirected. We do not discuss this part in more detail, as it is easy to check.

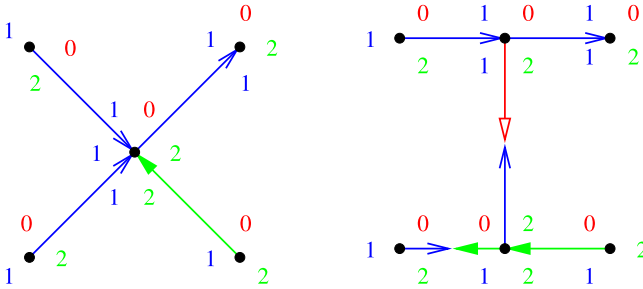


Fig. 24 Example of (T1') preservation during decontraction

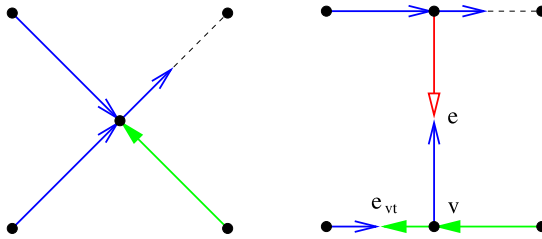


Fig. 25 Example of (T3') preservation during decontraction

(T3') One can easily check that in all the cases $\alpha.k.l$, property (T3') is satisfied for G . If (T3') is not satisfied in G after applying one of the colorings $\alpha.k.l$, then there exist two monochromatic cycles C, C' of different colors that are reversal. By property (T3') of Lemma 12, there are no reversal cycles in G' . Thus C, C' have to use a bidirected edge e' of the figures that is newly created and distinct from edge e and distinct from the half-dotted edges (otherwise the cycles are still reversal when e is contracted). Only some cases have such an edge, and one can note that, for all these cases, the cycle, after entering u or v by edge e' , must use the edge e that is either unidirected or bidirected with different colors than e' , a contradiction. For example, in case $c.2.1$ of Fig. 25, two reversal cycles of G that do not correspond to reversal cycles when e is contracted, have to use edge e_{vt} . Then one of the two cycles is entering v by e_{vt} in color 1 and thus has to continue by using the only edge leaving v in color 1, edge e . As e and e_{vt} are colored differently, this is not possible. We do not further detail this part, which is easy to check.

(T2') Proving property (T2') is the main difficulty of the proof. For each case $\alpha.k$, there is a case analysis considering the different ways in which the monochromatic cycles of G' go through w or not. We say that a monochromatic cycle C of G' is *safe* if C does not contain w . Depending on whether there are safe monochromatic cycles or not for each color, there may be a different case $\alpha.k.l$ and a different argument that is used to prove that property (T2') is preserved.

- *Case a.1: e_{wx} and e_{wy} are entering w in different colors.*

We can assume by symmetry that $e_{wx} = e_0(x)$ and $e_{wy} = e_2(y)$ (case a.1.0 of Fig. 21). We apply one of the colorings a.1.1, a.1.2, and a.1.3 of Fig. 21.

We have a case analysis corresponding to whether there are monochromatic cycles of G' that are safe.

★ *Subcase a.1.*{0, 1, 2}: *There are safe monochromatic cycles of colors {0, 1, 2}.*

Let C'_0, C'_1, C'_2 be safe monochromatic cycles of color 0, 1, 2 in G' . As the Schnyder wood of G' is of Type 1, they pairwise intersect in G' . Apply the coloring a.1.1 on G . As C'_0, C'_1, C'_2 do not contain vertex w , they are not modified in G . Thus, they still pairwise intersect in G . So (T2') is satisfied.

★ *Subcase a.1.*{0, 2}: *There are safe monochromatic cycles of colors exactly {0, 2}.*

Let C'_0, C'_2 be safe monochromatic cycles of color 0, 2 in G' . Let C'_1 be a 1-cycle in G' . As the Schnyder wood of G' is of Type 1, C'_0, C'_1, C'_2 pairwise intersect in G' . None of those intersections contains w as C'_0 and C'_2 do not contain w . By (T1), the cycle C'_1 enters w in the sector $]e_{wx}, e_{wy}[$ and leaves in the sector $]e_{wy}, e_{wx}[$. Apply the coloring a.1.1 on G . The cycle C'_1 is replaced by a new cycle $C_1 = C'_1 \setminus \{w\} \cup \{u, v\}$. The cycles C'_0, C'_1, C'_2 were intersecting outside w in G' so C'_0, C_1, C'_2 are intersecting in G . So (T2') is satisfied.

★ *Subcase a.1.*{1, 2}: *There are safe monochromatic cycles of colors exactly {1, 2}.*

Let C'_1, C'_2 be safe monochromatic cycles of color 1, 2 in G' . Let C'_0 be a 0-cycle in G' . The cycles C'_0, C'_1, C'_2 pairwise intersect outside w . The cycle C'_0 enters w in the sector $[e_1(w), e_{wx}[$, $[e_{wx}, e_{wx}]$, or $]e_{wx}, e_2(w)[$. Apply the coloring a.1.2 on G . Depending on which of the three sectors C'_0 enters, it is replaced by one of the three following cycles: $C_0 = C'_0 \setminus \{w\} \cup \{u, v\}$, $C_0 = C'_0 \setminus \{w\} \cup \{x, v\}$, $C_0 = C'_0 \setminus \{w\} \cup \{v\}$. In any of the three possibilities, C_0, C'_1, C'_2 are intersecting in G . So (T2') is satisfied.

★ *Subcase a.1.*{0, 1}: *There are safe monochromatic cycles of colors exactly {0, 1}.*

This case is completely symmetric to the case a.1.{1, 2}.

★ *Subcase a.1.*{2}: *There are safe monochromatic cycles of color 2 only.*

Let C'_2 be a safe 2-cycle in G' . Let C'_0, C'_1 be monochromatic cycles of color 0, 1 in G' .

Suppose that there exists a path Q'_0 of color 0 from y to w such that this path does not intersect C'_2 . Suppose also that there exists a path Q'_1 of color 1 from y to w such that this path does not intersect C'_2 . Let $C''_0 = Q'_0 \cup \{e_{wy}\}$ and $C''_1 = Q'_1 \cup \{e_{wy}\}$. By Lemma 1, C''_0, C''_1, C'_2 are not contractible. Both C''_0, C''_1 do not intersect C'_2 , so by Lemma 2, they are both homotopic to C'_2 . Thus, cycles C''_0, C''_1 are homotopic to each other, contradicting Lemma 15 (with $i = 2, w, y, Q'_0, Q'_1$). So we can assume that one of Q'_0 or Q'_1 as above does not exist.

Suppose that in G' , there does not exist a path of color 0 from y to w such that this path does not intersect C'_2 . Apply the coloring a.1.1 on G . Cycle C'_1 is replaced by $C_1 = C'_1 \setminus \{w\} \cup \{u, v\}$, and intersects C'_2 . Let C_0 be a 0-cycle of G . Cycle C_0 has to contain u or v or both, otherwise it is a safe cycle of G' of color 0. In any case it intersects C_1 . If C_0 contains v , then $C'_0 = C_0 \setminus \{v\} \cup \{w\}$, and so C_0 is intersecting C'_2 and (T2') is satisfied. Suppose now that C_0 does not contain v . Then C_0 contains u and y , the extremity of the edge leaving u in color 0. Let Q_0 be the part of C_0 consisting of the path from y to u . The path $Q'_0 = Q_0 \setminus \{u\} \cup \{w\}$ is from y to w . Thus, by assumption, Q'_0 intersects C'_2 . So C_0 intersects C'_2 and (T2') is satisfied.

Suppose now that in G' , there does not exist a path of color 1 from y to w such that this path does not intersect C'_2 . Apply the coloring a.1.2 on G . Depending on which of the three sectors C'_0 enters, $[e_1(w), e_{wx}[$, $[e_{wx}, e_{wx}]$, or $]e_{wx}, e_2(w)[$, it is replaced

by one of the following three cycles: $C_0 = C'_0 \setminus \{w\} \cup \{u, v\}$, $C_0 = C'_0 \setminus \{w\} \cup \{x, v\}$, $C_0 = C'_0 \setminus \{w\} \cup \{v\}$. In any of the three possibilities, C_0 contains v and intersects C'_2 . Let C_1 be a 1-cycle of G . Cycle C_1 has to contain u or v or both, otherwise it is a safe cycle of G' of color 1. Vertex u has no edge entering it in color 1, so C_1 does not contain u and thus it contains v and intersects C_0 . Then C_1 contains y , the extremity of the edge leaving v in color 1. Let Q_1 be the part of C_1 consisting of the path from y to v . The path $Q'_1 = Q_1 \setminus \{v\} \cup \{w\}$ is from y to w . Thus, by assumption, Q'_1 intersects C'_2 . So C_1 intersects C'_2 and (T2') is satisfied.

★ *Subcase a.1.{0}: There are safe monochromatic cycles of color 0 only.*

This case is completely symmetric to the case a.1.{2}.

★ *Subcase a.1.{1}: There are safe monochromatic cycles of color 1 only.*

Let C'_1 be a safe 1-cycle in G' . Let C'_0 and C'_2 be monochromatic cycles of color 0 and 2 in G' .

Suppose C'_0 is entering w in the sector $]e_{wx}, e_2(w)[$. Apply the coloring a.1.3 on G . The 0-cycle C'_0 is replaced by $C_0 = C'_0 \setminus \{w\} \cup \{v\}$ and thus contains v and still intersects C'_1 . Depending on which of the three sectors C'_2 enters, $[e_0(w), e_{wy}[$, $[e_{wy}, e_{wy}]$, or $]e_{wy}, e_1(w)[$, it is replaced by one of the following three cycles: $C_2 = C'_2 \setminus \{w\} \cup \{v\}$, $C_2 = C'_2 \setminus \{w\} \cup \{y, v\}$, $C_2 = C'_2 \setminus \{w\} \cup \{u, v\}$. In any case, C_2 contains v and still intersects C'_1 . Cycle C_0 and C_2 intersect on v . So (T2') is satisfied.

The case where C'_2 is entering w in the sector $[e_0(w), e_{wy}[$ is completely symmetric and we apply the coloring a.1.2 on G .

It remains to deal with the case where C'_0 is entering w in the sector $[e_1(w), e_{wx}]$ and C'_2 is entering w in the sector $[e_{wy}, e_1(w)]$. Suppose that there exists a path Q'_0 of color 0, from y to w , entering w in the sector $[e_1(w), e_{wx}]$, such that this path does not intersect C'_1 . Suppose also that there exists a path Q'_2 of color 2, from x to w , entering w in the sector $[e_{wy}, e_1(w)]$, such that this path does not intersect C'_1 . Let $C''_0 = Q'_0 \cup \{e_{wy}\}$ and $C''_2 = Q'_2 \cup \{e_{wx}\}$. By Lemma 1, C''_0, C'_1, C''_2 are not contractible. Cycles C''_0, C''_2 do not intersect C'_1 , so by Lemma 2 they are homotopic to C'_1 . Thus, cycles C''_0, C''_2 are homotopic to each other. Thus, by Lemma 16 (with $i = 1, w, x, y, Q'_0, Q'_2$), we have $C''_0 = (C''_2)^{-1}$, contradicting (T3') in G' . So we can assume that one of Q'_0 or Q'_2 as above does not exist. By symmetry, suppose that in G' there does not exist a path of color 0, from y to w , entering w in the sector $[e_1(w), e_{wx}]$, such that this path does not intersect C'_1 . Apply the coloring a.1.3 on G . Depending on which of the two sectors C'_2 enters, $[e_{wy}, e_{wy}]$ or $]e_{wy}, e_1(w)[$, it is replaced by one of the following two cycles: $C_2 = C'_2 \setminus \{w\} \cup \{y, v\}$, $C_2 = C'_2 \setminus \{w\} \cup \{u, v\}$. In any case, C_2 still intersects C'_1 . Let C_0 be a 0-cycle of G . Cycle C_0 has to contain u or v or both, otherwise it is a safe cycle of G' of color 0. Suppose C_0 does not contain u ; then $C'_0 = C_0 \setminus \{v\} \cup \{w\}$ and C'_0 is not entering w in the sector $[e_1(w), e_{wx}]$, a contradiction. So C_0 contains u . Thus, C_0 contains y , the extremity of the edge leaving u in color 0, and it intersects C_2 . Let Q_0 be the part of C_0 consisting of the path from y to u . The path $Q'_0 = Q_0 \setminus \{u\} \cup \{w\}$ is from y to w and entering w in the sector $[e_1(w), e_{wx}]$. Thus, by assumption, Q'_0 intersects C'_1 . So C_0 intersects C'_1 and (T2') is satisfied.

★ *Subcase a.1.{1}: There are no safe monochromatic cycles.*

Let C'_0, C'_1, C'_2 be monochromatic cycles of color 0, 1, 2 in G' . They all pairwise intersect on w .

Suppose first that C'_0 is entering w in the sector $]e_{wx}, e_2(w)[$. Apply the coloring a.1.3 on G . The 0-cycle C'_0 is replaced by $C_0 = C'_0 \setminus \{w\} \cup \{v\}$ and thus contains v . Depending on which of the three sectors C'_2 enters, $[e_0(w), e_{wy}[$, $[e_{wy}, e_{wy}]$, or $]e_{wy}, e_1(w)[$, it is replaced by one of the following three cycles: $C_2 = C'_2 \setminus \{w\} \cup \{v\}$, $C_2 = C'_2 \setminus \{w\} \cup \{y, v\}$, $C_2 = C'_2 \setminus \{w\} \cup \{u, v\}$. In any case, C_2 contains v . Let C_1 be a 1-cycle in G . Cycle C_1 has to contain u or v or both, otherwise it is a safe cycle of G' of color 1. Vertex u has no edge entering it in color 1, so C_1 does not contain u and thus it contains v . So C_0, C_1, C_2 all intersect on v and (T2') is satisfied.

The case where C'_2 is entering w in the sector $[e_0(w), e_{wy}[$ is completely symmetric and we apply the coloring a.1.2 on G .

It remains to deal with the case where C'_0 is entering w in the sector $[e_1(w), e_{wx}]$ and C'_2 is entering w in the sector $[e_{wy}, e_1(w)[$. Apply the coloring a.1.1 on G . Cycle C'_1 is replaced by $C_1 = C'_1 \setminus \{w\} \cup \{u, v\}$. Let C_0 be a 0-cycle in G . Cycle C_0 has to contain u or v or both, otherwise it is a safe cycle of G' of color 0. Suppose $C_0 \cap \{v, x\} = \{v\}$; then $C_0 \setminus \{v\} \cup \{w\}$ is a 0-cycle of G' entering w in the sector $]e_{wx}, e_2(w)[$, contradicting the assumption on C'_0 . Suppose C_0 contains u ; then C_0 contains y , the extremity of the edge leaving u in color 0. So C_0 contains $\{v, x\}$ or $\{u, y\}$. Similarly, C_2 contains $\{v, y\}$ or $\{u, x\}$. In any case, C_0, C_1, C_2 pairwise intersect. So (T2') is satisfied.

• *Case a.2: e_{wx} and e_{wy} have the same color; one is entering w , the other is leaving w .*

We can assume by symmetry that $e_{wx} = e_1(x)$ and $e_{wy} = e_1(w)$ (case a.2.0 of Fig. 21). We apply one of the colorings a.2.1 and a.2.2 of Fig. 21.

We have a case analysis corresponding to whether there are monochromatic cycles of G' that are safe.

★ *Subcase a.2.{0, 1, 2}: There are safe monochromatic cycles of colors {0, 1, 2}.*

Let C'_0, C'_1, C'_2 be safe monochromatic cycles of color 0, 1, 2 in G' . They pairwise intersect in G' . Apply the coloring a.2.1 on G . C'_0, C'_1, C'_2 still pairwise intersect in G . So (T2') is satisfied.

★ *Subcase a.2.{0, 2}: There are safe monochromatic cycles of colors exactly {0, 2}.*

Let C'_0, C'_2 be safe monochromatic cycles of color 0, 2 in G' . Let C'_1 be a 1-cycle in G' . Cycles C'_0, C'_2 still intersect in G . Apply the coloring a.2.1 on G . Depending on which of the three sectors C'_1 enters, $[e_2(w), e_{wx}[$, $[e_{wx}, e_{wx}]$, or $]e_{wx}, e_0(w)[$, it is replaced by one of the following three cycles: $C_1 = C'_1 \setminus \{w\} \cup \{u, y\}$, $C_1 = C'_1 \setminus \{w\} \cup \{x, v, y\}$, $C_1 = C'_1 \setminus \{w\} \cup \{v, y\}$. In any of the three possibilities, C_1 still intersects both C'_0, C'_2 . So (T2') is satisfied.

★ *Subcase a.2.{1, 2}: There are safe monochromatic cycles of colors exactly {1, 2}.*

Let C'_1, C'_2 be safe monochromatic cycles of color 1, 2 in G' . Let C'_0 be a 0-cycle in G' . Cycles C'_1, C'_2 still intersect in G . Apply the coloring a.2.2 on G . Depending on which of the two sectors C'_0 enters, $[e_{wy}, e_{wy}]$ or $]e_{wy}, e_2(w)[$, it is replaced by one of the following two cycles: $C_0 = C'_0 \setminus \{w\} \cup \{y, v\}$, $C_0 = C'_0 \setminus \{w\} \cup \{u, v\}$. In either of the two possibilities, C_0 still intersects both C'_1, C'_2 . So (T2') is satisfied.

★ *Subcase a.2.{0, 1}: There are safe monochromatic cycles of colors exactly {0, 1}.*

This case is completely symmetric to the case a.2.{1, 2}.

★ *Subcase a.2.{2}: There are safe monochromatic cycles of color 2 only.*

Let C'_2 be a safe 2-cycle in G' . Let C'_0, C'_1 be monochromatic cycles of color 0, 1 in G' .

Apply the coloring a.2.2 on G . Depending on which of the three sectors C'_1 enters, $[e_2(w), e_{wx}]$, $[e_{wx}, e_{wy}]$, or $]e_{wx}, e_0(w)[$, it is replaced by one of the following three cycles: $C_1 = C'_1 \setminus \{w\} \cup \{u, y\}$, $C_1 = C'_1 \setminus \{w\} \cup \{x, u, y\}$, $C_1 = C'_1 \setminus \{w\} \cup \{v, y\}$. Depending on which of the two sectors C'_0 enters, $[e_{wy}, e_{wy}]$ or $]e_{wy}, e_2(w)[$, it is replaced by one of the following two cycles: $C_0 = C'_0 \setminus \{w\} \cup \{y, v\}$, $C_0 = C'_0 \setminus \{w\} \cup \{u, v\}$. In any case, C_0 and C_1 intersect each other and intersect C'_2 . So $(T2')$ is satisfied.

★ *Subcase a.2.{0}: There are safe monochromatic cycles of color 0 only.*

This case is completely symmetric to the case a.2.{0}.

★ *Subcase a.2.{1}: There are safe monochromatic cycles of color 1 only.*

Let C'_1 be a safe 1-cycle in G' . Let C'_0, C'_2 be monochromatic cycles of color 0, 2 in G' . Suppose that there exists a path Q'_0 of color 0, from x to w , that does not intersect C'_1 . Suppose also that there exists a path Q'_2 of color 2, from x to w , that does not intersect C'_1 . Let $C''_0 = Q'_0 \cup \{e_{wx}\}$ and $C''_2 = Q'_2 \cup \{e_{wx}\}$. By Lemma 1, C''_0, C'_1, C''_2 are not contractible. Both of C''_0, C''_2 do not intersect C'_1 , so by Lemma 2, they are both homotopic to C'_1 . Thus, cycles C''_0, C''_2 are homotopic to each other, contradicting Lemma 15 (with $i = 1, w, x, Q'_0, Q'_2$). So we can assume that one of Q'_0 or Q'_2 as above does not exist.

By symmetry, suppose that in G' there does not exist a path of color 0, from x to w , that does not intersect C'_1 . Apply the coloring a.2.1 on G . Depending on which of the two sectors C'_2 enters, $[e_1(w), e_{wy}]$, $[e_{wy}, e_{wy}]$, it is replaced by one of the following two cycles: $C_2 = C'_2 \setminus \{w\} \cup \{v, u\}$, $C_2 = C'_2 \setminus \{w\} \cup \{y, u\}$. In either of the two possibilities C_2 intersects C'_1 . Let C_0 be a 0-cycle of G . Cycle C_0 has to contain u or v or both, otherwise it is a safe cycle of G' of color 0. Vertex v has no edge entering it in color 0, so C_0 does not contain v and so it contains u and x , the extremity of the edge leaving u in color 0. Thus, C_0 intersects C_2 . Let Q_0 be the part of C_0 consisting of the path from x to u . The path $Q'_0 = Q_0 \setminus \{u\} \cup \{w\}$ of G' is from x to w , and thus by assumption Q'_0 intersects C'_1 . So C_0 intersects C'_1 and $(T2')$ is satisfied.

★ *Subcase a.2.{}: There are no safe monochromatic cycles.*

Let C'_0, C'_1, C'_2 be monochromatic cycles of color 0, 1, 2 in G' .

Suppose C'_1 is entering w in the sector $[e_2(w), e_{wx}]$. Apply the coloring a.2.1 on G . Cycle C'_1 is replaced by $C_1 = C'_1 \setminus \{w\} \cup \{u, y\}$ or $C_1 = C'_1 \setminus \{w\} \cup \{x, v, y\}$. Cycle C'_0 is replaced by $C_0 = C'_0 \setminus \{w\} \cup \{u, x\}$ or $C_0 = C'_0 \setminus \{w\} \cup \{y, u, x\}$. Cycle C'_2 is replaced by $C_2 = C'_2 \setminus \{w\} \cup \{v, u\}$ or $C_2 = C'_2 \setminus \{w\} \cup \{y, u\}$. So C_0, C_1, C_2 all intersect each other and $(T2')$ is satisfied.

The case where C'_1 is entering w in the sector $[e_{wx}, e_0(w)]$ is completely symmetric, and we apply the coloring a.2.2 on G .

● *Cases a.3, a.4, a.5:*

The proof is simpler for the remaining cases (cases a.3.0, a.4.0, a.5.0 on Fig. 21). For each situation, there is only one way to extend the coloring to G in order to preserve $(T1')$ and this coloring also preserves $(T2')$. Indeed, in each coloring of G , for cases a.3.1, a.4.1, a.5.1 on Fig. 21, one can check that every non-safe monochromatic cycle C' is replaced by a cycle C with $C' \setminus \{w\} \cup \{u\} \subseteq C$. Thus, all non-safe cycles intersect on u and a non-safe cycle of color i intersects all safe cycles of colors $i - 1$ and $i + 1$. So $(T2')$ is always satisfied.

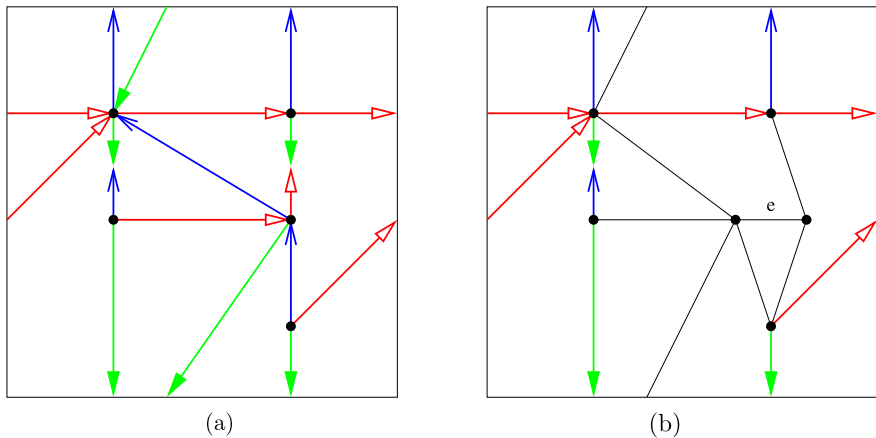


Fig. 26 (a) The graph obtained by contracting the edge e of the graph (b). It is not possible to color and orient the black edges of (b) to obtain a Schnyder wood

It remains to analyze the situation for the decontraction cases (b) and (c). The colorings that are needed are represented on Figs. 22 and 23. The proofs are similar to those for case (a) and we omit them. \square

Note that we are not able to prove a lemma analogous to Lemma 14 for Type 2 Schnyder woods. In the example of Fig. 26, it is not possible to decontract the graph G' (Fig. 26(a)) and extend its Schnyder wood to G (Fig. 26(b)) without modifying the edges that are not incident to the contracted edge e . Indeed, if we keep the edges non-incident to e unchanged, there are only two possible ways to extend the coloring in order to preserve (T1), but none of them fulfills (T2).

9 Existence for Essentially 3-Connected Toroidal Maps

We are given a map G embedded on a surface. The *angle map* [22] of G is a map $A(G)$ on this surface whose vertices are the vertices of G plus the vertices of G^* (i.e., the faces of G), and whose edges are the angles of G , each angle being incident with the corresponding vertex and face of G . Note that if G contains no homotopic multiple edges, then every face of G has degree at least three in $A(G)$.

Mohar and Rosenstiehl [23] proved that a map G is essentially 2-connected if and only if the angle map A of G has no pair of (multiple) edges bounding a disk (i.e., no walk of length 2 bounding a disk). As every face in an angle map is a quadrangle, such a disk contains some vertices of G . The following claim naturally extends this characterization to essentially 3-connected toroidal maps.

Lemma 17 *A toroidal map G is essentially 3-connected if and only if the angle map $A(G)$ has no walk of length at most 4 bounding a disk which is not a face.*

Proof In G^∞ any minimal separator of size 1 or 2, $S = \{v_1\}$ or $S = \{v_1, v_2\}$, corresponds to a separating cycle of length 2 or 4 in $A(G^\infty)$, $C = (v_1, f_1)$ or $C = (v_1, f_1, v_2, f_2)$, i.e., a cycle of length at most 4 bounding a disk D which is not a face.

(\implies) Any walk in $A(G)$ of length at most 4 bounding a disk which is not a face lifts to a cycle of length at most 4 bounding a disk which is not a face in $A(G^\infty)$. Thus, such a walk implies the existence of a small separator in G^∞ , contradicting its 3-connectedness.

(\impliedby) According to [23], if G is essentially 2-connected, $A(G)$ has no walk of length 2 bounding a disk. Let us now show that if G is essentially 2-connected but not essentially 3-connected, $A(G)$ has a walk of length 4 bounding a disk which is not a face.

If G is essentially 2-connected but not essentially 3-connected, then $A(G^\infty)$ has a cycle C of length 4 bounding a disk which is not a face, and this cycle corresponds to a contractible walk W of length 4 in $A(G)$. Since W is contractible, it contains a subwalk bounding a disk. $A(G)$ being bipartite, this subwalk has even length, and since $A(G)$ is essentially 2-connected, it has no such walk of length 2. Thus, W bounds a disk. Finally, this disk is not a single face, since otherwise C would bound a single face in $A(G^\infty)$. \square

A non-loop edge e of an essentially 3-connected toroidal map is *contractible* if the contraction of e keeps the map essentially 3-connected. We have the following lemma.

Lemma 18 *An essentially 3-connected toroidal map that is not reduced to a single vertex has a contractible edge.*

Proof Let G be an essentially 3-connected toroidal map with at least 2 vertices. Note that for any non-loop e , the map $A(G/e)$ has no walk of length 2 bounding a disk which is not a face; otherwise, $A(G)$ contains a walk of length at most 4 bounding a disk which is not a face and thus, by Lemma 17, G is not essentially 3-connected.

Suppose by contradiction that contracting any non-loop edge e of G yields a non-essentially 3-connected map G/e . By Lemma 17, it means that the angle map $A(G)$ has no walk of length at most 4 bounding a disk which is not a face. For any non-loop e , let $W_4(e)$ be the 4-walk of $A(G/e)$ bounding a disk, which is maximal in terms of the faces it contains. Among all the non-loop edges, let e be the one such that the number of faces in $W_4(e)$ is minimum. Let $W_4(e) = (v_1, f_1, v_2, f_2)$ and assume that the endpoints of e , say a and b , are contracted into v_2 (see Fig. 27(a)). Note that, by maximality of $W_4(e)$, v_1 and v_2 do not have any common neighbor f out of $W_4(e)$, such that (v_1, f, v_2, f_1) bounds a disk.

Assume one of f_1 or f_2 has a neighbor inside $W_4(e)$. By symmetry, assume v_3 is a vertex inside $W_4(e)$ such that there is a face $F = (v_1, f_1, v_3, f_w)$ in $A(G/e)$, with eventually $f_w = f_2$. Consider now the contraction of the edge v_1v_3 . Let $P(v_1, v_3) = (v_1, f_x, v_y, f_z, v_3)$ be the path from v_1 to v_3 corresponding to $W_4(v_1v_3)$ and $P(a, b) = (a, f_2, v_1, f_1, b)$ the path corresponding to $W_4(e)$. Suppose that $f_z = f_2$; then (v_1, f_2, v_3, f_w) bounds a face by Lemma 17 and f_w has degree two in $A(G)$, a contradiction. So $f_z \neq f_2$.

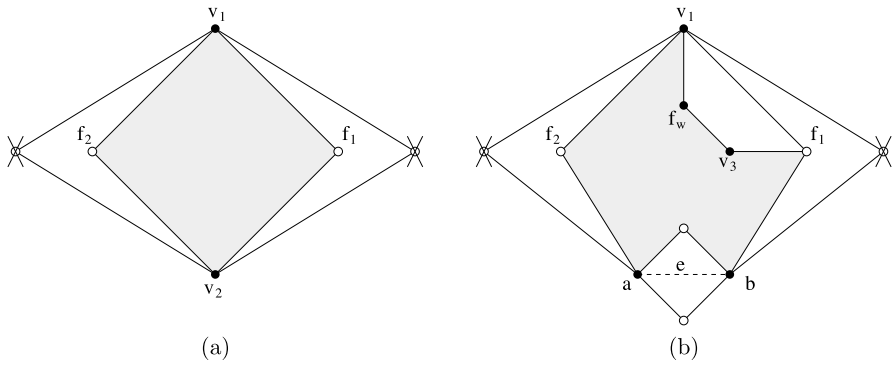
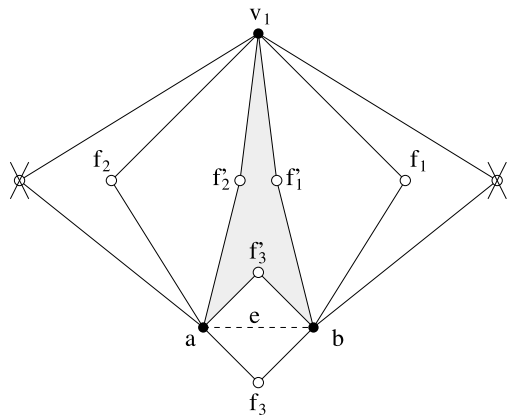


Fig. 27 Notation of the proof of Lemma 18

Fig. 28 Notation of the proof of Lemma 18



Suppose that all the faces of $W_4(v_1v_3)$ are in $W_4(e)$. Then with F , $W_4(e)$ contains more faces than $W_4(v_1v_3)$, a contradiction to the choice of e . So in $A(G)$, $P(v_1, v_3)$ must cross the path $P(a, b)$. Then v_y or f_z must intersect $P(a, b)$. Suppose $f_z \neq f_1$. Then $v_y = a$ or b . In this case, (v_1, f_x, v_2, f_1) bounds a disk, a contradiction. Thus, $f_z = f_1$ and the cycle (v_1, f_x, v_y, f_1) bounds a face by Lemma 17. This implies that $W_4(v_1v_3)$ bounds a face, a contradiction.

Assume now that neither f_1 nor f_2 has a neighbor inside $W_4(e)$. Let f'_1, f'_2, f_3 , and f'_3 be vertices of $A(G)$ such that (v_1, f_1, b, f'_1) , (v_1, f_2, a, f'_2) , and (a, f_3, b, f'_3) are faces (see Fig. 28). Suppose $f'_1 = f'_2 = f'_3$. Then in $A(G/e)$, the face f'_1 is deleted (of the two homotopic multiple edges between v_1, v_2 that are created, only one is kept in G/e). Then $W_4(e)$ bounds a face, a contradiction. Thus, there exists some i such that $f'_i \neq f'_{i+1}$. Assume that $i = 1$ (resp. $i = 2$ or 3), and let v_3 and f'' be such that there is a face (v_1, f'_1, v_3, f'') in $A(G)$ (resp. (a, f'_2, v_3, f'') or (b, f'_3, v_3, f'')). As above, considering the contraction of the edge v_1v_3 (resp. av_3 or bv_3) yields a contradiction. \square

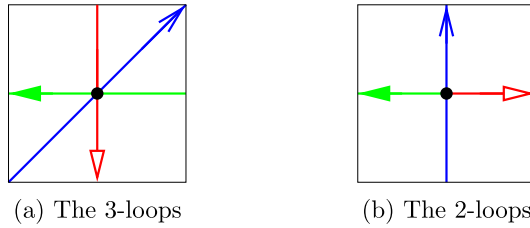


Fig. 29 The two essentially 3-connected toroidal maps on one vertex

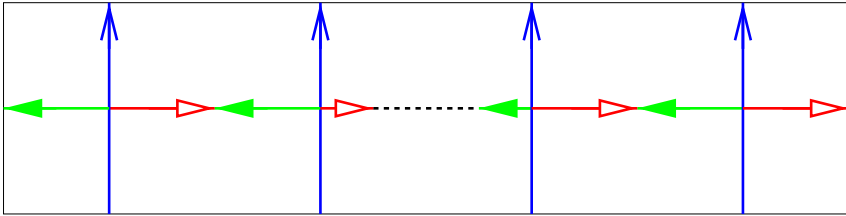
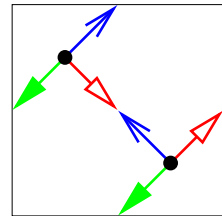


Fig. 30 The family of basic toroidal maps, having only Schnyder woods of Type 2

Fig. 31 The brick, an essentially 3-connected toroidal map with two vertices



Lemma 18 shows that an essentially 3-connected toroidal map can be contracted step by step by keeping it essentially 3-connected until a map with just one vertex is obtained. The two essentially 3-connected toroidal maps on one vertex are represented on Fig. 29 with a Schnyder wood. The graph of Fig. 29(a), the *3-loops*, admits a Schnyder wood of Type 1, and the graph of Fig. 29(b), the *2-loops*, admits a Schnyder wood of Type 2.

It would be convenient if one could contract any essentially 3-connected toroidal map to obtain one of the two graphs of Fig. 29 and then decontract the graph to obtain a Schnyder wood of the original graph. Unfortunately, for Type 2 Schnyder woods we are not able to prove that property (T2) can be preserved during the decontraction process (see Sect. 8). Fortunately, most essentially 3-connected toroidal maps admit Schnyder woods of Type 1. A toroidal map is *basic* if it consists of a non-contractible cycle on n vertices, $n \geq 1$, plus n homotopic loops (see Fig. 30). We prove in this section that non-basic essentially 3-connected toroidal maps admit Schnyder woods of Type 1. For this purpose, instead of contracting these maps to one of the two graphs of Fig. 29, we contract them to the graph of Fig. 29(a) or to the graph of Fig. 31, *the brick*. (One can draw the universal cover of the brick to understand its name.)

Lemma 19 *A non-basic essentially 3-connected toroidal map can be contracted to the 3-loops (Fig. 29(a)) or to the brick (Fig. 31).*

Proof Let us prove the lemma by induction on the number of edges of the map. As the 3-loop and the brick are the only non-basic essentially 3-connected toroidal maps with at most 3 edges, the lemma holds for the maps with at most 3 edges. Consider now a non-basic essentially 3-connected toroidal map G with at least 4 edges. As G has at least 2 vertices, it has at least one contractible edge by Lemma 18. If G has a contractible edge e whose contraction yields a non-basic map G' , then by the induction hypothesis on G' we are done. Let us prove that such an edge always exists. We assume, by contradiction, that the contraction of any contractible edge e yields a basic map G' . Let us denote v_i , with $1 \leq i \leq n$, the vertices of G' in such a way that (v_1, v_2, \dots, v_n) is a cycle of G' . We can assume that v_1 is the vertex resulting from the contraction of e . Let u and v be the endpoints of e in G .

Suppose first that u or v is incident to a loop in G . By symmetry, we can assume that v is incident to a loop and that u is in the cylinder between the loops around v and v_n (note that if $n = 1$ then $v_n = v$), and note that u is the only vertex here. Since G is non-basic and u has at least 3 incident edges, 2 of them go to the same vertex but are non-homotopic. Since after the contraction of e there is only one edge left in the cylinder, we can deduce that u has at least 2 edges in common with v . On the other side since G is essentially 3-connected u has an edge e' with v_n . This edge e' is contractible, since its contraction yields a graph containing the basic graph on n vertices. But since this graph has 2 non-homotopic edges linking (uv_n) and v , it is non-basic. So G has a contractible edge whose contraction produces a non-basic graph, contradicting our assumption.

Suppose now that u and v do not have an incident loop; we thus have that G contains a cycle C of length 2 containing e . Let e' be the other edge of C . Since G is essentially 3-connected, both u and v have at least degree three, and at least one of them has an incident edge on the left (resp. right) of C . If $n = 1$, since G has at least 4 edges, there are 2 (non-homotopic) edges, say f_1 and f_2 between u and v and distinct from e and e' . In this case, since the cycles (e, f_1) and (e, f_2) were not homotopic, the edges f_1 and f_2 remain non-homotopic in G' . So in this case G has one vertex and 3 edges, and it is thus non-basic. Assume now that $n \geq 2$. In this case, u and v are contained in a cylinder bordered by the loops at v_2 and at v_n (with eventually $n = 2$). In this case, we can assume that u has at least one incident edge f_1 on the left of C to v_n , and that v has at least one incident edge f_2 on the right of C to v_2 . In this case, one can contract f_1 and note that the obtained graph, which contains at least 3 non-homotopic edges around v (e , e' and f_2), is essentially 3-connected and non-basic. So G has a contractible edge whose contraction produces a non-basic graph, contradicting our assumption. \square

Lemma 20 *A basic toroidal map admits only Schnyder woods of Type 2.*

Proof A basic toroidal map admits Schnyder woods of Type 2, as shown by Fig. 30. Suppose that a basic toroidal map G on n vertices admits a Schnyder wood of Type 1. Consider one of the vertical loops e and suppose by symmetry that it is oriented

upward in color 1. In a Schnyder wood of Type 1, all the monochromatic cycles of different colors are not homotopic; thus, all the loops homotopic to e are also oriented upward in color 1 and they are not bi-oriented. There remains just a cycle on n vertices for edges of color 0 and 2. Thus, the Schnyder wood is the one of Fig. 30, a contradiction. \square

We are now able to prove the following theorem.

Theorem 10 *A toroidal graph admits a Schnyder wood of Type 1 if and only if it is an essentially 3-connected non-basic toroidal map.*

Proof (\implies) If G is a toroidal graph given with a Schnyder wood of Type 1, then, by Lemma 9, G is essentially 3-connected and by Lemma 20, G is not basic.

(\impliedby) Let G be a non-basic essentially 3-connected toroidal map. By Lemma 19, G can be contracted to the 3-loops or to the brick. Both of these graphs admit Schnyder woods of Type 1 (see Figs. 29(a) and 31). So by Lemma 14 applied successively, G admits a Schnyder wood of Type 1. \square

Theorem 10 and Lemma 20 imply Theorem 1. One related open problem is to characterize which essentially 3-connected toroidal maps have Schnyder woods of Type 2.

Here is a remark about how to compute a Schnyder wood for an essentially 3-connected toroidal triangulation. Instead of looking carefully at the technical proof of Lemma 14 to determine which coloring of the decontracted graph must be chosen among the possible choices, one can try the possible cases $\alpha.k.l$, $\ell \geq 1$, and then check which obtained coloring is a Schnyder wood. To do so, one just has to check if (T2') is satisfied. Checking that (T2') is satisfied can be done by the following method: start from any vertex v , walk along $P_0(v)$, $P_1(v)$, $P_2(v)$, and mark the three monochromatic cycles C_0, C_1, C_2 reached by the three paths P_i . Property (T2') is then satisfied if the cycles C_0, C_1, C_2 pairwise intersect.

The existence of Schnyder woods for toroidal triangulations implies the following theorem.

Theorem 11 *A toroidal triangulation contains three non-contractible and non-homotopic cycles that are pairwise edge-disjoint.*

Proof One just has to apply Theorem 10 to obtain a Schnyder wood of Type 1 and then, for each color i , choose arbitrarily an i -cycle. These cycles are edge-disjoint as, by Euler's formula, there are no bi-oriented edges in Schnyder woods of toroidal triangulations. \square

The conclusion of Theorem 11 is weaker than the one of Theorem 8, but it is not restricted to simple toroidal triangulations. Recall that Theorem 8 is not true for general toroidal triangulations, as shown by the graph of Fig. 17.

A non-empty family \mathcal{R} of linear orders on the vertex set V of a simple graph G is called a *realizer* of G if for every edge e , and every vertex x not in e , there is some

order $<_i \in \mathcal{R}$ so that $y <_i x$ for every $y \in e$. The *dimension* [10] of G is defined as the least positive integer t for which G has a realizer of cardinality t . Realizers are usually used on finite graphs, but here we allow G to be an infinite simple graph.

Schnyder woods were originally defined by Schnyder [26] to prove that a finite planar graph G has dimension at most three. A consequence of Theorem 1 is an analogous result for the universal cover of a toroidal graph.

Theorem 12 *The universal cover of a toroidal graph has dimension at most three.*

Proof By eventually adding edges to G , we may assume that G is a toroidal triangulation. By Theorem 1, it admits a Schnyder wood. For $i \in \{0, 1, 2\}$, let $<_i$ be the order induced by the inclusion of the regions R_i in G^∞ . That is, $u <_i v$ if and only if $R_i(u) \subsetneq R_i(v)$. Let $<'_i$ be any linear extension of $<_i$ and consider $\mathcal{R} = \{<'_0, <'_1, <'_2\}$. Let e be any edge of G^∞ and v be any vertex of G^∞ not in e . Edge e is in a region $R_i(v)$ for some i ; thus, $R_i(u) \subseteq R_i(v)$ for every $u \in e$ by Lemma 8(i). As there are no edges oriented in two directions in a Schnyder wood of a toroidal triangulation, we have $R_i(u) \neq R_i(v)$ and so $u <_i v$. Thus \mathcal{R} is a realizer of G^∞ . \square

10 Orthogonal Surfaces

Given two points $u = (u_0, u_1, u_2)$ and $v = (v_0, v_1, v_2)$ in \mathbb{R}^3 , we note $u \vee v = (\max(u_i, v_i))_{i=0,1,2}$ and $u \wedge v = (\min(u_i, v_i))_{i=0,1,2}$. We define an order \geq among the points in \mathbb{R}^3 , in such a way that $u \geq v$ if $u_i \geq v_i$ for $i = 0, 1, 2$.

Given a set \mathcal{V} of pairwise incomparable elements in \mathbb{R}^3 , we define the set of vertices that dominates \mathcal{V} as $\mathcal{D}_{\mathcal{V}} = \{u \in \mathbb{R}^3 \mid \exists v \in \mathcal{V} \text{ such that } u \geq v\}$. The *orthogonal surface* $\mathcal{S}_{\mathcal{V}}$ generated by \mathcal{V} is the boundary of $\mathcal{D}_{\mathcal{V}}$. (Note that orthogonal surfaces are well defined even when \mathcal{V} is an infinite set.) If $u, v \in \mathcal{V}$ and $u \vee v \in \mathcal{S}_{\mathcal{V}}$, then $\mathcal{S}_{\mathcal{V}}$ contains the union of the two line segments joining u and v to $u \vee v$. Such arcs are called *elbow geodesics*. The *orthogonal arc* of $v \in \mathcal{V}$ in the direction of the standard basis vector e_i is the intersection of the ray $v + \lambda e_i$ with $\mathcal{S}_{\mathcal{V}}$.

Let G be a planar map. A *geodesic embedding* of G on the orthogonal surface $\mathcal{S}_{\mathcal{V}}$ is a drawing of G on $\mathcal{S}_{\mathcal{V}}$ satisfying the following:

- (D1) There is a bijection between the vertices of G and \mathcal{V} .
- (D2) Every edge of G is an elbow geodesic.
- (D3) Every orthogonal arc in $\mathcal{S}_{\mathcal{V}}$ is part of an edge of G .
- (D4) There are no crossing edges in the embedding of G on $\mathcal{S}_{\mathcal{V}}$.

Miller [20] (see also [8, 11]) proved that a geodesic embedding of a planar map G on an orthogonal surface $\mathcal{S}_{\mathcal{V}}$ induces a Schnyder wood of G . The edges of G are colored with the direction of the orthogonal arc contained in the edge. An orthogonal arc intersecting the ray $v + \lambda e_i$ corresponds to the edge leaving v in color i . Edges represented by two orthogonal arcs correspond to edges oriented in two directions.

Conversely, it has been proved that a Schnyder wood of a planar map G can be used to obtain a geodesic embedding of G . Let G be a planar map given with a Schnyder wood. The method is the following (see [8] for more details): For every

vertex v , one can divide G into the three regions bounded by the three monochromatic paths going out from v . The *region vector* associated to v is the vector obtained by counting the number of faces in each of these three regions. The mapping of each vertex on its region vector gives the geodesic embedding. (Note that in this approach, the vertices are all mapped on the same plane, as the sum of the coordinates of each region vector is equal to the total number of inner faces of the map.)

Our goal is to generalize geodesic embedding to the torus. More precisely, we want to represent the universal cover of a toroidal map on an infinite and periodic orthogonal surface.

Let G be a toroidal map. Consider any flat torus representation of G in a parallelogram P . The graph G^∞ is obtained by replicating P to tile the plane. Given any of these parallelograms Q , let Q^{top} (resp. Q^{right}) be the copy of P just above (resp. on the right of) Q . Given a vertex v in Q , we denote v^{top} (resp. v^{right}) its copies in Q^{top} (resp. Q^{right}).

A mapping of the vertices of G^∞ in \mathbb{R}^d , $d \in \{2, 3\}$, is *periodic* with respect to vectors S and S' of \mathbb{R}^d , if there exists a flat torus representation P of G such that for any vertex v of G^∞ , vertex v^{top} is mapped on $v + S$ and v^{right} is mapped on $v + S'$. A *geodesic embedding* of a toroidal map G is a geodesic embedding of G^∞ on $S_{\mathcal{V}^\infty}$, where \mathcal{V}^∞ is a periodic mapping of G^∞ with respect to two non-collinear vectors (see example of Fig. 5).

As in the plane, Schnyder woods can be used to obtain geodesic embeddings of toroidal maps. For that purpose, we need to generalize the region vector method. The idea is to use the regions $R_i(v)$ to compute the coordinates of the vertex v of G^∞ . The problem is that, contrarily to the planar case, these regions are unbounded and contain an infinite number of faces. The method is thus generalized by the following.

Let G be a toroidal map, given with a Schnyder wood and a flat torus representation in a parallelogram P .

Recall that $\mathcal{C}_i = \{C_i^0, \dots, C_i^{k_i-1}\}$ denotes the set of i -cycles of G such that there is no i -cycle in the region $R(C_i^j, C_i^{j+1})$. Recall that \mathcal{L}_i^j denotes the set of i -lines of G^∞ corresponding to C_i^j . The *positive side* of an i -line is defined as the right side while “walking” along the directed path by following the orientation of the edges colored i .

Lemma 21 *For any vertex v , the two monochromatic lines $L_{i-1}(v)$ and $L_{i+1}(v)$ intersect. Moreover, if the Schnyder wood is of Type 2.i, then $L_{i+1}(v) = (L_{i-1}(v))^{-1}$ and v is situated on the right of $L_{i+1}(v)$.*

Proof Let j, j' be such that $L_{i-1}(v) \in \mathcal{L}_{i-1}^j$ and $L_{i+1}(v) \in \mathcal{L}_{i+1}^{j'}$. If the Schnyder wood is of Type 1 or Type 2.j with $j \neq i$, then the two cycles C_{i-1}^j and $C_{i+1}^{j'}$ are not homotopic, and so the two lines $L_{i-1}(v)$ and $L_{i+1}(v)$ intersect.

If the Schnyder wood is of Type 2.i, we consider the case where $v \in L_{i-1}(v)$, and the case where v does not belong to either $L_{i-1}(v)$ or $L_{i+1}(v)$. Then v lies between two consecutive $(i + 1)$ -lines (which are also $(i - 1)$ -lines). Let us denote those two lines L_{i+1} and L'_{i+1} , such that L'_{i+1} is situated on the right of L_{i+1} and $v \notin L'_{i+1}$. By property (T1), $P_{i+1}(v)$ and $P_{i-1}(v)$ cannot reach L'_{i+1} . Thus, $L_{i+1} = L_{i+1}(v) = (L_{i-1}(v))^{-1}$. □

The *size* of the region $R(C_i^j, C_i^{j+1})$ of G , denoted $f_i^j = |R(C_i^j, C_i^{j+1})|$, is equal to the number of faces in $R(C_i^j, C_i^{j+1})$. Remark that for each color, we have that $\sum_{j=0}^{k_i-1} f_i^j$ equals the total number of faces f of G . If L and L' are consecutive i -lines of G^∞ with $L \in \mathcal{L}_i^j$ and $L' \in \mathcal{L}_i^{j+1}$, then the *size* of the (unbounded) region $R(L, L')$, denoted $|R(L, L')|$, is equal to f_i^j . If L and L' are any i -lines, the *size* of the (unbounded) region $R(L, L')$, denoted $|R(L, L')|$, is equal to the sum of the size of all the regions delimited by consecutive i -lines inside $R(L, L')$. For each color i , choose arbitrarily an i -line L_i^* in \mathcal{L}_i^0 that is used as an origin for i -lines. Given an i -line L , we define the value $f_i(L)$ of L as follows: $f_i(L) = |R(L, L_i^*)|$ if L is on the positive side of L_i^* and $f_i(L) = -|R(L, L_i^*)|$ otherwise.

Consider two vertices u, v such that $L_{i-1}(u) = L_{i-1}(v)$ and $L_{i+1}(u) = L_{i+1}(v)$. Even if the two regions $R_i(u)$ and $R_i(v)$ are unbounded, their *difference* is bounded. Let $d_i(u, v)$ be the number of faces in $R_i(u) \setminus R_i(v)$ minus the number of faces in $R_i(v) \setminus R_i(u)$. For any vertex, by Lemma 21, there exists $z_i(v)$, a vertex on the intersection of the two lines $L_{i-1}(v)$ and $L_{i+1}(v)$. Let N be a constant $\geq n$ (in this section we can have $N = n$, but in Sect. 12 we need to choose N bigger). We are now able to define the region vector of a vertex of G^∞ , that is, a mapping of this vertex in \mathbb{R}^3 .

Definition 4 (Region vector) The i -th coordinate of the *region vector* of a vertex v of G^∞ is equal to $v_i = d_i(v, z_i(v)) + N \times (f_{i+1}(L_{i+1}(v)) - f_{i-1}(L_{i-1}(v)))$ (see Fig. 32).

For each color i , let c_i (resp. c'_i), be the algebraic number of times an i -cycle is traversing the vertical (resp. horizontal) side of the parallelogram P (which was the parallelogram containing the flat torus representation of G) from right to left (resp. from bottom to top). This number increases by one each time a monochromatic cycle traverses the side in the given direction and decreases by one when it traverses in the other direction. Let S and S' be the two vectors of \mathbb{R}^3 with coordinates $S_i = N(c_{i+1} - c_{i-1})f$ and $S'_i = N(c'_{i+1} - c'_{i-1})f$. Note that $S_0 + S_1 + S_2 = 0$ and $S'_0 + S'_1 + S'_2 = 0$

We use the example of the toroidal map G of Fig. 2 to illustrate the region vector method. This toroidal map has $n = 3$ vertices, $f = 4$ faces, and $e = 7$ edges. Let $N = n = 3$. There are two edges that are oriented in two directions. The Schnyder wood is of Type 1, with two 1-cycles. We choose as origin the three bold monochromatic lines of Fig. 33. We give them value 0 and compute the other values $f_i(L)$ as explained formally at the beginning of this section; i.e., we compute the “number” of faces between L and the origin L^* and put a minus if we are on the left of L^* . (This corresponds to values indicated on the border of Fig. 33, which are values 0, -4 , -8 , -12 for lines of color 0, values -4 , -2 , 0 , 2 , 4 for lines of color 1, and values 0, 4 for lines of color 2.) Then we compute the region vector of the points according to Definition 4. For example, the point v of Fig. 33 has the following values (the three points $z_i(v)$ are represented on the figure): $v_0 = d_0(v, z_0(v)) + N \times (f_1(L_1(v)) - f_2(L_2(v))) = 0 + 3(0 - 0) = 0$, $v_1 = d_1(v, z_1(v)) + N \times (f_2(L_2(v)) - f_0(L_0(v))) = 0 + 3(0 - (-4)) = 12$, $v_2 = d_2(v, z_2(v)) + N \times (f_0(L_0(v)) - f_1(L_1(v))) = 1 + 3(-4 - 0) = -11$. We compute

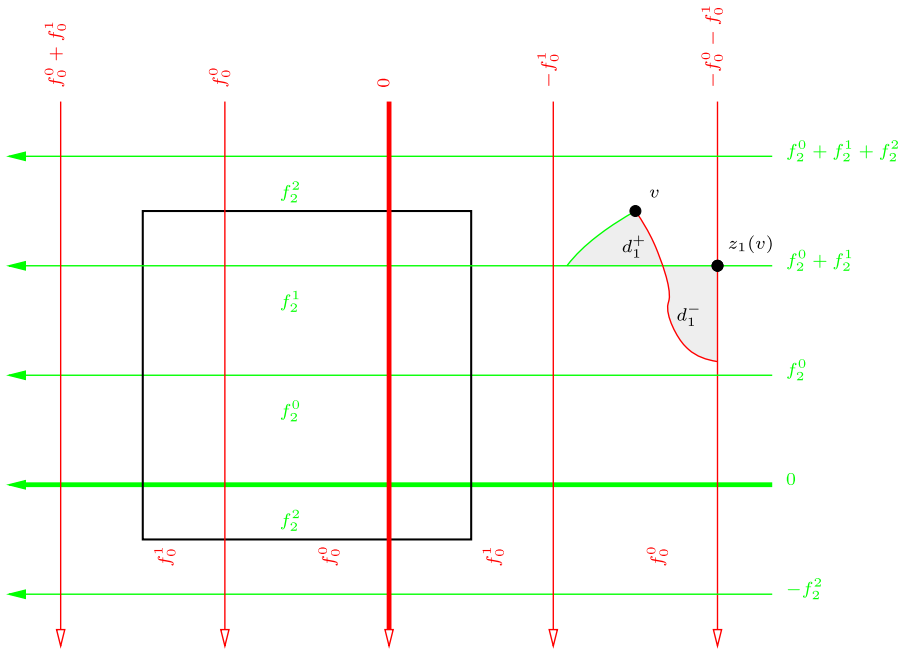


Fig. 32 Coordinate 1 of vertex v is equal to the number of faces in the region d_1^+ , minus the number of faces in the region d_1^- , plus N times $(f_2^0 + f_2^1) - (-f_0^0 - f_0^1)$

similarly the region vectors of all the vertices that are in the black box representing one copy of the graph and let $\mathcal{V} = \{(0, 0, 0), (0, 12, -11), (6, 12, -18)\}$ be the set of these vectors. Then we compute the c_i 's and c'_i 's by algebraically counting the number of times the monochromatic cycles cross the sides of the black box. A monochromatic cycle of color 0 goes -1 time from right to left and 2 times from bottom to top. So $c_0 = -1$ and $c'_0 = -2$. Similarly, $c_1 = 0$, $c'_1 = 1$, $c_2 = 1$, $c'_2 = 0$. Then we compute $S_i = N(c_{i+1} - c_{i-1})f$ and $S'_i = N(c'_{i+1} - c'_{i-1})f$ and obtain $S = (-12, 24, -12)$, $S' = (12, 24, -36)$. Then the region vectors of the vertices of G^∞ are $\{u \in \mathbb{R}^3 \mid \exists v \in \mathcal{V}, k_1, k_2 \in \mathbb{Z} \text{ such that } u = v + k_1 S + k_2 S'\}$. In this example, the points are not coplanar; they lie on the two different planes of equations $x + y + z = 0$ and $x + y + z = 1$. The geodesic embedding that is obtained by mapping each vertex to its region vector is the geodesic embedding of Fig. 5. The black parallelogram has as sides the vectors S, S' and represents a basic tile.

Lemma 22 *The sum of the coordinates of a vertex v equals the number of faces in the bounded region delimited by the lines $L_0(v), L_1(v)$, and $L_2(v)$ if the Schnyder wood is of Type 1, and this sum equals zero if the Schnyder wood is of Type 2.*

Proof We have $v_0 + v_1 + v_2 = d_0(v, z_0(v)) + d_1(v, z_1(v)) + d_2(v, z_2(v)) = \sum_i (|R_i(v) \setminus R_i(z_i(v))| - |R_i(z_i(v)) \setminus R_i(v)|)$. We use the characteristic function $\mathbf{1}$ to deal with infinite regions. We note $\mathbf{1}(R)$, the function defined on the faces of G^∞ that has value 1 on each face of region R and 0 elsewhere. Given a function

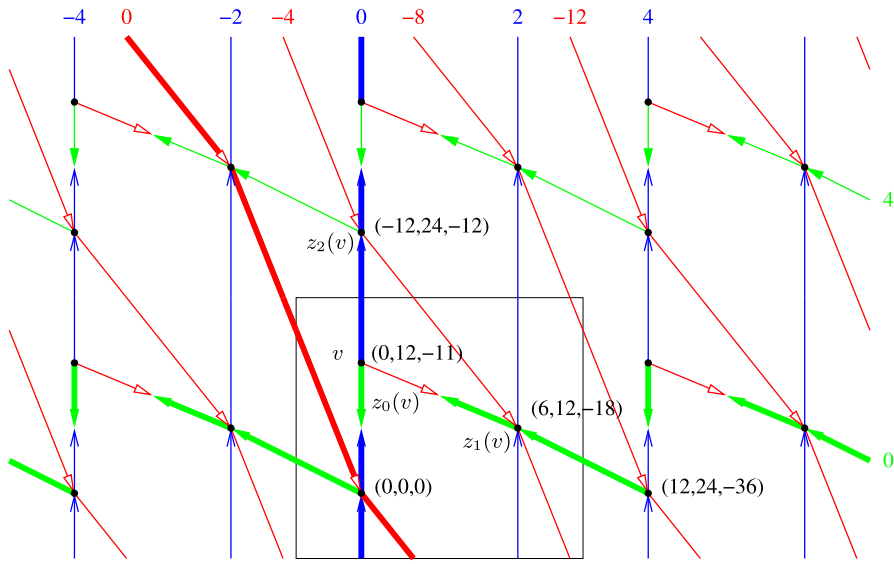


Fig. 33 Computation of the region vectors for the Schnyder wood of Fig. 2

$g : F(G^\infty) \rightarrow \mathbb{Z}$, we note that $|g| = \sum_{F \in F(G^\infty)} g(F)$ (when the sum is finite). Thus, $\sum_i v_i = \sum_i (|\mathbf{1}(R_i(v) \setminus R_i(z_i(v)))| - |\mathbf{1}(R_i(z_i(v)) \setminus R_i(v))|) = |\sum_i (\mathbf{1}(R_i(v) \setminus R_i(z_i(v))) - \mathbf{1}(R_i(z_i(v)) \setminus R_i(v)))|$. Now we compute $g = \sum_i (\mathbf{1}(R_i(v) \setminus R_i(z_i(v))) - \mathbf{1}(R_i(z_i(v)) \setminus R_i(v)))$. We have:

$$g = \sum_i (\mathbf{1}(R_i(v) \setminus R_i(z_i(v))) + \mathbf{1}(R_i(v) \cap R_i(z_i(v))) - \mathbf{1}(R_i(z_i(v)) \setminus R_i(v)) - \mathbf{1}(R_i(v) \cap R_i(z_i(v))))$$

As $R_i(v) \setminus R_i(z_i(v))$ and $R_i(z_i(v)) \setminus R_i(v)$ are disjoint from $R_i(v) \cap R_i(z_i(v))$, we have:

$$g = \sum_i (\mathbf{1}(R_i(v)) - \mathbf{1}(R_i(z_i(v)))) = \sum_i \mathbf{1}(R_i(v)) - \sum_i \mathbf{1}(R_i(z_i(v)))$$

Because the interior of the three regions $R_i(v)$, for $i = 0, 1, 2$, is disjoint and spans the whole plane \mathbb{P} (by definition), we have $\sum_i \mathbf{1}(R_i(v)) = \mathbf{1}(\cup_i (R_i(v))) = \mathbf{1}(\mathbb{P})$. Moreover, the regions $R_i(z_i(v))$, for $i = 0, 1, 2$, are also disjoint and $\sum_i \mathbf{1}(R_i(z_i(v))) = \mathbf{1}(\cup_i (R_i(z_i(v)))) = \mathbf{1}(\mathbb{P} \setminus T)$, where T is the bounded region delimited by the lines $L_0(v)$, $L_1(v)$, and $L_2(v)$. So $g = \mathbf{1}(\mathbb{P}) - \mathbf{1}(\mathbb{P} \setminus T) = \mathbf{1}(T)$. And thus $\sum_i v_i = |g| = |\mathbf{1}(T)|$. \square

Lemma 22 shows that if the Schnyder wood is of Type 1, then the set of points are not necessarily coplanar as in the planar case [12], but all the copies of a vertex lie on the same plane (the bounded region delimited by the lines $L_0(v)$, $L_1(v)$ and $L_2(v)$ has the same number of faces for any copies of a vertex v). Surprisingly, for Schnyder woods of Type 2, all the points are coplanar.

Lemma 23 *The mapping is periodic with respect to S and S' .*

Proof Let v be any vertex of G^∞ . Then $v_i^{\text{top}} - v_i = N(f_{i+1}(L_{i+1}(v^{\text{top}})) - f_{i+1}(L_{i+1}(v))) - N(f_{i-1}(L_{i-1}(v^{\text{top}})) - f_{i-1}(L_{i-1}(v))) = N(c_{i+1} - c_{i-1})f$. So $v^{\text{top}} = v + S$. Similarly, $v^{\text{right}} = v + S'$. \square

For each color i , let γ_i be the integer such that two monochromatic cycles of G of respective colors $i - 1$ and $i + 1$ intersect exactly γ_i times, with the convention that $\gamma_i = 0$ if the Schnyder wood is of Type 2.i. By Lemma 3, γ_i is properly defined and does not depend on the choice of the monochromatic cycles. Note that if the Schnyder wood is of Type 2.i, then $\gamma_{i-1} = \gamma_{i+1}$ and if the Schnyder wood is not of Type 2.i, then $\gamma_i \neq 0$. Let $\gamma = \max(\gamma_0, \gamma_1, \gamma_2)$. Let $Z_0 = ((\gamma_1 + \gamma_2)Nf, -\gamma_1Nf, -\gamma_2Nf)$, $Z_1 = (-\gamma_0Nf, (\gamma_0 + \gamma_2)Nf, -\gamma_2Nf)$, and $Z_2 = (-\gamma_0Nf, -\gamma_1Nf, (\gamma_0 + \gamma_1)Nf)$.

Lemma 24 *For any vertex u , we have $\{u + k_0Z_0 + k_1Z_1 + k_2Z_2 \mid k_0, k_1, k_2 \in \mathbb{Z}\} \subseteq \{u + kS + k'S' \mid k, k' \in \mathbb{Z}\}$.*

Proof Let u, v be two copies of the same vertex, such that v is the first copy of u in the direction of $L_0(u)$. (That is, $L_0(u) = L_0(v)$ and on the path $P_0(u) \setminus P_0(v)$ there are not two copies of the same vertex.) Then $v_i - u_i = N(f_{i+1}(L_{i+1}(v)) - f_{i+1}(L_{i+1}(u))) - N(f_{i-1}(L_{i-1}(v)) - f_{i-1}(L_{i-1}(u)))$. We have $|R(L_0(v), L_0(u))| = 0$, $|R(L_1(v), L_1(u))| = \gamma_2f$, and $|R(L_2(v), L_2(u))| = \gamma_1f$. So $v_0 - u_0 = N(\gamma_1 + \gamma_2)f$, $v_1 - u_1 = -N\gamma_1f$, and $v_2 - u_2 = -N\gamma_2f$. Thus, $v = u + Z_0$, and similarly for the other colors. So the first copy of u in the direction of $L_i(u)$ is equal to $u + Z_i$. By Lemma 23, all the copies of u are mapped on $\{u + kS + k'S' \mid k, k' \in \mathbb{Z}\}$, and so we have the result. \square

Lemma 25 *We have $\dim(Z_0, Z_1, Z_2) = 2$, and if the Schnyder wood is not of Type 2.i, then $\dim(Z_{i-1}, Z_{i+1}) = 2$.*

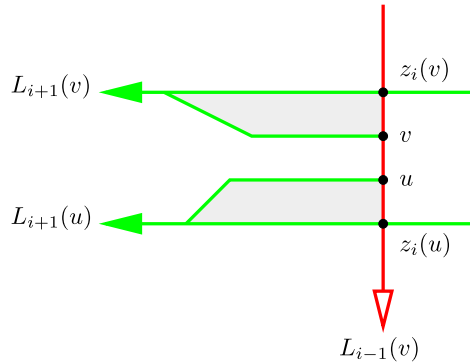
Proof We have $\gamma_0Z_0 + \gamma_1Z_1 + \gamma_2Z_2 = 0$ and so $\dim(Z_0, Z_1, Z_2) \leq 2$. We can assume by symmetry that the Schnyder wood is not of Type 2.1 and so $\gamma_1 \neq 0$. Thus, $Z_0 \neq 0$ and $Z_2 \neq 0$. Suppose by contradiction that $\dim(Z_0, Z_2) = 1$. Then there exist $\alpha \neq 0, \beta \neq 0$, such that $\alpha Z_0 + \beta Z_2 = 0$. The sum of this equation for the coordinates 0 and 2 gives $(\alpha + \beta)\gamma_1 = 0$ and thus $\alpha = -\beta$. Then the equation for coordinate 0 gives $\gamma_0 + \gamma_1 + \gamma_2 = 0$, contradicting the fact that $\gamma_1 > 1$ and $\gamma_0, \gamma_2 \geq 0$. \square

Lemma 26 *The vectors S, S' are not collinear.*

Proof By Lemma 24, the set $\{u + k_0Z_0 + k_1Z_1 + k_2Z_2 \mid k_0, k_1, k_2 \in \mathbb{Z}\}$ is a subset of $\{u + kS + k'S' \mid k, k' \in \mathbb{Z}\}$. By Lemma 25, we have $\dim(Z_0, Z_1, Z_2) = 2$, thus $\dim(S, S') = 2$. \square

Lemma 27 *If u, v are two distinct vertices such that v is in $L_{i-1}(v)$, u is in $P_{i-1}(v)$, both u and v are in the region $R(L_{i+1}(u), L_{i+1}(v))$, and $L_{i+1}(u)$ and $L_{i+1}(v)$ are two consecutive $(i + 1)$ -lines with $L_{i+1}(u) \in \mathcal{L}_{i+1}^j$ (see Fig. 34), then $d_i(z_i(v), v) + d_i(u, z_i(u)) < (n - 1) \times f_{i+1}^j$.*

Fig. 34 The gray area, corresponding to the quantity $d_i(z_i(v), v) + d_i(u, z_i(u))$, has size bounded by $(n - 1) \times f_{i+1}^j$



Proof Let $Q_{i+1}(v)$ the subpath of $P_{i+1}(v)$ between v and $L_{i+1}(v)$ (maybe $Q_{i+1}(v)$ has length 0 if $v = z_i(v)$). Let $Q_{i+1}(u)$ be the subpath of $P_{i+1}(u)$ between u and $L_{i+1}(u)$ (maybe $Q_{i+1}(u)$ has length 0 if $u = z_i(u)$). The path $Q_{i+1}(v)$ cannot contain two different copies of a vertex of G , otherwise $Q_{i+1}(v)$ will correspond to a non-contractible cycle of G and thus will contain an edge of $L_{i+1}(v)$. So the length of $Q_{i+1}(v)$ is $\leq n - 1$.

The total number of times a copy of a given face of G can appear in the region $R = R_i(z_i(v)) \setminus R_i(v)$, corresponding to $d_i(z_i(v), v)$, can be bounded as follows. Region R is between two consecutive copies of $L_{i+1}(u)$. So in R , all the copies of a given face are separated by a copy of $L_{i-1}(v)$. Each copy of $L_{i-1}(v)$ intersecting R must intersect $Q_{i+1}(v)$ on a specific vertex. As $Q_{i+1}(v)$ has at most n vertices, a given face can appear at most $n - 1$ times in R . Similarly, the total number of times that a copy of a given face of G can appear in the region $R_i(u) \setminus R_i(z_i(u))$, corresponding to $d_i(u, z_i(u))$, is $\leq (n - 1)$.

A given face of G can appear in only one of the two gray regions of Fig. 34. So a face is counted $\leq n - 1$ times in the quantity $d_i(z_i(v), v) + d_i(u, z_i(u))$. Only the faces of the region $R(C_{i+1}^j, C_{i+1}^{j+1})$ can be counted, and there is at least one face of $R(C_{i+1}^j, C_{i+1}^{j+1})$ (for example, one incident to v) that is not counted. So in total $d_i(z_i(v), v) + d_i(u, z_i(u)) \leq (n - 1) \times (f_{i+1}^j - 1) < (n - 1) \times f_{i+1}^j$. \square

Clearly, the symmetric of Lemma 27, where the roles of $i + 1$ and $i - 1$ are exchanged, is also true.

The bound of Lemma 27 is somehow sharp. In the example of Fig. 35, the rectangle represents a toroidal map G and the universal cover is partially represented. If the map G has n vertices and f faces ($n = 5$ and $f = 5$ in the example), then the gray region, representing the quantity $d_1(z_1(v), v) + d_1(u, z_1(u))$, has size $\frac{n(n-1)}{2} = \Omega(n \times f)$.

Lemma 28 *Let u, v be vertices of G^∞ such that $R_i(u) \subseteq R_i(v)$, then $u_i \leq v_i$. Moreover, if $R_i(u) \subsetneq R_i(v)$, then $v_i - u_i > (N - n)(|R(L_{i-1}(u), L_{i-1}(v))| + |R(L_{i+1}(u), L_{i+1}(v))|) \geq 0$.*

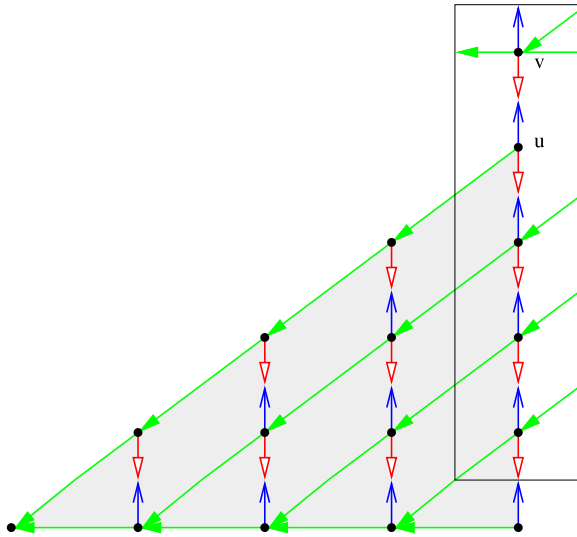


Fig. 35 Example of a toroidal map where $d_1(u, z_1(u))$ has size $\Omega(n \times f)$

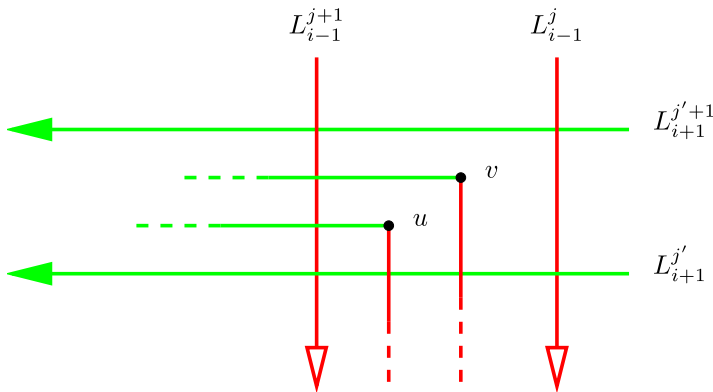


Fig. 36 Positions of u and v in the proof of Lemma 28

Proof We distinguish two cases depending on whether the Schnyder wood is of Type 2.i or not.

• *Case 1: The Schnyder wood is not of Type 2.i.*

Suppose first that u and v are both in a region delimited by two consecutive lines of color $i - 1$ and two consecutive lines of color $i + 1$. Let $L_{i-1}^j, L_{i-1}^{j+1}, L_{i+1}^{j'}, L_{i+1}^{j'+1}$ be these lines such that L_{i-1}^{j+1} is on the positive side of $L_{i-1}^j, L_{i+1}^{j'+1}$ is on the positive side of $L_{i+1}^{j'}$, and $L_k^\ell \in \mathcal{L}_k^\ell$ (see Fig. 36). We distinguish cases corresponding to equality or not between lines $L_{i-1}(u), L_{i-1}(v)$ and $L_{i+1}(u), L_{i+1}(v)$.

★ *Case 1.1:* $L_{i-1}(u) = L_{i-1}(v)$ and $L_{i+1}(u) = L_{i+1}(v)$. Then $v_i - u_i = d_i(v, z_i(v)) - d_i(u, z_i(u)) = d_i(v, u)$. Thus clearly, if $R_i(u) \subseteq R_i(v)$, then $u_i \leq v_i$ and if $R_i(u) \subsetneq R_i(v)$, $v_i - u_i > 0 = (N - n)(|R(L_{i-1}(u), L_{i-1}(v))| + |R(L_{i+1}(u), L_{i+1}(v))|)$.

★ *Case 1.2:* $L_{i-1}(u) = L_{i-1}(v)$ and $L_{i+1}(u) \neq L_{i+1}(v)$. As $u \in R_i(v)$, we have $L_{i+1}(u) = L_{i+1}^j$ and $L_{i+1}(v) = L_{i+1}^{j+1}$. Then $v_i - u_i = d_i(v, z_i(v)) - d_i(u, z_i(u)) + N(f_{i+1}(L_{i+1}(v)) - f_{i+1}(L_{i+1}(u))) = d_i(v, z_i(v)) - d_i(u, z_i(u)) + Nf_{i+1}^j$. Let u' be the intersection of $P_{i+1}(u)$ with L_{i-1}^{j+1} (maybe $u = u'$). Let v' be the intersection of $P_{i+1}(v)$ with L_{i-1}^{j+1} (maybe $v = v'$). Since $L_{i+1}(u) \neq L_{i+1}(v)$, we have $u' \neq v'$. Since $u \in R_i(v)$, we have $u' \in R_i(v')$ and so $u' \in P_{i-1}(v')$. Then, by Lemma 27, $d_i(z_i(v'), v') + d_i(u', z_i(u')) < (n - 1)f_{i+1}^{j+1}$. If $L_{i-1}(u) = L_{i-1}^{j+1}$, then one can see that $d_i(v, z_i(v)) - d_i(u, z_i(u)) \geq d_i(v', z_i(v')) - d_i(u', z_i(u'))$. If $L_{i-1}(u) = L_{i-1}^j$, one can see that $d_i(v, z_i(v)) - d_i(u, z_i(u)) \geq d_i(v', z_i(v')) - d_i(u', z_i(u')) - f_{i+1}^j$. So finally, $v_i - u_i = d_i(v, z_i(v)) - d_i(u, z_i(u)) + Nf_{i+1}^j \geq d_i(v', z_i(v')) - d_i(u', z_i(u')) + (N - 1)f_{i+1}^j > (N - n)f_{i+1}^j = (N - n)(|R(L_{i-1}(u), L_{i-1}(v))| + |R(L_{i+1}(u), L_{i+1}(v))|) \geq 0$.

★ *Case 1.3:* $L_{i-1}(u) \neq L_{i-1}(v)$ and $L_{i+1}(u) = L_{i+1}(v)$. This case is completely symmetric to the previous case.

★ *Case 1.4:* $L_{i-1}(u) \neq L_{i-1}(v)$ and $L_{i+1}(u) \neq L_{i+1}(v)$. As $u \in R_i(v)$, we have $L_{i+1}(u) = L_{i+1}^j$, $L_{i+1}(v) = L_{i+1}^{j+1}$, $L_{i-1}(u) = L_{i-1}^{j+1}$, and $L_{i-1}(v) = L_{i-1}^j$. Then $v_i - u_i = d_i(v, z_i(v)) - d_i(u, z_i(u)) + N(f_{i+1}(L_{i+1}(v)) - f_{i+1}(L_{i+1}(u))) - N(f_{i-1}(L_{i-1}(v)) - f_{i-1}(L_{i-1}(u))) = d_i(v, z_i(v)) - d_i(u, z_i(u)) + Nf_{i+1}^j + Nf_{i-1}^j$. Let u' be the intersection of $P_{i+1}(u)$ with L_{i-1}^{j+1} (maybe $u = u'$). Let u'' be the intersection of $P_{i-1}(u)$ with L_{i+1}^j (maybe $u = u''$). Let v' be the intersection of $P_{i+1}(v)$ with L_{i-1}^{j+1} (maybe $v = v'$). Let v'' be the intersection of $P_{i-1}(v)$ with L_{i+1}^j (maybe $v = v''$). Since $L_{i+1}(u) \neq L_{i+1}(v)$, we have $u' \neq v'$. Since $u \in R_i(v)$, we have $u' \in R_i(v')$ and so $u' \in P_{i-1}(v')$. Then, by Lemma 27, $d_i(z_i(v'), v') + d_i(u', z_i(u')) < (n - 1)f_{i+1}^j$. Symmetrically, $d_i(z_i(v''), v'') + d_i(u'', z_i(u'')) < (n - 1)f_{i-1}^j$. Moreover, we have $d_i(v, z_i(v)) - d_i(u, z_i(u)) \geq d_i(v', z_i(v')) - d_i(u', z_i(u')) + d_i(v'', z_i(v'')) - d_i(u'', z_i(u'')) - f_{i+1}^j - f_{i-1}^j$. So finally, $v_i - u_i = d_i(v, z_i(v)) - d_i(u, z_i(u)) + Nf_{i+1}^j + Nf_{i-1}^j \geq d_i(v', z_i(v')) - d_i(u', z_i(u')) + d_i(v'', z_i(v'')) - d_i(u'', z_i(u'')) + (N - 1)f_{i+1}^j + (N - 1)f_{i-1}^j > (N - n)f_{i+1}^j + (N - n)f_{i-1}^j = (N - n)(|R(L_{i-1}(u), L_{i-1}(v))| + |R(L_{i+1}(u), L_{i+1}(v))|) \geq 0$.

Suppose now that u and v do not lie in a region delimited by two consecutive lines of color $i - 1$ and/or in a region delimited by two consecutive lines of color $i + 1$. One can easily find distinct vertices w_0, \dots, w_r ($w_i, 1 \leq i < r$ chosen at intersections of monochromatic lines of colors $i - 1$ and $i + 1$) such that $w_0 = u, w_r = v$, and for $0 \leq \ell \leq r - 1$, we have $R_i(w_\ell) \subsetneq R_i(w_{\ell+1})$ and $w_\ell, w_{\ell+1}$ are both in a region delimited by two consecutive lines of color $i - 1$ and in a region delimited by two consecutive lines of color $i + 1$. Thus, by the first part of the proof, $(w_\ell)_i - (w_{\ell+1})_i > (N - n)(|R(L_{i-1}(w_{\ell+1}), L_{i-1}(w_\ell))| + |R(L_{i+1}(w_{\ell+1}), L_{i+1}(w_\ell))|)$. Thus $v_i - u_i >$

$(N - n) \sum_{\ell} (|R(L_{i-1}(w_{\ell+1}), L_{i-1}(w_{\ell}))| + |R(L_{i+1}(w_{\ell+1}), L_{i+1}(w_{\ell}))|)$. For any a, b, c such that $R_i(a) \subseteq R_i(b) \subseteq R_i(c)$, we have $|R(L_j(a), L_j(b))| + |R(L_j(b), L_j(c))| = |R(L_j(a), L_j(c))|$. Thus, we obtain the result by summing the size of the regions.

• *Case 2: The Schnyder wood is of Type 2.i.*

Suppose first that u and v are both in a region delimited by two consecutive lines of color $i + 1$.

Let L_{i+1}^j, L_{i+1}^{j+1} be these lines such that L_{i+1}^{j+1} is on the positive side of L_{i+1}^j , and $L_{i+1}^{\ell} \in \mathcal{L}_{i+1}^{\ell}$. We can assume that we do not have both u and v in L_{i+1}^{j+1} (by eventually choosing other consecutive lines of color $i + 1$). We consider two cases:

★ *Case 2.1: $v \notin L_{i+1}^{j+1}$.* Then by Lemma 21, $L_{i+1}^j = L_{i+1}(u) = (L_{i-1}(u))^{-1} = L_{i+1}(v) = (L_{i-1}(v))^{-1}$. Then $v_i - u_i = d_i(v, z_i(v)) - d_i(u, z_i(u)) = d_i(v, u)$. Thus clearly, if $R_i(u) \subseteq R_i(v)$, then $u_i \leq v_i$ and if $R_i(u) \subsetneq R_i(v)$, then $v_i - u_i > 0 = (N - n)(|R(L_{i-1}(u), L_{i-1}(v))| + |R(L_{i+1}(u), L_{i+1}(v))|)$.

★ *Case 2.2: $v \in L_{i+1}^{j+1}$.* Then $L_{i+1}^{j+1} = L_{i+1}(v) = (L_{i-1}(v))^{-1}$ and $d_i(v, z_i(v)) = 0$. By assumption $u \notin L_{i+1}^{j+1}$ and by Lemma 21, $L_{i+1}^j = L_{i+1}(u) = (L_{i-1}(u))^{-1}$. Then $v_i - u_i = d_i(v, z_i(v)) - d_i(u, z_i(u)) + N(f_{i+1}(L_{i+1}(v)) - f_{i+1}(L_{i+1}(u))) - N(f_{i-1}(L_{i-1}(v)) - f_{i-1}(L_{i-1}(u))) = -d_i(u, z_i(u)) + 2Nf_{i+1}^j$. Let L_i and L'_i be two consecutive i -lines such that u lies in the region between them and L'_i is on the right of L_i . Let u' be the intersection of $P_{i+1}(u)$ with L_i (maybe $u = u'$). Let u'' be the intersection of $P_{i-1}(u)$ with L'_i (maybe $u = u''$). Then, by Lemma 27, $d_i(u', z_i(u')) < (n - 1)f_{i+1}^j$ and $d_i(u'', z_i(u'')) < (n - 1)f_{i+1}^j$. Thus, we have $d_i(u, z_i(u)) \leq d_i(u', z_i(u')) + d_i(u'', z_i(u'')) + f_{i+1}^j < (2(n - 1) + 1)f_{i+1}^j$. So finally, $v_i - u_i > -(2n - 1)f_{i+1}^j + 2Nf_{i+1}^j > 2(N - n)f_{i+1}^j = (N - n) \times (|R(L_{i-1}(u), L_{i-1}(v))| + |R(L_{i+1}(u), L_{i+1}(v))|) \geq 0$.

If u and v do not lie in a region delimited by two consecutive lines of color $i + 1$, then as in case 1, one can find intermediate vertices to obtain the result. □

Lemma 29 *If two vertices u, v are adjacent, then for each color i , we have $|v_i - u_i| \leq 2Nf$.*

Proof Since u, v are adjacent, they are both in a region delimited by two consecutive lines of color $i - 1$ and in a region delimited by two consecutive lines of color $i + 1$. Let L_{i-1}^j, L_{i-1}^{j+1} be these two consecutive lines of color $i - 1$ and L_{i+1}^j, L_{i+1}^{j+1} these two consecutive lines of color $i + 1$ where $L_k^{\ell} \in \mathcal{L}_k^{\ell}$, L_{i-1}^{j+1} is on the positive side of L_{i-1}^j , and L_{i+1}^{j+1} is on the positive side of L_{i+1}^j (see Fig. 36 when the Schnyder wood is not of Type 2.i). If the Schnyder wood is of Type 2.i, we assume that $L_{i-1}^{j+1} = (L_{i+1}^j)^{-1}$ and $L_{i-1}^j = (L_{i+1}^{j+1})^{-1}$. Let z be a vertex on the intersection of L_{i-1}^{j+1} and L_{i+1}^j . Let z' be a vertex on the intersection of L_{i-1}^j and L_{i+1}^{j+1} . Thus, we have $R_i(z) \subseteq R_i(u) \subseteq R_i(z')$ and $R_i(z) \subseteq R_i(v) \subseteq R_i(z')$. So by Lemma 28, $z_i \leq u_i \leq z'_i$ and $z_i \leq v_i \leq z'_i$. So $|v_i - u_i| \leq z'_i - z_i = N(f_{i+1}(L_{i+1}^{j+1}) - f_{i+1}(L_{i+1}^j)) - N(f_{i-1}(L_{i-1}^j) - f_{i-1}(L_{i-1}^{j+1})) = Nf_{i+1}^{j'} + Nf_{i-1}^j \leq 2Nf$. □

We are now able to prove the following theorem.

Theorem 13 *If G is a toroidal map given with a Schnyder wood, then the mapping of each vertex of G^∞ on its region vector gives a geodesic embedding of G .*

Proof By Lemmas 23 and 26, the mapping of G^∞ on its region vector is periodic with respect to S, S' that are not collinear. For any pair u, v of distinct vertices of G^∞ , by Lemma 8(iii), there exists i, j with $R_i(u) \subsetneq R_i(v)$ and $R_j(v) \subsetneq R_j(u)$; thus, by Lemma 28, $u_i < v_i$ and $v_j < u_j$. So \mathcal{V}^∞ is a set of pairwise incomparable elements of \mathbb{R}^3 .

(D1) \mathcal{V}^∞ is a set of pairwise incomparable elements, so the mapping between vertices of G^∞ and \mathcal{V}^∞ is a bijection.

(D2) Let $e = uv$ be an edge of G^∞ . We show that $w = u \vee v$ is on the surface $S_{\mathcal{V}^\infty}$. By definition, $u \vee v$ is in $\mathcal{D}_{\mathcal{V}^\infty}$. Suppose, by contradiction, that $w \notin S_{\mathcal{V}^\infty}$. Then there exists $x \in \mathcal{V}^\infty$ with $x < w$. Let x also denote the corresponding vertex of G^∞ . Edge e is in a region $R_i(x)$ for some i . So $u, v \in R_i(x)$ and thus by Lemma 8(i), $R_i(u) \subseteq R_i(x)$ and $R_i(v) \subseteq R_i(x)$. Then by Lemma 28, $w_i = \max(u_i, v_i) \leq x_i$, a contradiction. Thus, the elbow geodesic between u and v is on the surface.

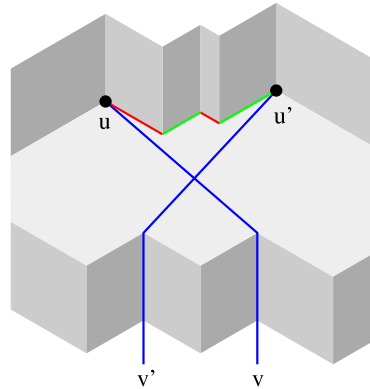
(D3) Consider a vertex $v \in \mathcal{V}$ and a color i . Let u be the extremity of the arc $e_i(v)$. We have $u \in R_{i-1}(v)$ and $u \in R_{i+1}(v)$, so by Lemma 8(i), $R_{i-1}(u) \subseteq R_{i-1}(v)$ and $R_{i+1}(u) \subseteq R_{i+1}(v)$. Thus, by Lemma 8(iii), $R_i(v) \subsetneq R_i(u)$. So, by Lemma 28, $v_i < u_i, u_{i-1} \leq v_{i-1}$, and $u_{i+1} \leq v_{i+1}$. So the orthogonal arc of vertex v in the direction of the basis vector e_i is part of the elbow geodesic of the edge $e_i(v)$.

(D4) Suppose there exists a pair of crossing edges $e = uv$ and $e' = u'v'$ on the surface $S_{\mathcal{V}^\infty}$. The two edges e, e' cannot intersect on orthogonal arcs, so they intersect on a plane orthogonal to one of the coordinate axes. Up to symmetry we may assume that we are in the situation of Fig. 37 with $u_1 = u'_1, u_2 > u'_2$, and $v_2 < v'_2$. Between u and u' , there is a path consisting of orthogonal arcs only. With (D3), this implies that there is a bidirected path P^* colored 0 from u to u' and colored 2 from u' to u . We have $u \in R_2(v)$, so by Lemma 8(i), $R_2(u) \subseteq R_2(v)$. We have $u' \in R_2(u)$, so $u' \in R_2(v)$. If $P_0(v)$ contains u' , then there is a contractible cycle containing v, u, u' in $G_1 \cup G_0^{-1} \cup G_2^{-1}$, contradicting Lemma 1, so $P_0(v)$ does not contain u' . If $P_1(v)$ contains u' , then $u' \in P_1(u) \cap P_0(u)$, contradicting Lemma 7. So $u' \in R_2^o(v)$. Thus, the edge $u'v'$ implies that $v' \in R_2(v)$. So by Lemma 28, $v'_2 \leq v_2$, a contradiction. \square

Theorems 1 and 13 imply Theorem 3.

One can ask: What is the “size” of the obtained geodesic embedding of Theorem 13? Of course, this mapping is infinite so there is no real size, but as the object is periodic, one can consider the smallest size of the vectors such that the mapping is periodic with respect to them. There are several such pairs of vectors, one is S, S' . Recall that $S_i = N(c_{i+1} - c_{i-1})f$ and $S'_i = N(c'_{i+1} - c'_{i-1})f$. Unfortunately, the size of S, S' can be arbitrarily large. Indeed, the values of $c_{i+1} - c_{i-1}$ and $c'_{i+1} - c'_{i-1}$ are unbounded, as a toroidal map can be artificially “very twisted” in the considered flat torus representation (independent of the number of vertices or faces). Nevertheless, we can prove the existence of bounded size vectors for which the mapping is periodic with respect to them.

Fig. 37 A pair of crossing elbow geodesics



Lemma 30 *If G is a toroidal map given with a Schnyder wood, then the mapping of each vertex of G^∞ on its region vector gives a periodic mapping of G^∞ with respect to non-collinear vectors Y and Y' , where the size of Y and Y' is in $\mathcal{O}(\gamma Nf)$. In general, we have $\gamma \leq n$, and in the case where G is a simple toroidal triangulation given with a Schnyder wood obtained by Theorem 9, we have $\gamma = 1$.*

Proof By Lemma 24, the vectors Z_{i-1}, Z_{i+1} (when the Schnyder wood is not of Type 2.i) span a subset of S, S' (it can happen that this subset is strict). Thus, in the parallelogram delimited by the vectors Z_{i-1}, Z_{i+1} (that is, a parallelogram by Lemma 25), there is a parallelogram with sides Y, Y' containing a copy of V . The size of the vectors Z_i is in $\mathcal{O}(\gamma Nf)$ and so the size of Y and Y' is also.

In general, we have $\gamma_i \leq n$, as each intersection between two monochromatic cycles of G of color $i - 1$ and $i + 1$ corresponds to a different vertex of G and thus $\gamma \leq n$. In the case of simple toroidal triangulation given with a Schnyder wood obtained by Theorem 9, we have, for each color i , $\gamma_i = 1$, and thus $\gamma = 1$. □

As in the plane, one can give weights to faces of G . Then all their copies in G^∞ have the same weight, and instead of counting the number of faces in each region one can compute the weighted sum.

Note that the geodesic embeddings of Theorem 13 are not necessarily rigid. A geodesic embedding is *rigid* [11, 20] if for every pair $u, v \in \mathcal{V}$ such that $u \vee v$ is in S_γ , u and v are the only elements of \mathcal{V} that are dominated by $u \vee v$. The geodesic embedding of Fig. 5 is not rigid, as the bend corresponding to the loop of color 1 is dominated by three vertices of G^∞ . We do not know if it is possible to build a rigid geodesic embedding from the Schnyder wood of a toroidal map. Maybe a technique similar to the one presented in [11] can be generalized to the torus.

It has already been mentioned that in the geodesic embeddings of Theorem 13 the points corresponding to vertices are not coplanar. The problem of building a coplanar geodesic embedding from the Schnyder wood of a toroidal map is open. In the plane, there are some examples of maps G [11] for which it is not possible to require both rigidity and coplanarity. Thus, the same is true in the torus for the graph G^+ .

Another question related to coplanarity is whether one can require that the points of the orthogonal surface corresponding to edges of the graph (i.e., bends) are copla-

nar. This property is related to contact representation by homotopic triangles [11]. It is known that in the plane, not all Schnyder woods are supported by such surfaces. Kratochvil’s conjecture [19], recently proved [17], states that every 4-connected planar triangulation admits a contact representation by homothetic triangles. Can this be extended to the torus?

When considering not necessarily homothetic triangles, it has been proved [14] that there is a bijection between Schnyder woods of planar triangulations and contact representations by triangles. This result has been generalized to internally 3-connected planar maps [16] by exhibiting a bijection between Schnyder woods of internally 3-connected planar maps and primal-dual contact representations by triangles (i.e., representations where both the primal and the dual are represented). It would be interesting to generalize these results to the torus.

11 Duality of Orthogonal Surfaces

Given an orthogonal surface generated by \mathcal{V} , let $\mathcal{F}_{\mathcal{V}}$ be the maximal points of $\mathcal{S}_{\mathcal{V}}$, i.e., the points of $\mathcal{S}_{\mathcal{V}}$ that are not dominated by any vertex of $\mathcal{S}_{\mathcal{V}}$. If $A, B \in \mathcal{F}_{\mathcal{V}}$ and $A \wedge B \in \mathcal{S}_{\mathcal{V}}$, then $\mathcal{S}_{\mathcal{V}}$ contains the union of the two line segments joining A and B to $A \wedge B$. Such arcs are called *dual elbow geodesics*. The *dual orthogonal arc* of $A \in \mathcal{F}_{\mathcal{V}}$ in the direction of the standard basis vector e_i is the intersection of the ray $A + \lambda e_i$ with $\mathcal{S}_{\mathcal{V}}$.

Given a toroidal map G , let $G^{\infty*}$ be the dual of G^{∞} . A *dual geodesic embedding* of G is a drawing of $G^{\infty*}$ on the orthogonal surface $\mathcal{S}_{\mathcal{V}^{\infty}}$, where \mathcal{V}^{∞} is a periodic mapping of G^{∞} with respect to two non-collinear vectors, satisfying the following (see the example of Fig. 38):

- (D1*) There is a bijection between the vertices of $G^{\infty*}$ and $\mathcal{F}_{\mathcal{V}^{\infty}}$.
- (D2*) Every edge of $G^{\infty*}$ is a dual elbow geodesic.
- (D3*) Every dual orthogonal arc in $\mathcal{S}_{\mathcal{V}^{\infty}}$ is part of an edge of $G^{\infty*}$.
- (D4*) There are no crossing edges in the embedding of $G^{\infty*}$ on $\mathcal{S}_{\mathcal{V}^{\infty}}$.

Let G be a toroidal map given with a Schnyder wood. Consider the mapping of each vertex on its region vector. We consider the dual of the Schnyder wood of G . By Lemma 11, it is a Schnyder wood of G^* . A face F of G^{∞} is mapped on the point $\bigvee_{v \in F} v$. Let \widetilde{G}^{∞} be a simultaneous drawing of G^{∞} and $G^{\infty*}$ such that only dual edges intersect. To avoid confusion, we denote R_i the regions of the primal Schnyder wood and R_i^* the regions of the dual Schnyder wood.

Lemma 31 *For any face F of G^{∞} , we have that $\bigvee_{v \in F} v$ is a maximal point of $\mathcal{S}_{\mathcal{V}^{\infty}}$.*

Proof Let F be a face of G^{∞} . For any vertex u of \mathcal{V}^{∞} , there exists a color i , such that the face F is in the region $R_i(u)$. Thus for $v \in F$, we have $v \in R_i(u)$. By Lemma 28, we have $v_i \leq u_i$ and so $F_i \leq u_i$. So $F = \bigvee_{v \in F} v$ is a point of $\mathcal{S}_{\mathcal{V}^{\infty}}$.

Suppose, by contradiction, that F is not a maximal point of $\mathcal{S}_{\mathcal{V}^{\infty}}$. Then there is a point $\alpha \in \mathcal{S}_{\mathcal{V}^{\infty}}$ that dominates F and, for at least one coordinate j , we have $F_j < \alpha_j$. By Lemma 10, the angles at F form, in counterclockwise order, non-empty intervals

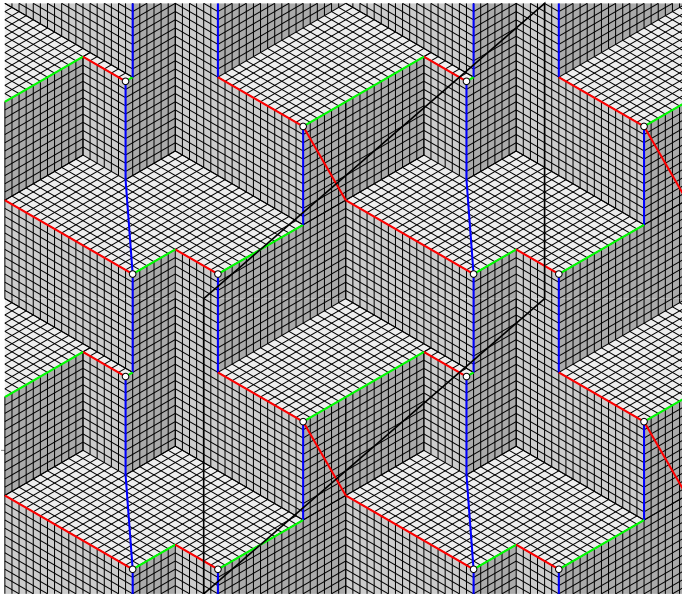


Fig. 38 Dual geodesic embedding of the toroidal map of Fig. 2

of 0’s, 1’s, and 2’s. For each color, let z^i be a vertex of F with angle i . We have that F is in the region $R_i(z^i)$. So $z^{i-1} \in R_i(z^i)$ and by Lemma 8(i), we have $R_i(z^{i-1}) \subseteq R_i(z^i)$. Since F is in $R_{i-1}(z^{i-1})$, it is not in $R_i(z^{i-1})$ and thus $R_i(z^{i-1}) \subsetneq R_i(z^i)$. Then by Lemma 28, we have $(z^{i-1})_i < (z^i)_i$ and symmetrically $(z^{i+1})_i < (z^i)_i$. So $F_{j-1} = (z^{j-1})_{j-1} > (z^j)_{j-1}$ and $F_{j+1} > (z^j)_{j+1}$. Thus, α strictly dominates z^j , a contradiction to $\alpha \in \mathcal{S}_{\mathcal{V}^\infty}$. Thus, F is a maximal point of $\mathcal{S}_{\mathcal{V}^\infty}$. \square

Lemma 32 *If two faces A, B are such that $R_i^*(B) \subseteq R_i^*(A)$, then $A_i \leq B_i$.*

Proof Let $v \in B$ be a vertex whose angle at B is labeled i . We have $v \in R_i^*(B)$ and so $v \in R_i^*(A)$. In \widetilde{G}^∞ , the path $P_i(v)$ cannot leave $R_i^*(A)$, the path $P_{i+1}(v)$ cannot intersect $P_{i+1}(A)$, and the path $P_{i-1}(v)$ cannot intersect $P_{i-1}(A)$. Thus, $P_{i+1}(v)$ intersects $P_{i-1}(A)$ and the path $P_{i-1}(v)$ cannot intersect $P_{i+1}(A)$. So $A \in R_i(v)$. Thus, for all $u \in A$, we have $u \in R_i(v)$, so $R_i(u) \subseteq R_i(v)$, and so $u_i \leq v_i$. Then $A_i = \max_{u \in A} u_i \leq v_i \leq \max_{w \in B} w_i = B_i$. \square

Theorem 14 *If G is a toroidal map given with a Schnyder wood and each vertex of G^∞ is mapped on its region vector, then the mapping of each face of $G^{\infty*}$ on the point $\bigvee_{v \in F} v$ gives a dual geodesic embedding of G .*

Proof By Lemmas 23 and 26, the mapping is periodic with respect to non-collinear vectors.

(D1*) Consider a counting of elements on the orthogonal surface, where we count two copies of the same object just once (note that we are on an infinite and periodic

object). We have that the sum of primal orthogonal arcs plus dual ones is exactly $3m$. There are $3n$ primal orthogonal arcs and thus there are $3m - 3n = 3f$ dual orthogonal arcs. Each maximal point of $\mathcal{S}_{\mathcal{V}^\infty}$ is incident to 3 dual orthogonal arcs and there is no dual orthogonal arc incident to two distinct maximal points. So there are f maximal points. Thus by Lemma 31, we have a bijection between faces of G^∞ and maximal points of $\mathcal{S}_{\mathcal{V}^\infty}$.

Let $\mathcal{V}^{\infty*}$ be the maximal points of $\mathcal{S}_{\mathcal{V}^\infty}$. Let $\mathcal{D}_{\mathcal{V}^\infty}^* = \{A \in \mathbb{R}^3 \mid \exists B \in \mathcal{V}^{\infty*} \text{ such that } A \leq B\}$. Note that the boundary of $\mathcal{D}_{\mathcal{V}^\infty}^*$ is $\mathcal{S}_{\mathcal{V}^\infty}$.

(D2*) Let $e = AB$ be an edge of $G^{\infty*}$. We show that $w = A \wedge B$ is on the surface $\mathcal{S}_{\mathcal{V}^\infty}$. By definition, w is in $\mathcal{D}_{\mathcal{V}^\infty}^*$. Suppose, by contradiction, that $w \notin \mathcal{S}_{\mathcal{V}^\infty}$. Then there exists C , a maximal point of $\mathcal{S}_{\mathcal{V}^\infty}$ with $w < C$. By the bijection (D1*) between maximal points and vertices of $G^{\infty*}$, the point C corresponds to a vertex of $G^{\infty*}$, also denoted C . Edge e is in a region $R_i^*(C)$ for some i . So $A, B \in R_i^*(C)$ and thus, by Lemma 8(i), $R_i^*(A) \subseteq R_i^*(C)$ and $R_i^*(B) \subseteq R_i^*(C)$. Then by Lemma 32, we have $C_i \leq \min(A_i, B_i) = w_i$, a contradiction. Thus, the dual elbow geodesic between A and B is also on the surface.

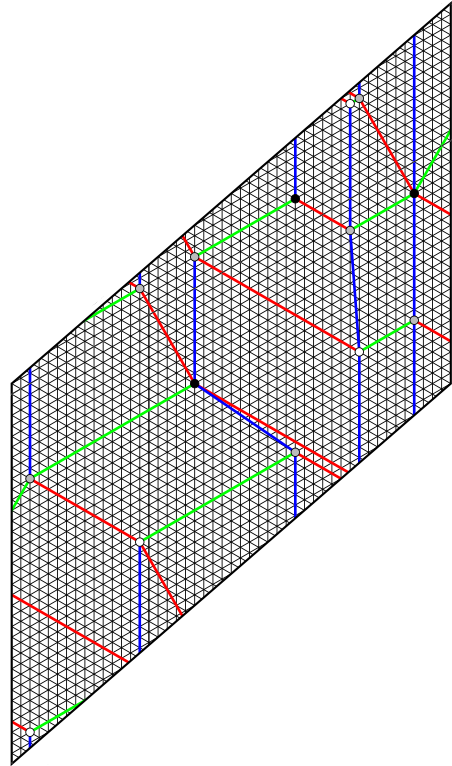
(D3*) Consider a vertex A of $G^{\infty*}$ and a color i . Let B be the extremity of the arc $e_i(A)$. We have $B \in R_{i-1}^*(A)$ and $B \in R_{i+1}^*(A)$, so by Lemma 8(i), $R_{i-1}^*(B) \subseteq R_{i-1}^*(A)$ and $R_{i+1}^*(B) \subseteq R_{i+1}^*(A)$. Thus by Lemma 32, $A_{i-1} \leq B_{i-1}$ and $A_{i+1} \leq B_{i+1}$. As A and B are distinct maximal points of $\mathcal{S}_{\mathcal{V}^\infty}$, they are incomparable, and thus $B_i < A_i$. So the dual orthogonal arc of vertex A in the direction of the basis vector e_i is part of edge $e_i(A)$.

(D4*) Suppose there exists a pair of crossing edges $e = AB$ and $e' = A'B'$ of $G^{\infty*}$ on the surface $\mathcal{S}_{\mathcal{V}^\infty}$. The two edges e, e' cannot intersect on orthogonal arcs, so they intersect on a plane orthogonal to one of the coordinate axes. Up to symmetry we may assume that we are in the situation $A_1 = A'_1, A'_0 > A_0$, and $B'_0 < B_0$. Between A and A' there is a path consisting of orthogonal arcs only. With (D3*), this implies that there is a bidirected path P^* colored 2 from A to A' and colored 0 from A' to A . We have $A \in R_0(B)$, so by Lemma 8(i), $R_0(A) \subseteq R_0(B)$. We have $A' \in R_0(A)$, so $A' \in R_0(B)$. If $P_2(B)$ contains A' , then there is a contractible cycle containing A, A', B in $G_1^* \cup G_0^{*-1} \cup G_2^{*-1}$, contradicting Lemma 1, so $P_2(B)$ does not contain A' . If $P_1(B)$ contains A' , then $A' \in P_1(A) \cap P_2(A)$, contradicting Lemma 7. So $A' \in R_0(B)$. Thus, the edge $A'B'$ implies that $B' \in R_0(B)$. So by Lemma 32, $B'_0 \geq B_0$, a contradiction. \square

Theorems 13 and 14 can be combined to obtain a simultaneous representation of a Schnyder wood and its dual on an orthogonal surface. The projection of this 3-dimensional object on the plane of the equation $x + y + z = 0$ gives a representation of the primal and the dual where edges are allowed to have one bend and two dual edges have to cross on their bends (see the example of Fig. 39).

Theorem 15 *An essentially 3-connected toroidal map admits a simultaneous flat torus representation of the primal and the dual where edges are allowed to have one bend and two dual edges have to cross on their bends. Such a representation is contained in a (triangular) grid of size $\mathcal{O}(n^2 f) \times \mathcal{O}(n^2 f)$ in general and $\mathcal{O}(nf) \times \mathcal{O}(nf)$ if the map is a simple triangulation. Furthermore, the length of the edges are in $\mathcal{O}(nf)$.*

Fig. 39 Simultaneous representation of the primal and the dual of the toroidal map of Fig. 2 with edges having one bend (in gray)



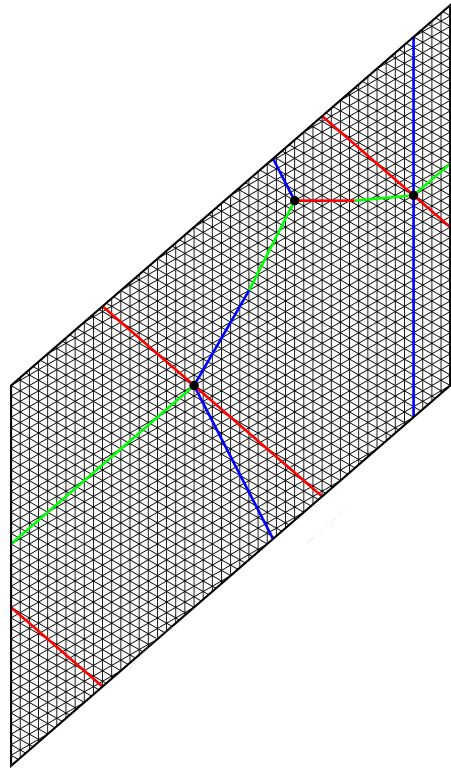
Proof Let G be an essentially 3-connected toroidal map. By Theorem 1 (or Theorem 9 if G is a simple triangulation), G admits a Schnyder wood (where monochromatic cycles of different colors intersect just once if G is simple). By Theorems 13 and 14, the mapping of each vertex of G^∞ on its region vector gives a primal and dual geodesic embedding. Thus, the projection of this embedding on the plane of the equation $x + y + z = 0$ gives a representation of the primal and the dual of G^∞ where edges are allowed to have one bend and two dual edges have to cross on their bends.

By Lemma 30, the obtained mapping is a periodic mapping of G^∞ with respect to non-collinear vectors Y and Y' where the size of Y and Y' is in $\mathcal{O}(\gamma Nf)$, with $\gamma \leq n$ in general and $\gamma = 1$ in case of a simple triangulation. Let $N = n$. The embedding gives a representation in the flat torus of sides Y, Y' where the size of the vectors Y and Y' is in $\mathcal{O}(n^2 f)$ in general and in $\mathcal{O}(nf)$ if the graph is simple and the Schnyder wood is obtained by Theorem 9. By Lemma 29, the lengths of the edges in this representation are in $\mathcal{O}(nf)$. □

12 Straight-Line Representation of Toroidal Maps

The geodesic embedding obtained by the region vector method can be used to obtain a straight-line representation of a toroidal map (see Fig. 40). For this purpose, we

Fig. 40 Straight-line representation of the graph of Fig. 2 obtained by projecting the geodesic embedding of Fig. 5



have to choose N bigger than previously. Note that Fig. 40 is the projection of the geodesic embedding of Fig. 5 obtained with the value of $N = n$. In this particular case this gives a straight-line representation, but in this section we only prove that such a technique works for triangulations and for N sufficiently large. To obtain a straight-line representation of a general toroidal map, one first has to triangulate it.

Let G be a toroidal triangulation given with a Schnyder wood and V^∞ the set of region vectors of vertices of G^∞ . The Schnyder wood is of Type 1 by Theorem 7. Recall that γ_i is the integer such that two monochromatic cycles of G of colors $i - 1$ and $i + 1$ intersect exactly γ_i times.

Lemma 33 *For any vertex v , the number of faces in the bounded region delimited by the three lines $L_i(v)$ is strictly less than $(5 \min(\gamma_i) + \max(\gamma_i))f$.*

Proof Suppose by symmetry that $\min(\gamma_i) = \gamma_1$. Let $L_i = L_i(v)$ and $z_i = z_i(v)$. Let T be the bounded region delimited by the three monochromatic lines L_i . The boundary of T is a cycle C oriented clockwise or counterclockwise. Assume that C is oriented counterclockwise (the proof is similar if oriented clockwise). The region T is on the left sides of the lines L_i . We have $z_{i-1} \in P_i(z_{i+1})$.

We define, for $j, k \in \mathbb{N}$, monochromatic lines $L_2(j)$, $L_0(k)$ and vertices $z(j, k)$ as follows (see Fig. 41). Let $L_2(1)$ be the first 2-line intersecting $L_0 \setminus \{z_1\}$ while walking from z_1 , along L_0 in the direction of L_0 . Let $L_0(1)$ be the first 0-line of color 0

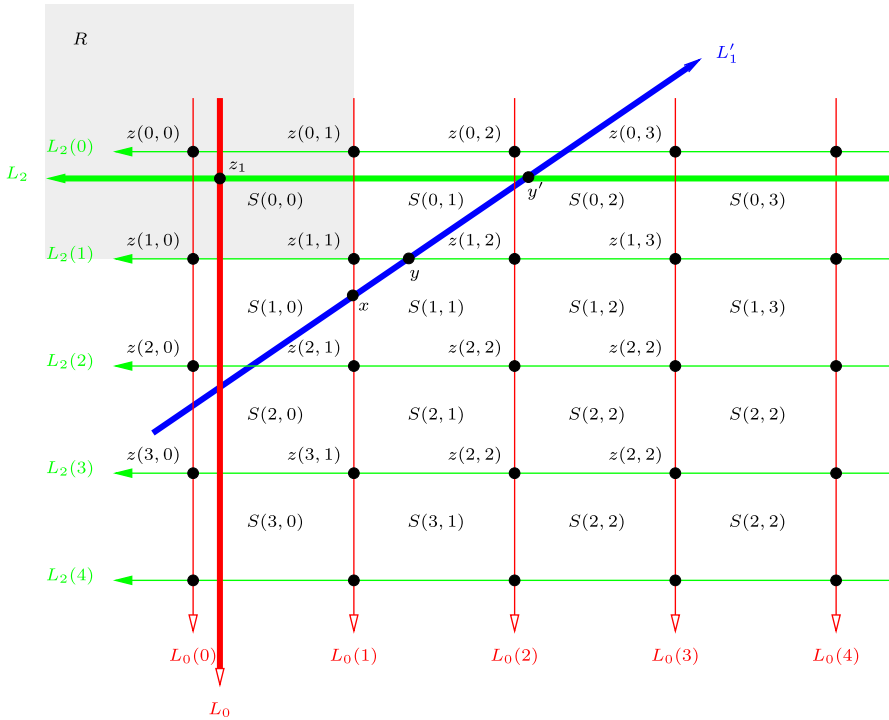


Fig. 41 Notation of the proof of Lemma 33

intersecting $L_2 \setminus \{z_1\}$ while walking from z_1 , along L_2 in the reverse direction of L_2 . Let $z(1, 1)$ be the intersection between $L_2(1)$ and $L_0(1)$. Let $z(j, 1)$, $j \geq 0$, be the consecutive copies of $z(1, 1)$ along $L_0(1)$ such that $z(j + 1, 1)$ is after $z(j, 1)$ in the direction of $L_0(1)$. Let $L_2(j)$, $j \geq 0$, be the 2-line of color 2 containing $z(j, 1)$. Note that we may have $L_2 = L_2(0)$, but in any case L_2 is between $L_2(0)$ and $L_2(1)$. Let $z(j, k)$, $k \geq 0$, be the consecutive copies of $z(j, 1)$ along $L_2(j)$ such that $z(j, k + 1)$ is after $z(j, k)$ in the reverse direction of $L_2(j)$. Let $L_0(k)$, $k \geq 0$, be the 0-line containing $z(1, k)$. Note that we may have $L_0 = L_0(0)$, but in any case L_0 is between $L_0(0)$ and $L_0(1)$. Let $S(j, k)$ be the region delimited by $L_2(j)$, $L_2(j + 1)$, $L_0(k)$, $L_0(k + 1)$. All the regions $S(j, k)$ are copies of $S(0, 0)$. The region $S(0, 0)$ may contain several copies of a face of G , but the number of copies of a face in $S(0, 0)$ is equal to γ_1 . Let R be the unbounded region situated on the right of $L_0(1)$ and on the right of $L_2(1)$. As $P_0(v)$ cannot intersect $L_0(1)$ and $P_2(v)$ cannot intersect $L_2(1)$, vertex v is in R . Let $P(j, k)$ be the subpath of $L_0(k)$ between $z(j, k)$ and $z(j + 1, k)$. All the lines $L_0(k)$ are composed only of copies of $P(0, 0)$. The interior vertices of the path $P(0, 0)$ cannot contain two copies of the same vertex, otherwise there will be a vertex $z(j, k)$ between $z(0, 0)$ and $z(1, 0)$. Thus, all interior vertices of a path $P(j, k)$ correspond to distinct vertices of G .

The Schnyder wood is of Type 1, thus 1-lines are crossing 0-lines. As a line $L_0(k)$ is composed only of copies of $P(0, 0)$, any path $P(j, k)$ is crossed by a 1-line. Let

L'_1 be the first 1-line crossing $P(1, 1)$ on a vertex x while walking from $z(1, 1)$ along $L_0(1)$. By (T1), line L'_1 is not intersecting $R \setminus \{z(1, 1)\}$. As $v \in R$, we have that L_1 is on the left of L'_1 (maybe $L_1 = L'_1$). Thus, the region T is included in the region T' delimited by L_0, L'_1, L_2 .

Let y be the vertex where L'_1 is leaving $S(1, 1)$. We claim that $y \in L_2(1)$. Note that by (T1), we have $y \in L_2(1) \cup P(1, 2)$. Suppose, by contradiction, that y is an interior vertex of $P(1, 2)$. Let d_x be the length of the subpath of $P(1, 1)$ between $z(1, 1)$ and x . Let d_y be the length of the subpath of $P(1, 2)$ between $z(1, 2)$ and y . Suppose $d_y < d_x$; then there should be a distinct copy of L'_1 intersecting $P(1, 1)$ between $z(1, 1)$ and x on a copy of y , a contradiction to the choice of L'_1 . So $d_x \leq d_y$. Let A be the subpath of L'_1 between x and y . Let B be the subpath of $P(1, 1)$ between x and the copy of y (if $d_x = d_y$, then B is just a single vertex). Consider all the copies of A and B between lines $L_2(1)$ and $L_2(2)$. They form an infinite line L situated on the right of $L_2(1)$ that prevents L'_1 from crossing $L_2(1)$, a contradiction.

By the positions of x and y , we have that L'_1 intersects $S(0, 1)$ and $S(1, 0)$. We claim that L'_1 cannot intersect both $S(0, 3)$ and $S(3, 0)$. Suppose by contradiction that L'_1 intersects both $S(0, 3)$ and $S(3, 0)$. Then L'_1 is crossing $S(0, 2)$ without crossing $L_2(0)$ or $L_2(1)$. Similarly, L'_1 is crossing $S(2, 0)$ without crossing $L_0(0)$ or $L_0(1)$. Thus, by superposing what happens in $S(0, 2)$ and $S(2, 0)$ in a square $S(j, k)$, we have that there are two crossing 1-lines, a contradiction. Thus, L'_1 intersects at most one of $S(0, 3)$ and $S(3, 0)$.

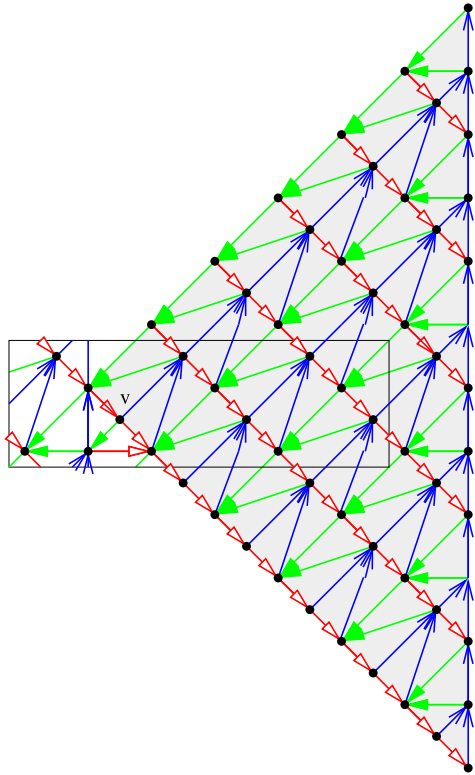
Suppose that L'_1 does not intersect $S(3, 0)$. Then the part of T' situated right of $L_0(2)$ (the left part of Fig. 41) is strictly included in $(S(0, 0) \cup S(1, 0) \cup S(2, 0) \cup S(0, 1) \cup S(1, 1))$. Thus, this part of T' contains at most $5\gamma_1 f$ faces. Now consider the part of T' situated on the left of $L_0(2)$ (the right part of Fig. 41). Let y' be the intersection of L'_1 with L_2 . Let Q be the subpath of L'_1 between y and y' . By the definition of $L_2(1)$, there are no 2-lines between L_2 and $L_2(1)$. So Q cannot intersect a 2-line on one of its interior vertices. Thus, Q is crossing at most γ_2 consecutive 0-lines (that are not necessarily lines of type $L_0(k)$). Let L'_0 be the $\gamma_2 + 1$ -th consecutive 0-line that is on the left of $L_0(2)$ (counting $L_0(2)$). Then the part of T' situated on the left of $L_0(2)$ is strictly included in the region delimited by $L_0(2), L'_0, L_2, L_2(1)$, and thus contains at most γ_2 copies of a face of G . Thus, T' contains at most $(\gamma_2 + 5\gamma_1) f$ faces.

Symmetrically, if L'_1 does not intersect $S(0, 3)$ we have that T' contains at most $(\gamma_0 + 5\gamma_1) f$ faces. Then in any case, T' contains at most $(\max(\gamma_0, \gamma_2) + 5\gamma_1) f$ faces and the lemma is true. □

The bound of Lemma 33 is somehow sharp. In the example of Fig. 42, the rectangle represents a toroidal triangulation G and the universal cover is partially represented. For each value of $k \geq 0$, there is a toroidal triangulation G with $n = 4(k + 1)$ vertices, where the gray region, representing the region delimited by the three monochromatic lines $L_i(v)$, contains $4 \sum_{j=1}^{2k+1} + 3(2k + 2) = \Omega(n \times f)$ faces. Fig-ure 42 represents such a triangulation for $k = 2$.

For planar graphs the region vector method gives vertices that all lie on the same plane. This property is very helpful in proving that the positions of the points on P give straight-line representations. In the torus, things are more complicated, as

Fig. 42 Example of a toroidal triangulation where the number of faces in the region delimited by the three monochromatic lines $L_i(v)$ contains $\Omega(n \times f)$ faces



our generalization of the region vector method does not give coplanar points. But Lemmas 22 and 33 show that all the points lie in the region situated between the two planes of equations $x + y + z = 0$ and $x + y + z = t$, with $t = (5 \min(\gamma_i) + \max(\gamma_i))f$. Note that t is bounded by $6nf$ by Lemma 30 and this is independent from N . Thus, from “far away” it looks like the points are coplanar and by taking N sufficiently large, non-coplanar points are “far enough” from each other to enable the region vector method to give straight-line representations.

Let $N = t + n$.

Lemma 34 *Let u, v be two vertices such that $e_{i-1}(v) = uv$, $L_i = L_i(u) = L_i(v)$, and such that both u, v are in the region $R(L_i, L'_i)$ for L'_i an i -line consecutive to L_i . Then $v_{i+1} - u_{i+1} < |R(L_i, L'_i)|$ and $e_{i-1}(v)$ is going counterclockwise around the closed disk bounded by $\{e_{i-1}(v)\} \cup P_i(u) \cup P_i(v)$.*

Proof Let y be the first vertex of $P_i(v)$ that is also in $P_i(u)$. Let Q_u (resp. Q_v) be the part of $P_i(u)$ (resp. $P_i(v)$) between u (resp. v) and y .

Let D be the closed disk bounded by the cycle $C = (Q_v)^{-1} \cup \{e_{i-1}(v)\} \cup Q_u$. If C is going clockwise around D , then $P_{i+1}(v)$ is leaving v in D and thus has to intersect Q_u or Q_v . In both cases, there is a cycle in $G_{i+1} \cup (G_i)^{-1} \cup (G_{i-1})^{-1}$, a contradiction to Lemma 6. So C is going clockwise around D .

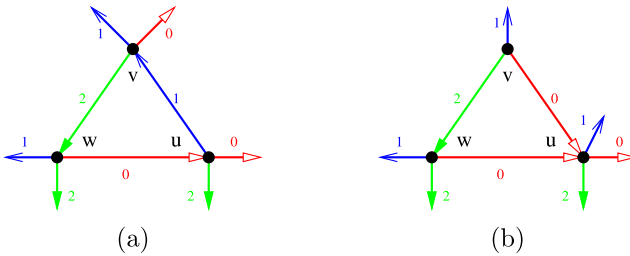


Fig. 43 (a) Case 1 and (b) case 2 of the proof of Lemma 35

As $L_i(u) = L_i(v)$ and $L_{i-1}(u) = L_{i-1}(v)$, we have $v_{i+1} - u_{i+1} = d_{i+1}(v, u)$, and this is equal to the number of faces in D . We have $D \subsetneq R(L_i, L'_i)$. Suppose D contains two copies of a given face. Then, these two copies are on different sides of a 1-line. By property (T1), it is not possible to have a 1-line entering D . So D contains at most one copy of each face of $R(L_i, L'_i)$. \square

Lemma 35 For any face F of G^∞ , incident to vertices u, v, w (given in counterclockwise order around F), the cross product $\vec{vw} \wedge \vec{vu}$ has strictly positive coordinates.

Proof Consider the angle labeling corresponding to the Schnyder wood. By Lemma 10, the angles at F are labeled in counterclockwise order 0, 1, 2. As $\vec{uv} \wedge \vec{uw} = \vec{vw} \wedge \vec{vu} = \vec{wu} \wedge \vec{wv}$, we may assume that u, v, w are such that u is in the angle labeled 0, vertex v in the angle labeled 1, and vertex w in the angle labeled 2. The face F is either a cycle completely directed into one direction or it has two edges oriented in one direction and one edge oriented in the other. Let

$$\vec{X} = \vec{vw} \wedge \vec{vu} = \begin{pmatrix} (w_1 - v_1)(u_2 - v_2) - (w_2 - v_2)(u_1 - v_1) \\ -(w_0 - v_0)(u_2 - v_2) + (w_2 - v_2)(u_0 - v_0) \\ (w_0 - v_0)(u_1 - v_1) - (w_1 - v_1)(u_0 - v_0) \end{pmatrix}$$

By symmetry, we consider the following two cases:

- *Case 1: The edges of the face F are in counterclockwise order $e_1(u), e_2(v), e_0(w)$ (see Fig. 43(a)).*

We have $v \in P_1(u)$, so $v \in R_0(u) \cap R_2(u)$ and $u \in R_1^\circ(v)$ (as there are no edges oriented in two directions). By Lemma 8, we have $R_0(v) \subseteq R_0(u)$, $R_2(v) \subseteq R_2(u)$, and $R_1(u) \subsetneq R_1(v)$. In fact, the first two inclusions are strict as $u \notin R_0(v) \cup R_2(v)$. So by Lemma 28, we have $v_0 < u_0, v_2 < u_2, u_1 < v_1$. We can prove similar inequalities for the other pairs of vertices and we obtain $w_0 < v_0 < u_0, u_1 < w_1 < v_1, v_2 < u_2 < w_2$. By just studying the signs of the different terms occurring in the values of the coordinates of \vec{X} , it is clear that \vec{X} has strictly positive coordinates. (For the first coordinates, it is easier if written in the following form: $X_0 = (u_1 - w_1)(v_2 - w_2) - (u_2 - w_2)(v_1 - w_1)$.)

- *Case 2: The edges of the face F are in counterclockwise order $e_0(v), e_2(v), e_0(w)$ (see Fig. 43(b)).*

As in the previous case, one can easily obtain the following inequalities: $w_0 < v_0 < u_0, u_1 < w_1 < v_1, u_2 < v_2 < w_2$ (the only difference with case 1 is between u_2

and v_2). Exactly as in the previous case, it is clear that X_0 and X_2 are strictly positive. But there is no way to reformulate X_1 to have a similar proof. Let $A = w_2 - v_2$, $B = u_0 - v_0$, $C = v_0 - w_0$, and $D = v_2 - u_2$, so $X_1 = AB - CD$ and A, B, C, D are all strictly positive.

Vertices u, v, w are in the region $R(L_1, L'_1)$ for L'_1 a 1-line consecutive to L_1 . We consider two cases depending on equality or not between $L_1(u)$ and $L_1(v)$.

★ *Subcase 2.1: $L_1(u) = L_1(v)$.*

We have $X_1 = A(B - D) + D(A - C)$.

We have $B - D = (u_0 + u_2) - (v_0 + v_2) = (v_1 - u_1) + (\sum u_i - \sum v_i)$. Since $u \in P_0(v)$, we have $L_0(u) = L_0(v)$. Suppose that $L_2(u) = L_2(v)$; then by Lemma 22, we have $\sum u_i = \sum v_i$, and thus $B - D = v_1 - u_1 > 0$. Suppose now that $L_2(u) \neq L_2(v)$. By Lemmas 22 and 33, $\sum u_i - \sum v_i > -t$. By Lemma 28, $v_1 - u_1 > (N - n)|R(L_2(u), L_2(v))| \geq N - n$. So $B - D > N - n - t \geq 0$.

We have $A - C = (w_0 + w_2) - (v_0 + v_2) = (v_1 - w_1) + (\sum w_i - \sum v_i) > \sum w_i - \sum v_i$. Suppose that $L_1(w) = L_1(v)$; then by Lemma 22, we have $\sum v_i = \sum w_i$ and thus $A - C = v_1 - w_1 > 0$. Then $X_1 > 0$. Suppose now that $L_1(v) \neq L_1(w)$. By Lemma 34, $D = v_2 - u_2 < |R(L_1, L'_1)|$. By Lemma 28, $A = w_2 - v_2 > (N - n) \times |R(L_1, L'_1)|$. By Lemmas 22 and 33, $\sum w_i - \sum v_i > -t$, so $A - C > -t$. Then $X_1 > (N - n - t)|R(L_1, L'_1)| > 0$.

★ *Subcase 2.2: $L_1(u) \neq L_1(v)$.*

We have $X_1 = B(A - C) + C(B - D)$.

Suppose that $L_1(w) \neq L_1(v)$. Then $L_1(w) = L_1(u)$. By Lemma 34 $e_0(w)$ is going counterclockwise around the closed disk D bounded by $\{e_0(w)\} \cup P_1(w) \cup P_1(u)$. Then v is inside D and $P_1(v)$ has to intersect $P_1(w) \cup P_1(u)$, so $L_1(v) = L_1(u)$, contradicting our assumption. So $L_1(v) = L_1(w)$.

By Lemma 28, $B = u_0 - v_0 > (N - n)|R(L_1, L'_1)|$. We have $A - C = (w_0 + w_2) - (v_0 + v_2) = (v_1 - w_1) + (\sum w_i - \sum v_i)$. By Lemma 22, we have $\sum v_i = \sum w_i$ and thus $A - C = v_1 - w_1 > 0$. By (the symmetric of) Lemma 34, $C = v_0 - w_0 < |R(L_1, L'_1)|$. By Lemmas 22 and 33, $B - D = (u_0 + u_2) - (v_0 + v_2) = (v_1 - u_1) + (\sum u_i - \sum v_i) > -t$. So $X_1 > (N - n - t)|R(L_1, L'_1)| > 0$. □

Let G be an essentially 3-connected toroidal map. Consider a periodic mapping of G^∞ , embedded graph H (finite or infinite), and a face F of H . Denote (f_1, f_2, \dots, f_t) the counterclockwise facial walk around F . Given a mapping of the vertices of H in \mathbb{R}^2 , we say that F is *correctly oriented* if for any triplet $1 \leq i_1 < i_2 < i_3 \leq t$, the points f_{i_1}, f_{i_2} , and f_{i_3} form a counterclockwise triangle. Note that a correctly oriented face is drawn as a convex polygon.

Lemma 36 *Let G be an essentially 3-connected toroidal map given with a periodic mapping of G^∞ such that every face of G^∞ is correctly oriented. This mapping gives a straight-line representation of G^∞ .*

Proof We proceed by induction on the number of vertices n of G . Note that the theorem holds for $n = 1$, so we assume that $n > 1$. Given any vertex v of G , let $(u_0, u_1, \dots, u_{d-1})$ be the sequence of its neighbors in counterclockwise order (subscript understood modulo d). Every face being correctly oriented, for every

$i \in [0, d - 1]$ the oriented angle (oriented counterclockwise) $(\overrightarrow{vu_i}, \overrightarrow{vu_{i+1}}) < \pi$. Let the winding number k_v of v be the integer such that $2k_v\pi = \sum_{i \in [0, d-1]} (\overrightarrow{vu_i}, \overrightarrow{vu_{i+1}})$. It is clear that $k_v \geq 1$. Let us prove that $k_v = 1$ for every vertex v .

Claim 4 For any vertex v , its winding number $k_v = 1$.

Proof of Claim 4 In a flat torus representation of G , we can sum up all the angles by grouping them around the vertices or around the faces.

$$\sum_{v \in V(G)} \sum_{u_i \in N(v)} (\overrightarrow{vu_i}, \overrightarrow{vu_{i+1}}) = \sum_{F \in F(G)} \sum_{f_i \in F} (\overrightarrow{f_i f_{i-1}}, \overrightarrow{f_i f_{i+1}})$$

The faces being correctly oriented, they form convex polygons. Thus, the angles of a face F sum at $(|F| - 2)\pi$.

$$\begin{aligned} \sum_{v \in V(G)} 2k_v\pi &= \sum_{F \in F(G)} (|F| - 2)\pi \\ \sum_{v \in V(G)} k_v &= \frac{1}{2} \sum_{F \in F(G)} |F| - f \\ \sum_{v \in V(G)} k_v &= m - f \end{aligned}$$

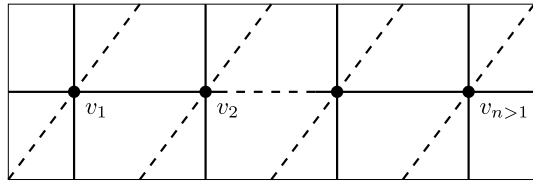
So by Euler’s formula $\sum_{v \in V(G)} k_v = n$, and thus $k_v = 1$ for every vertex v . This proves Claim 4. □

Let v be a vertex of G that minimizes the number of loops whose ends are on v . Thus, either v has no incident loop, or every vertex is incident to at least one loop.

Assume that v has no incident loop. Let v' be any copy of v in G^∞ and denote its neighbors $(u_0, u_1, \dots, u_{d-1})$ in counterclockwise order. As $k_v = 1$, the points u_0, u_1, \dots, u_{d-1} form a polygon P containing the point v' and the segments $[v', u_i]$ for any $i \in [0, d - 1]$. It is well known that any polygon admits a partition into triangles by adding some of the chords. Let us call O the outerplanar graph with outer boundary $(u_0, u_1, \dots, u_{d-1})$, obtained by this “triangulation” of P . Let us now consider the toroidal map $G' = (G \setminus \{v\}) \cup O$ and its periodic embedding obtained from the mapping of G^∞ by removing the copies of v . It is easy to see that in this embedding every face of G' is correctly oriented (including the inner faces of O , or the faces of G that have been shortened by an edge $u_i u_{i+1}$). Thus by the induction hypothesis, the mapping gives a straight-line representation of G'^∞ . It is also a straight-line representation of G^∞ minus the copies of v where the interiors of each copy of the polygons P are pairwise disjoint and do not intersect any vertex or edge. Thus, one can add the copies of v on their initial positions and add the edges with their neighbors without intersecting any edge. The obtained drawing is thus a straight-line representation of G^∞ .

Assume now that every vertex is incident to at least one loop. Since these loops are non-contractible and do not cross each other, they form homothetic cycles. Thus, G is as depicted in Fig. 44, where the dotted segments stand for edges that may be in G but not necessarily. Since the mapping is periodic, the edges corresponding to

Fig. 44 The graph G if every vertex is incident to a loop



loops of G form several parallel lines, cutting the plane into infinite strips. Since for any $1 \leq i \leq n, k_{v_i} = 1$, a line of copies of v_i divides the plane, in such a way that their neighbors which are copies of v_{i-1} and their neighbors which are copies of v_{i+1} are in distinct half-planes. Thus, adjacent copies of v_i and v_{i+1} are on two lines bounding a strip. Then one can see that the edges between copies of v_i and v_{i+1} are contained in this strip without intersecting each other. Thus, the obtained mapping of G^∞ is a straight-line representation. \square

A plane is *positive* if it has equation $\alpha x + \beta y + \gamma z = 0$ with $\alpha, \beta, \gamma \geq 0$.

Theorem 16 *If G is a toroidal triangulation given with a Schnyder wood, and V^∞ the set of region vectors of vertices of G^∞ , then the projection of V^∞ on a positive plane gives a straight-line representation of G^∞ .*

Proof Let $\alpha, \beta, \gamma \geq 0$ and consider the projection of V^∞ on the plane P of the equation $\alpha x + \beta y + \gamma z = 0$. A normal vector of the plane is given by the vector $\vec{n} = (\alpha, \beta, \gamma)$. Consider a face F of G^∞ . Suppose that F is incident to vertices u, v, w (given in counterclockwise order around F). By Lemma 35, $(\vec{u}\vec{v} \wedge \vec{u}\vec{w}) \cdot \vec{n}$ is positive. Thus, the projection of the face F on P is correctly oriented. So by Lemma 36, the projection of V^∞ on P gives a straight-line representation of G^∞ . \square

Theorems 1 and 16 imply Theorem 4. Indeed, any toroidal graph G can be transformed into a toroidal triangulation G' by adding a linear number of vertices and edges and such that G' is simple if and only if G is simple (see for example the proof of Lemma 2.3 of [21]). Then by Theorem 1, G' admits a Schnyder wood. By Theorem 16, the projection of the set of region vectors of vertices of G'^∞ on a positive plane gives a straight-line representation of G'^∞ . The grid where the representation is obtained can be the triangular grid, if the projection is done on the plane of equation $x + y + z = 0$, or the square grid, if the projection is done on one of the planes of equations $x = 0, y = 0, \text{ or } z = 0$. By Lemma 30, and the choice of N , the obtained mapping is a periodic mapping of G^∞ with respect to non-collinear vectors Y and Y' where the size of these vectors is in $\mathcal{O}(\gamma^2 n^2)$ with $\gamma \leq n$ in general and $\gamma = 1$ if the graph is simple and the Schnyder wood obtained by Theorem 9. By Lemma 29, the lengths of the edges in this representation are in $\mathcal{O}(n^3)$ in general and in $\mathcal{O}(n^2)$ if the graph is simple. When the graph is not simple, there is a non-contractible cycle of length 1 or 2 and thus the size of one of the two vectors Y, Y' is in $\mathcal{O}(n^3)$. Thus, the grid obtained in Theorem 4 has size in $\mathcal{O}(n^3) \times \mathcal{O}(n^4)$ in general and $\mathcal{O}(n^2) \times \mathcal{O}(n^2)$ if the graph is simple.

The method presented here gives a polynomial algorithm to obtain flat torus straight-line representations of any toroidal maps in polynomial size grids. Indeed, all the proofs lead to polynomial algorithms, even the proof of Theorem 8 [13], which uses results from Robertson and Seymour [25] on disjoint paths problems.

It would be nice to extend Theorem 16 to obtain convex straight-line representations for essentially 3-connected toroidal maps.

13 Conclusion

We have proposed a generalization of Schnyder woods to toroidal maps with application to graph drawing. Along these lines, several questions were raised. We recall some briefly:

- Does the set of Schnyder woods of a given toroidal map have a kind of lattice structure?
- Does any simple toroidal triangulation admit a Schnyder wood where the set of edges of each color induces a connected subgraph?
- Is it possible to use Schnyder woods to embed the universal cover of a toroidal map on rigid or coplanar orthogonal surfaces?
- Which toroidal maps admit (primal-dual) contact representation by (homothetic) triangles in a flat torus?
- Can geodesic embeddings be used to obtain convex straight-line representations for essentially 3-connected toroidal maps?

The guideline of Castelli Aleardi et al. [3] to generalize Schnyder woods to higher genus was to preserve the tree structure of planar Schnyder woods and to use this structure for efficient encoding. For that purpose they introduce several special rules (even in the case of genus 1). Our main guideline while working on this paper was that the surface of genus 1, the torus, seems to be the perfect surface to define Schnyder woods. Euler's formula gives exactly $m = 3n$ for toroidal triangulations. Thus, a simple and symmetric object can be defined by relaxing the tree constraint. For genus 0, the plane, there are not enough edges in planar triangulations to have out-degree three for every vertex. For higher genus (the double torus, ...) there are too many edges in triangulations. An open problem is to find what would be the natural generalization of our definition of toroidal Schnyder woods to higher genus.

The results presented here motivated Castelli Aleardi and Fusy [4] to develop direct methods to obtain straight-line representations for toroidal maps. They manage to generalize planar canonical ordering to the cylinder to obtain straight-line representations of simple toroidal triangulations in grids of size $\mathcal{O}(n) \times \mathcal{O}(n^2)$, thus improving the size of our grid, which is $\mathcal{O}(n^2) \times \mathcal{O}(n^2)$ in the case of a simple toroidal map. It should be interesting to investigate further the links between the two methods, as canonical orderings are strongly related to Schnyder woods.

Planar Schnyder woods appear to have many applications in various areas like enumeration [1], compact coding [24], representation by geometric objects [14, 16], graph spanners [2], graph drawing [7, 18], etc. In this paper we use a new definition of Schnyder wood for graph drawing purposes, and it would also be interesting to see if it can be used in other computer science domains.

Acknowledgements The authors thank Nicolas Bonichon, Luca Castelli Aleardi, and Eric Fusy for fruitful discussions about this work. They also thank student Chloé Desdouts for developing a software to visualize orthogonal surfaces.

References

1. Bonichon, N.: A bijection between realizers of maximal plane graphs and pairs of non-crossing Dyck paths. *Discrete Math.* **298**, 104–114 (2005)
2. Bonichon, N., Gavoille, C., Hanusse, N., Ilcinkas, D.: Connections between Theta-graphs, Delaunay triangulations, and orthogonal surfaces. In: *Proceeding WG'10 Proceedings of the 36th International Conference on Graph-Theoretic Concepts in Computer Science*, pp. 266–278. Springer, Berlin (2010)
3. Castelli Aleardi, L., Fusy, E., Lewiner, T.: Schnyder woods for higher genus triangulated surfaces, with applications to encoding. *Discrete Comput. Geom.* **42**, 489–516 (2009)
4. Castelli Aleardi, L., Fusy, E.: Canonical ordering for triangulations on the cylinder, with applications to periodic straight-line drawings. In: *Proceeding GD'12 Proceedings of the 20th International Conference on Graph Drawing*, pp. 376–387. Springer, Berlin (2012)
5. Chambers, E., Eppstein, D., Goodrich, M., Löffler, M.: Drawing graphs in the plane with a prescribed outer face and polynomial area. *Lect. Notes Comput. Sci.* **6502**, 129–140 (2011)
6. Duncan, C., Goodrich, M., Kobourov, S.: Planar drawings of higher-genus graphs. *J. Graph Algorithms Appl.* **15**, 13–32 (2011)
7. Felsner, S.: Convex drawings of planar graphs and the order dimension of 3-polytopes. *Order* **18**, 19–37 (2001)
8. Felsner, S.: Geodesic embeddings and planar graphs. *Order* **20**, 135–150 (2003)
9. Felsner, S.: Lattice structures from planar graphs. *Electron. J. Comb.* **11**(1), R15 (2004)
10. Felsner, S., Trotter, W.T.: Posets and planar graphs. *J. Graph Theory* **49**, 273–284 (2005)
11. Felsner, S., Zickfeld, F.: Schnyder woods and orthogonal surfaces. *Discrete Comput. Geom.* **40**, 103–126 (2008)
12. Felsner, S.: *Geometric Graphs and Arrangements*. Vieweg, Wiesbaden (2004)
13. Fijavz, G.: Personal communication (2011)
14. de Fraysseix, H., Ossona de Mendez, P., Rosenstiehl, P.: On triangle contact graphs. *Comb. Probab. Comput.* **3**, 233–246 (1994)
15. de Fraysseix, H., Ossona de Mendez, P.: On topological aspects of orientations. *Discrete Math.* **229**, 57–72 (2001)
16. Gonçalves, D., Lévêque, B., Pinlou, A.: Triangle contact representations and duality. *Discrete Comput. Geom.* **48**, 239–254 (2012)
17. Gonçalves, D., Lévêque, B., Pinlou, A.: Triangle contact representations and duality (GD'10). *Lect. Notes Comput. Sci.* **6502**, 262–273 (2011)
18. Kant, G.: Drawing planar graphs using the canonical ordering. *Algorithmica* **16**, 4–32 (1996)
19. Kratochvíl, J.: In: *Bertinoro Workshop on Graph Drawing* (2007)
20. Miller, E.: Planar graphs as minimal resolutions of trivariate monomial ideals. *Doc. Math.* **7**, 43–90 (2002)
21. Mohar, B.: Straight-line representations of maps on the torus and other flat surfaces. *Discrete Math.* **155**, 173–181 (1996)
22. Rosenstiehl, P.: Embedding in the plane with orientation constraints: The angle graph. *Annals New York Academy of Sciences* (1989)
23. Mohar, B., Rosenstiehl, P.: Tessellation and visibility representations of maps on the torus. *Discrete Comput. Geom.* **19**, 249–263 (1998)
24. Poulalhon, D., Schaeffer, G.: Optimal coding and sampling of triangulations. *Algorithmica* **46**, 505–527 (2006)
25. Robertson, N., Seymour, P.D.: Graph minors. VI. Disjoint paths across a disc. *J. Comb. Theory, Ser. B* **41**, 115–138 (1986)
26. Schnyder, W.: Planar graphs and poset dimension. *Order* **5**, 323–343 (1989)